SYNTHESIS AND PHOTOPOLYMERIZATION OF NOVEL ALKYL-α-HYDROXYMETHYL ACRYLATE BASED DENTAL CROSSLINKING MONOMERS

by

MUSTAFA BARIŞ YAĞCI

B.S. in Chem., Marmara University, 2002

Submitted to the Institute for Graduate Studies in
Science and Engineering in partial fulfillment of
the requirements for the degree of
Master of Science

Graduate Program in Chemistry
Boğaziçi University

2005

Annem ve Zeynep' ime …

ACKNOWLEDGEMENTS

I would like to express my sincere gratitude to my supervisor Prof. Duygu Avcı Semiz for her invaluable guidance, advice, and encouragements throughout this study. I enjoyed a lot working in her research group.

I am grateful to my committee members Assist. Prof. Ali Ersin Acar and Assoc. Prof. Safiye Erdem for their careful and constructive review of the final manuscript.

I would especially like to thank to my laboratory partner, Aylin Ziylan Albayrak for her helps and friendship. She was more a co-promoter than a lab mate. She taught a lot of things to me throughout my study. I am also very grateful to her for taking care of me during our days in USA.

I would like to extend my thanks to Ayla Türkekul, Dr. Bilge Uluocak, and Burcu Selen Çağlayan for NMR analyses.

I also thank to all members of Boğaziçi University Department of Chemistry, my instructors and my friends, and especially the secretary of the department Hülya Metiner (Hülya Abla) and Zahit Mehlep for their helps and friendship.

Finally, I would like to express my gratitude and respect to my loving family for their everlasting support and love throughout my life; and my sweet niece Zeynep for not watching cartoons while I was writing my thesis.

This study has been supported by Boğaziçi University Scientific Research Project (BAP05B502) and DPT (03K120250).

ABSTRACT

SYNTHESIS AND PHOTOPOLYMERIZATION OF NOVEL ALKYL-α-HYDROXYMETHYL ACRYLATE BASED DENTAL CROSSLINKING MONOMERS

The most commonly used dental restorative filling composites are composed of Bisphenol A glycolate dimethacrylate (Bis-GMA) monomer, an inorganic filler, and a polymerization initiator system. A comonomer such as triethyleneglycol dimethacrylate (TEGDMA) is added to adjust the viscosity of the dental resin.

In this study, five new dental crosslinking monomers with improved adhesion to tooth tissue, volume shrinkage and stability were synthesized. Four are based on t-butyl-α-hydroxymethyl acrylate (TBHMA): (i) via reaction of t-butyl-α-bromomethyl acrylate (TBBr) and Bisphenol A, (ii) by hydrolysis of t-butyl groups of the first monomer to give a diacid derivative, (iii) by conversion to amide derivative using benzyl amine, (iv) by conversion to amide derivative using (3-aminopropyl)-triethoxy silane (APTES). The AHM based monomer (v) was synthesized from the Michael addition of APTES to 3-acryloyloxy-2-hydroxypropyl methacrylate (AHM).

The photopolymerization behavior of the synthesized monomers with mixtures of commercial monomers Bisphenol A glycolate dimethacrylate (BisGMA)/triethyleneglycol dimethacrylate (TEGDMA) and BisGMA/2-hydroxyethyl methacrylate HEMA widely used in dentistry was investigated using photodifferential scanning calorimetry. The rate of polymerizations and conversions were found to be similar to the commercial materials, although adhesion and stability properties were improved.

ÖZET

ALKİL-α-HİDROKSİMETİL AKRİLAT BAZLI YENİ ÇAPRAZ BAĞLAYICI DİŞÇİLİK MONOMERLERİNİN SENTEZİ VE IŞIKLA POLİMERİZASYONU

En genel kullanılan dişçilik dolgu kompozitleri, Bisfenol A glikolat dimetakrilat (Bis-GMA) monomeri, inorganik bir katkı maddesi ve bir polimerizasyon başlatıcı sisteminden oluşmaktadır. Akışkanlığı ayarlamak amacı ile dişçilik reçinesinin içerisine bir yardımcı monomer, örneğin trietilenglikol dimetakrilat (TEGDMA) eklenir.

Bu çalışmada, diş dokusuna bağlanma kabiliyeti, hacim küçülmesi ve mukavemet özellikleri gelişmiş beş yeni dişçilik çapraz bağlayıcı monomeri sentezlenmiştir. Bunlardan dördü t-bütil-α-hidroksimetil akrilat (TBHMA) türevidir: (i) t-bütil-α-bromometil akrilat (TBBr) ile bisfenol A reaksiyonundan, (ii) ilk momomerin t-bütil gruplarının hidrolizi sonucu oluşan diasit türevi, (iii) benzil amin kullanılarak amid türevine dönüştürülmesinden, (iv) (3-aminopropil)-trietoksi silan (APTES) kullanılarak amid türevine dönüştürülmesinden, AHM türevi monomer, (v) APTES' in 3-akriloiloksi-2-hidroksipropil metakrilat (AHM) ile verdiği Michael reaksiyonu ile sentezlenmiştir.

Sentezlenen monomerlerin, dişçilikte çok kullanılan endüstriyel Bisfenol A glikolat dimetakrilat (BisGMA)/trietilenglikol dimetakrilat (TEGDMA) ve BisGMA/2-hidroksietil metakrilat HEMA karışımları ile oluşturduğu sistemlerin ışıkla polimerizasyon davranışları, Foto Diferansiyel Taramalı Kalorimetri (Photo-DSC) metoduyla incelenmiştir. Bağlanma ve mukavemet özelliklerindeki artışın yanı sıra, polimerizasyon hızları ve dönüşümlerinin endüstriyel malzemelerinki ile benzer olduğu saptanmıştır.

TABLE OF CONTENTS

LIST OF FIGURES

LIST OF TABLES

LIST OF SYMBOLS/ABBREVIATIONS

k_p	Propagation rate constant
R_p	Rate of polymerization
T_g	Glass transition temperature
AHM	3-acryloyloxy-2-hydroxypropyl methacrylate
APTES	(3-aminopropyl)-triethoxy silane
BisAcid	TBBr-Bisphenol A Diacid Derivative
BisAptes	TBBr-Bisphenol A – APTES Diamide Derivative
BisBenzyl	TBBr-Bisphenol A – Benzylamide Derivative
Bistbutyl	TBBr-Bisphenol A Diester Monomer
CI	Co-initiator
CQ	Camphorquinone
DMAB	Ethyl-4-dimethylaminobenzoate
DSC	Differential Scanning Calorimetry
NMR	Nuclear Magnetic Resonance Spectroscopy
PI	Photoinitiator
Poly(AA-*co*-IA)	Copolymer of acrylic acid and itaconic acid
RT-FTIR	Real time – Fourier transform Infra Red Spectroscopy
TBBr	tert-Butyl-α-Bromomethyl Acrylate
TBHMA	tert-Butyl-α-Hydroxymethyl Acrylate
UV	Ultra Violet Spectroscopy

1. INTRODUCTION

1.1. Introduction to the Anatomy of Tooth

A human tooth has three main parts which are, crown; the visible part of the tooth, neck; the layer between crown and the mouth tissue, and root; the anchor of the tooth that extends into the jawbone (Figure 1.1) [1].

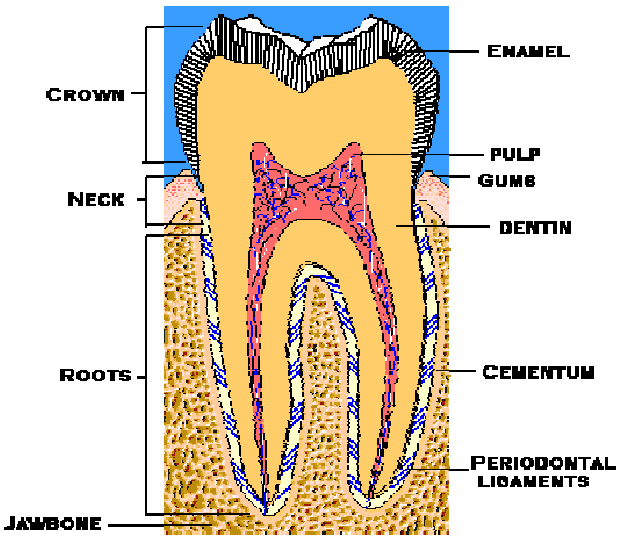

Figure 1.1. The anatomy of tooth

The tough, shiny, and white outer surface of the tooth is called enamel. The porous, yellowish, and hard dentin tissue which constitutes the main bulk of the tooth is located under enamel and cementum [2]. Both dentin and enamel consist of more than 95 vol% pure hydroxyapatite crystals and a small amount of other organic and inorganic components [3,4]. The pulp, the soft center of the tooth, contains blood vessels and nerves; it nourishes the dentin. Finally, the fleshy tissue between the tooth and tooth socket, so called periodontal ligaments hold the tooth in place. The fibers of this periodontal membrane are embedded within the cementum [2].

1.2. Introduction to Dental Restorative Filling Materials

Dental restoration is one of the most popular research areas in the field of biomaterials for hundreds of years. The search for the ideal restorative material for dentistry is an ongoing one [5]. To be successful, materials need to fulfill several chemical and physical requirements, which are stated below [5,6]:

- Rapid setting
- Easy handling and placing
- High resistance in oral conditions
- Low oral toxicity, no mutagenic or carcinogenic effect
- No or very low volume change during and after setting
- High light and coloration stability
- High adhesive and mechanical properties

Today, commonly used dental restorative filling materials are mainly classified into four groups, which are amalgams, composite resins, glass-ionomer cements, and hybrid materials [5].

1.2.1. Amalgams

Amalgam restorations were first used in France in 1826, and were introduced in the United States in 1833 [7]. Despite their lack of aesthetics and potential health hazard due to the high amount of mercury they contain [5], their long term durability (10-20 years) and low cost have made them preferred for years [8,9].

Early dental amalgams were made by mixing mercury (50 wt%) with powdered alloy (50 wt%) which was composed of 65-70 wt% Ag, 25-27 wt% Sn, 0-6 wt% Cu, 0-2 wt% Zn, and only minor changes in the basic composition have been made since then. In preparing the alloy for dental amalgam, the components are melted together, usually under an inert atmosphere, and then are homogenized at 400°C for 6-24 hr. When the powdered amalgam alloy and mercury are freshly mixed, a paste-like material is obtained. The cavity

is restored at this point and the chemical setting process, which can be described by the following reaction, takes place in the cavity [7].

$$Ag_3Sn + Hg \rightarrow Ag_2Hg_3 + Sn_{7-8}Hg$$

Amalgamation involves dissolution of Ag_3Sn powder in liquid mercury followed by the growth of reaction product from the mercury solution. Ag_2Hg_3 is formed as a solid reaction product separating Ag_3Sn and the liquid mercury. The amalgamation will then proceed by solid-state diffusion through Ag_2Hg_3, and Sn will be concentrated in the liquid until it solidifies as $Sn_{7-8}Hg$ [7].

Besides their long term durability and good mechanical properties, there are some serious drawbacks of dental amalgams, for instance, there is almost no adhesion between the amalgam and the tooth material. Saliva may penetrate into this interspace around the restoration resulting in corrosion. The condition of the amalgam surface is important since corrosion products and rough surface retain bacteria and debris. Another frequently observed failure is ditching which can be observed between the enamel and the amalgam. Ditching results from improper cavity preparation and may cause secondary caries [7].

Furthermore, any material used in contact with living tissue should be biocompatible. Dental amalgam, its corrosion products, and compounds, ions, or elements which leach out from the restoration may have a toxic effect on the human body [7]. The toxicity and other potential hazards of mercury is well documented [10,11].

1.2.2. Composite Resins

In restorative dentistry, tooth-colored resin-based composites have been used as direct restorative material for both posterior and anterior regions, for years. Many of the currently used commercial dental restorative composites are composed of a mixture of about 20-30 wt% of an organic matrix and 70-80 wt% of inorganic fillers, such as quartz or barium aluminoborate silica glass [12].

A three-dimensional organic network is formed by free radical photopolymerization of non-toxic dimethacrylates, which are capable of rapid polymerization in the presence of oxygen and water. The selection of monomers strongly influences the reactivity and other physical and mechanical properties. Some examples of commonly used dimethacrylate crosslinking monomers are shown in Figure 1.2.

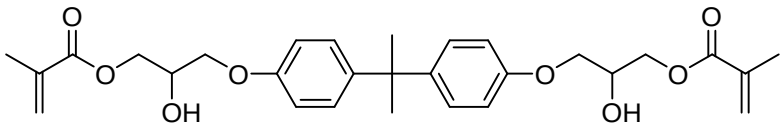

Bisphenol A glycolate dimethacrylate (Bis-GMA)

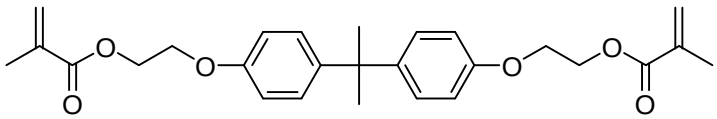

Bisphenol A ethoxylated dimethacrylate (Bis-EMA)

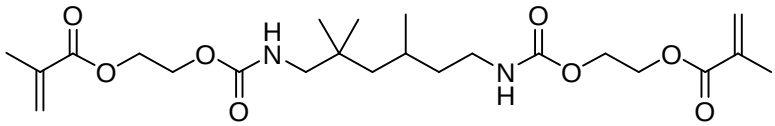

Urethane dimethacrylate (UDMA)

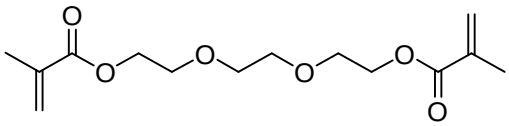

Triethyleneglycol dimethacrylate (TEGDMA)

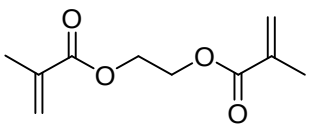

Ethyleneglycol dimethacrylate (EGDMA)

Figure 1.2. Structures of frequently used base resins in dental composite filling materials

Since its first development in 1960s, the ‘‘Bowen resin’’ (Bisphenol A glycolate dimethacrylate or Bis-GMA) is still the most commonly used base resin in current dental restorative composite formulations. The advantages of using Bis-GMA include its high modulus and glass transition temperature, low volatility, and relatively low volume shrinkage during polymerization. However, the extremely high viscosity of Bis-GMA requires dilution with 20-35 wt% low-viscosity monomer, such as triethyleneglycol dimethacrylate (TEGDMA) or ethyleneglycol dimethacrylate (EGDMA). This also provides easy handling, higher filler loading and greater extent of polymerization. On the other hand, incorporation of these reactive diluents affects mechanical properties, volume shrinkage, and water absorption [13]. By addition of particulate fillers which are harder than the polymeric matrix, these drawbacks resulting from the addition of reactive diluents are being tried to overcome.

Because they are cured by irradiation with visible light, these systems also include a photoinitiator (PI) or a photoinitiating system [14]. Camphorquinone (CQ) is a widely used photoinitiator in dental applications, in combination with tert-amines, such as ethyl-4-dimethylaminobenzoate (DMAB) as a co-initiator (CI) (Figure 1.3). The main reasons to use CQ/DMAB system is absorption in the visible range of the spectrum and biocompatibility [15].

Camphorquinone (CQ) Ethyl-4-dimethylaminobenzoate (DMAB)

Figure 1.3. Structures of camphorquinone (CQ) and ethyl-4-dimethylaminobenzoate (DMAB)

To improve the performance of these materials, a lot of investigations are being conducted [16-25]. For instance, the use of monomers with different structures and properties, such as cyclic [26-28], liquid-crystalline, highly-branched, and dendritic [29] monomers is under investigation. Also, the use of heavy-metal containing monomers

provides a certain degree of radiopacity, which is important for the detection of secondary caries, marginal defects, or other imperfections on X-rays [30]. Moreover, introduction of some adhesive moieties such as phosphonic acid groups, beside incorporation of hydroxyl and amide functions [31] to commonly used monomers, increases the adhesive properties of dental composites to dentine and enamel structures [31-33].

Overall, the current composite materials have good color and translucency, and fast setting time, but much lower wear resistance than the amalgams. The lifetime for anterior polymeric restorative materials is about 8 years, but for posterior materials is often not longer than 2–4 years. However, despite this deficiency there are diverse cogent reasons, such as aesthetics and avoidance of mercury pollution of the environment, which spur on their further developments [34].

1.2.3. Glass-Ionomer Cements (GIC's)

Glass-ionomer cements mainly consist of an acid-decomposable glass and water-soluble acid, i.e. a polyelectrolyte [6,35]. The systematic name of these materials is "glass-polyalkenoate", but they are known as "glass-ionomer" to the dental profession [5]. The invention of glass-ionomer dental cement occurred as a result of the pioneering studies of Alan Wilson and Brian Kent at the Laboratory of the Government Chemist, London, in the late 1960s [37]. This type of commercial dental cements became available in 1975 [38,39]. The uses of these materials include cavity lining beneath amalgam or composite resin fillings (to prevent thermal or chemical damage to the sensitive underlying pulp of the tooth), cementation of crowns and gum-line cavity filling [5].

Conventional glass-ionomer cements are formed by the setting reaction of an aqueous solution of a polyelectrolyte (40-50 wt%), derived from acids, such as those shown in Figure 1.4, with a calcium fluoro-aluminosilicate (CaFAlSi) glass powder (at ratio of 2:1 - 3.5:1) [5,6].

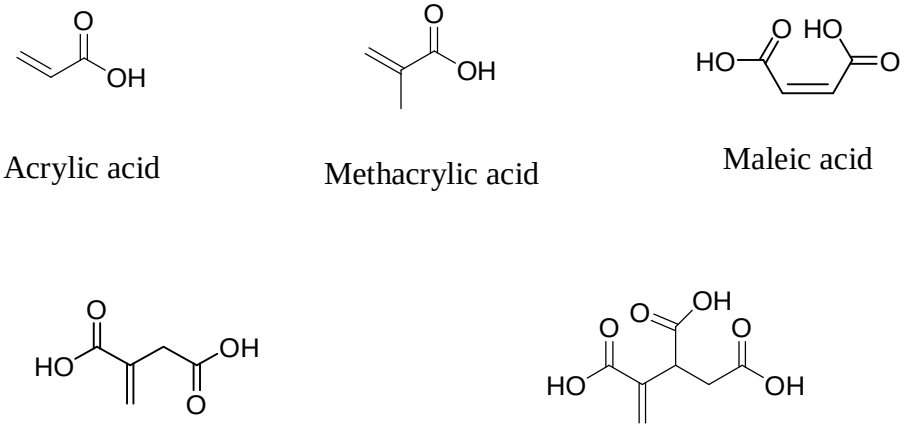

Figure 1.4. Commonly used monomers in glass-ionomer cements

Hydrogen ions released from the polymeric acid in the presence of water, attack the glass powder and lead to release of Ca^{2+} and Al^{3+} cations forming a silica gel (hydrogel) area on the glass surface (Figure 1.5) [5].

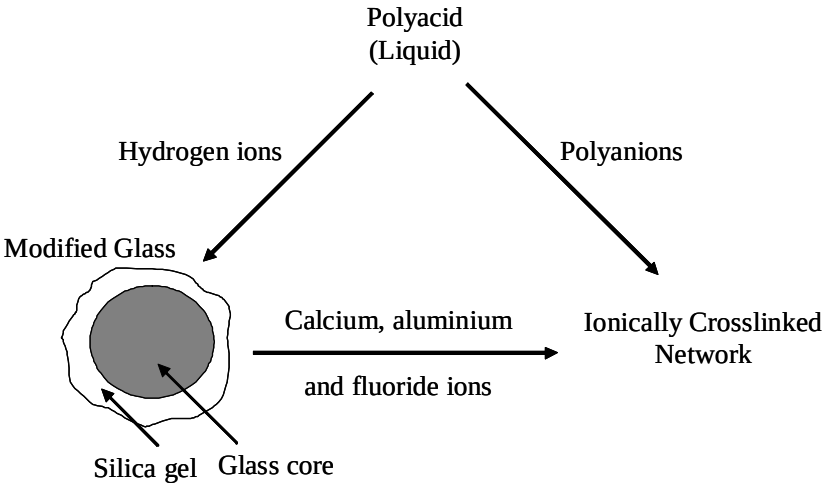

Figure 1.5. Setting mechanism of glass-ionomer cements

Then, the rapid complexation of the Ca^{2+} ions with polycarboxylate anions (after loosing H^+ protons), following by slower complexation of Al^{3+} species, gradually form a

hard, ionically cross-linked, ceramic-like matrix of the molecular structures as shown in Figure 1.6 [40].

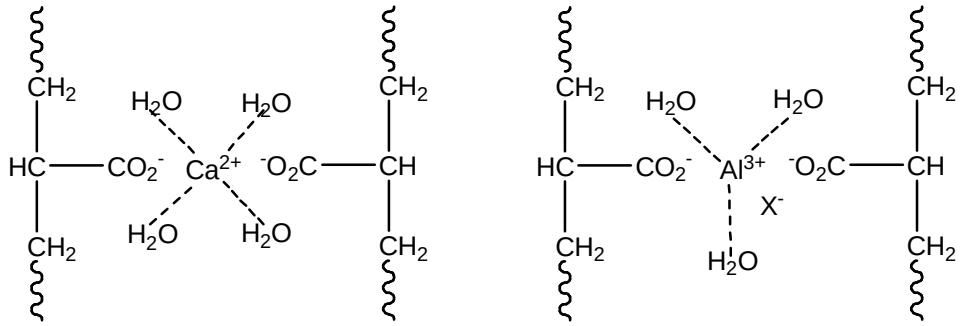

Figure 1.6. Possible intermolecular Ca^{2+} or Al^{3+} carboxylate complexes (salt-bridges) in cured glass-ionomer cements, where X represents OH^- or F^- anions

The carboxylate groups also form either strong ionic bonds to the calcium ions on the surface of enamel and dentin [41] or they displace phosphates from the calcium hydroxyapatite surface.

Glass-ionomers have good translucency, hence they can be used as restoratives in the front teeth, where aesthetics are important. They also release fluoride, since fluoride as CaF_2 is a constituent of the glass, and this protects the natural tooth material in the region immediately surrounding the filling and provide good antibacterial activity [42,43-51]. Fluoride ions also reduce microleakage [52,53], and help reduce occurrence of secondary caries [54-59]. Fluoride release appears to be an ion-exchange process between hydroxyl ions in the saliva and F^- ions in the cement matrix, and fluoride can be replenished by brushing the teeth with a fluoride containing toothpaste [5].

Beside fluoride release, glass-ionomers have a number of important advantages [6]:

a. They form hard materials upon setting [6,60],
b. They do not result in an exothermic reaction,
c. They exhibit little to no volume shrinkage during setting,
d. They have no free monomer in the set matrix,
e. They have good adhesion to the tooth tissue [6,61,62].

One disadvantage of glass-ionomer cements is their brittle structure due to the high amount of glass component. Furthermore, since these materials are ionically crosslinked, the possibility of water penetration into the matrix is higher than composite resins which are covalently bonded. This may result in moisture sensitivity in the early part of their life, soon after placement, because glass-ionomer cements undergo slower setting process when compared to photopolymerizable composites.

1.2.4. Hybrid Materials

After the discovery of first glass-ionomer cement more than 30 years ago, numerous developments have been taken place in order to improve properties of these materials. For instance, the first major breakthrough was the addition of tartaric acid for improved setting characteristics. Then, the incorporation of more reactive polyacids and various modified glass compositions were examined. Also, sintering the glass together with metals (e.g. silver) resulted in the so-called “cermets”, where the metal can absorb mechanical stress to a certain extent and reduce the brittleness of the cement [63].

However, despite all these improvements, two problems with glass-ionomers still remained: moisture sensitivity and the lack of command cure. To overcome these problems, in the late 1980s and early 1990s the first hybrid materials were released on the market [63].

Resin-modified glass-ionomers is the name given to these materials since, they are effectively hybrids of two other dental materials, namely, the glass-ionomer cements and composite resins [5,6,36,64]. They combine both water-soluble and water-immiscible components, and when set include both polyelectrolyte and nonionic polymer structures [5]. Resin-modified glass ionomer cements were introduced to dentistry as lining materials under the main filling, such as amalgam or composite resin, just like their glass-ionomer counterparts [5,65], and they also contain calcium fluoro-aluminosilicate type glasses, too. These glasses have two roles: they act as crosslinkers, via salt-bridge formation from the neutralization reaction, and as filler for the resin phase [5,6]. Water is essential to promote the neutralization reaction.

The setting mechanism of resin-modified glass-ionomers involves both the neutralization reaction (from the glass-ionomer phase) and photo-chemical process (from the organic phase), and due to the contrasting nature of the components, a natural tendency exists for resin modification to undergo phase separation while still liquid. To achieve a stable solution of the aqueous and organic phases, some water soluble organic components, such as 2-hydroxyethyl methacrylate (HEMA) (Figure 1.7) were employed. These components act both as a co-solvent and a free radical or photopolymerizable monomer [5,6].

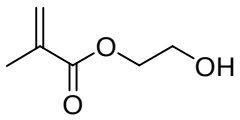

Figure 1.7. The structure of 2-hydroxyethyl methacrylate (HEMA)

After initial discovery, alternative monomers and concepts were used to make cements of this type. For instance, photopolymerizable side chains were grafted to the main polyacid polymer backbone via the reactions between 20-33 per cent of pendant carboxylic acid groups with something such as glycidyl methacrylate (Figure 1.8) or 2-isocyanatoethyl methacrylate (Figure 1.9) [6].

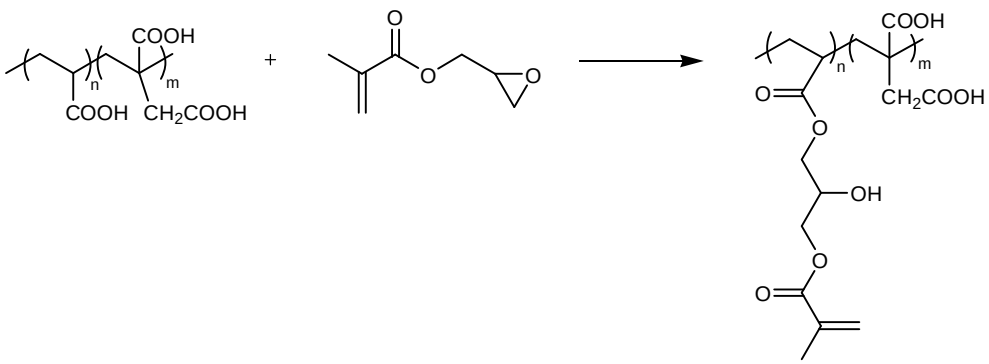

Figure 1.8. Poly(AA-*co*-IA) reaction with glycidyl methacrylate for producing a hybrid system

An extension of this type of cements was developed by 3M, so-called Vitrabond™ (Figure 1.9). This product has two modes of cure; neutralization and photocure.

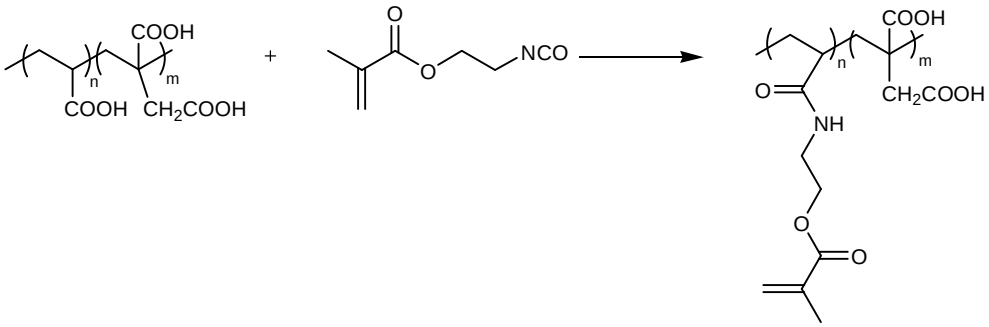

Figure 1.9. Poly(AA-*co*-IA) reaction with 2-isocyanatoethyl methacrylate for producing a hybrid system

The setting chemistry of resin-modified systems is complicated. As the acid-base reaction progresses, the polymeric acid becomes more neutralized and phase separates from the organic phase. The product contains domains of different compositions. Another approach to hybrid systems is the direct replacement of the carboxylic acid functionalized, water soluble polymers with polymerizable, carboxylic acid functionalized monomers or prepolymers. This method is called “compomer” approach (Figure 1.10) [30].

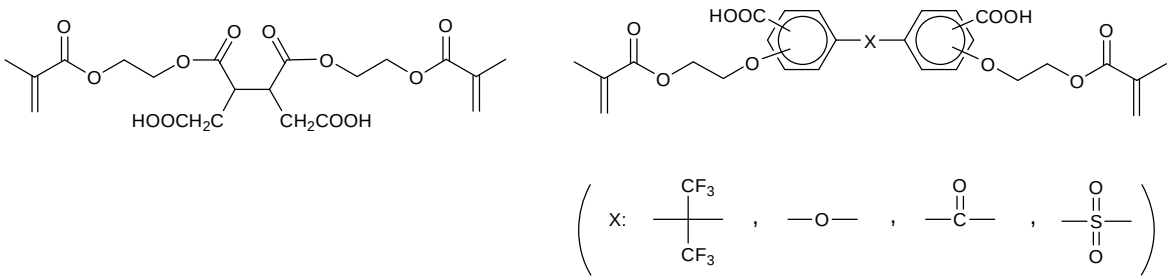

Figure 1.10. Aliphatic and aromatic COOH-containing dimethacrylates for compomers

Basically, these compomer monomers are able to react simultaneously with the methacrylate groups by free-radical polymerization and, in the presence of water from the environment, a limited acid-base reaction is also observed.

More recently, besides their use as lining materials, resin-modified glass-ionomer cements have found applications in where aesthetics are important, such as front teeth or to

seal small fissures on the surface of molars in children [66]. These materials are obtained by reducing the amount of organic resin component from 20 to 10 per cent to be stronger and more durable than the original liner versions [5].

In summary, resin-modified glass-ionomer cements are cured with visible light, and are white, translucent restorations. They also have been shown to have good adhesion to teeth and to release clinically useful amounts of fluoride. Furthermore, recent hybrid materials are showing improved handling and mechanical properties, coupled with a decrease in moisture sensitivity compared to glass-ionomer counterparts.

1.2.4.1. Ormocers. A further possibility to reduce the polymerization shrinkage, to improve the mechanical properties and biocompatibility is the use of new polymerizable sol-gel polycondensates which are also called “ormocers (organically modified ceramics)”.

The formation of ormocers starts from an alkoxy silane functionalized with a polymerizable group (Figure 1.11). The setting mechanism of ormocers firstly involves hydrolysis and condensation resulting an oligomeric Si-O-Si nanostructure. In the next step, a three-dimensional network is formed by the polymerization of the double bonds or other polymerizable groups [30]. In these hybrids, the organic and inorganic components are combined at a nanoscopic or molecular scale and, therefore, enable the fabrication of the materials with tailor-made properties. This makes ormocers very attractive for use in dentistry [12].

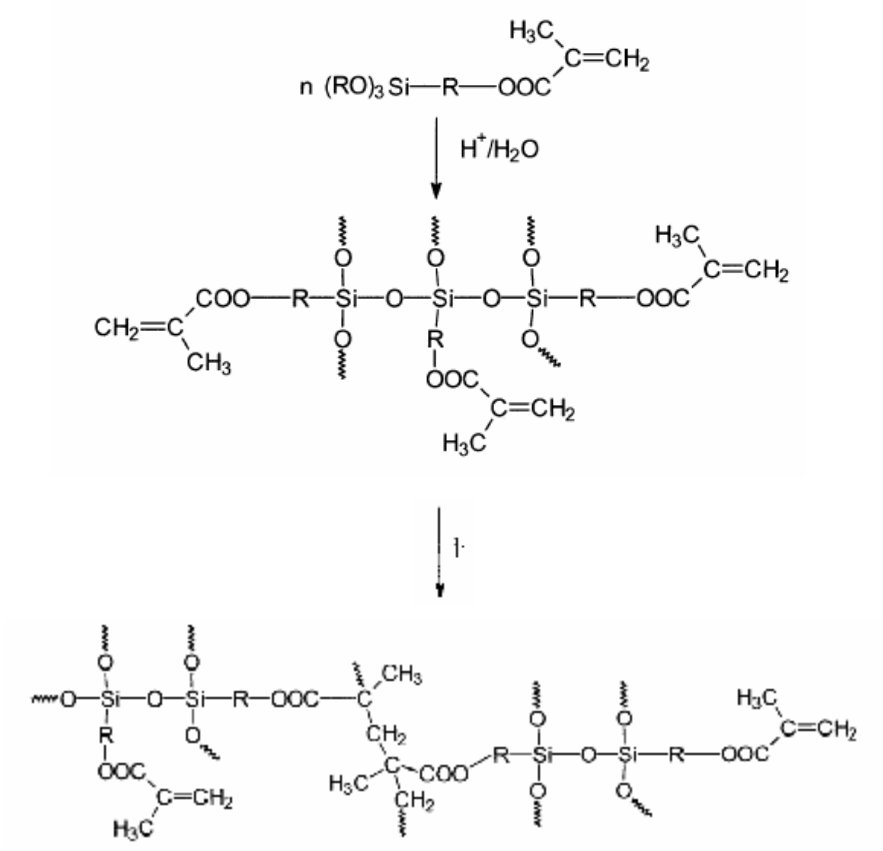

Figure 1.11. The general setting mechanism of ormocers

An example of methacrylate-functionalized alkoxy silane is obtained from the reaction of glycerol dimethacrylate (GDMA) with (3-isocyanatopropyl)-triethoxy silane (IPTES) (Figure 1.12) [30].

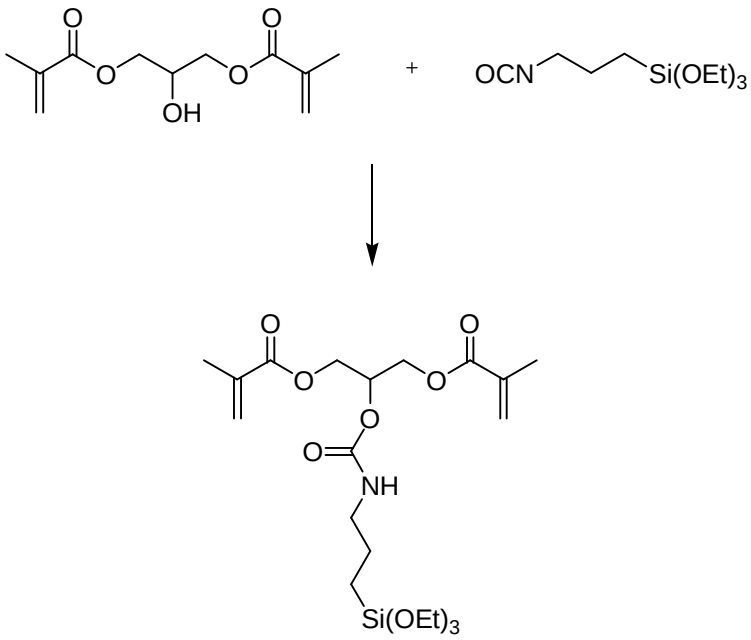

Figure 1.12. The reaction of GDMA with IPTES

The main problem of this type of material is high viscosity, comparable to that of Bis-GMA. To obtain good handling properties, dilution with a low viscous monomer, such as TEGDMA is needed as in composite materials. In this case, the biocompatibility requirements are no longer fulfilled. Recently, new ormoceric materials resulting condensates demonstrated a viscosity in the range 1-15 Pa.s were synthesized [67]. For example, a different type ormocer was obtained by Michael addition of 2-acryloyloxyethyl methacrylate (AEMA) to (3-aminopropyl)-triethoxy silane (APTES) (Figure 1.13).

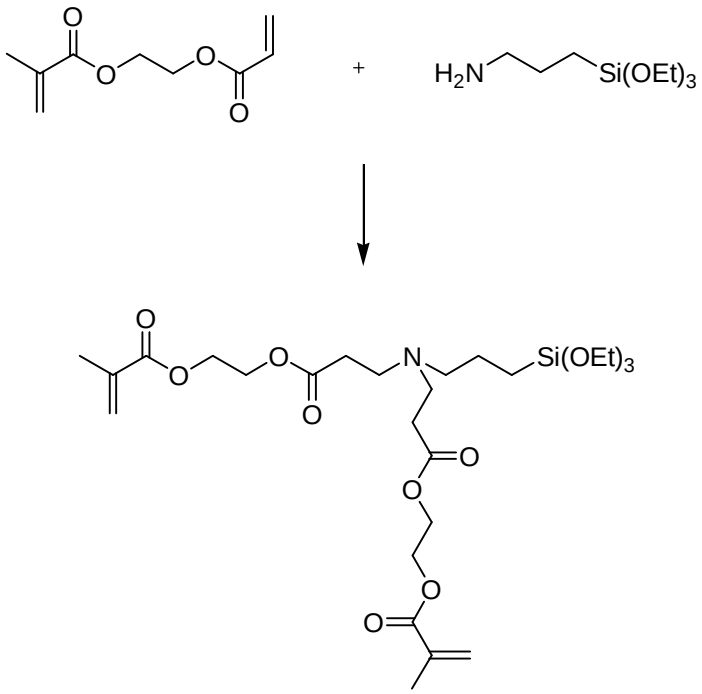

Figure 1.13. Michael addition of AEMA with APTES

Because these materials are in a convenient viscosity range, they do not need methacrylate diluents. In this way, the improved biocompatibility is provided [12].

1.3. Introduction to Photopolymerization

In dentistry, the curing process of dental filling systems must fulfill a basic requirement. It must be very fast at room temperature. Because photopolymerization satisfies this requirement, it is widely used in polymerizable dental systems.

Dental photopolymerizable formulations are usually made of three main components [68];

a) A photoinitiator that effectively absorbs the incident light and generates radicals or ions,
b) Functionalized monomer or oligomer that will constitute the backbone,
c) A reactive diluent to adjust viscosity.

Photopolymerization is mainly classified into two groups, depending whether on the reaction proceeds by a radical-type or cationic-type mechanism (Table 1.1). In photoinduced radical polymerization, aromatic ketones are used as initiators which decompose to generate free radicals. The produced radicals initiate the polymerization of vinyl monomers by a step-growth addition mechanism. On the other hand, in photoinduced cationic polymerization, a protonic acid is generated by photolysis of triarylsulfonium (TAS) or diaryliodonium salts to initiate the polymerization of epoxides or vinyl ethers [68].

Table 1.1. Different types of photo-curable resins

Mechanism	RADICAL	CATIONIC
Photoinitiator	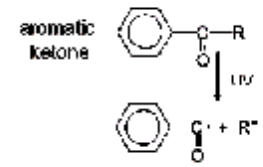	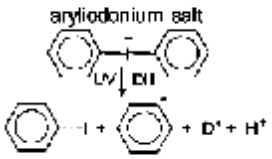
Monomers and functionalized polymers	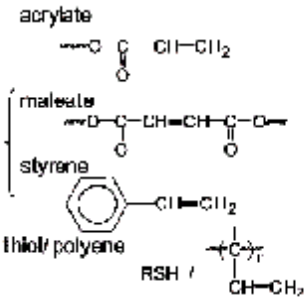	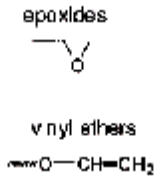

Radical-type systems are the most widely used in today's photo-curing applications.

1.3.1. Photoinitiators

The photoinitiators play a key role in that they govern both the rate of initiation and the penetration of incident light into the sample, and therefore control the depth of cure. It is essential to select a photoinitiator showing the highest initiation efficiency and undergoing a fast photobleaching upon UV exposure in order to achieve a deep-throug cure by frontal polymerization. Figure 1.14 gives the structures of some photoinitiators which are commonly used in both dentistry and other applications [68].

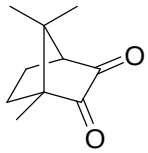

Camphorquinone (CQ)

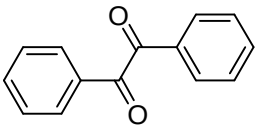

Benzil

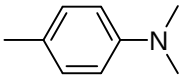

Dimethyl-p-toluidine

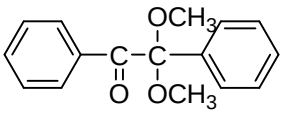

2,2-Dimethoxy-2-phenyl acetophenone (Irgacure 651)

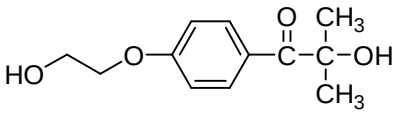

2-Hydroxy-1-[4-Hydroxyethoxyphenyl]-2-methyl-1-propane (Irgacure 2959)

Figure 1.14. Commonly used photoinitiators

1.3.2. Monomers

The most widely used monomers in photopolymerization are multifunctional acrylates and methacrylats due to their high reactivity and moderate to low volatility. Methacrylates are one of the most reactive monomers polymerizing by free radical mechanism. The use of methacrylate monomers in dental resins is very common. The polymerization of a dimethacrylate monomer, initiated by UV-generated benzoyl radicals, is assumed to develop according to the following scheme (Figure 1.15) [69].

The rate of polymerization initially depends on the reactivity of the functional group, its concentration and the viscosity of the resin. The chemical structure, distance and flexibility between the functional groups, and functionality of both monomer and/or oligomer are also important. These factors determine the final degree of polymerization, as well as the physical and chemical characteristics of the UV-cured polymer [70].

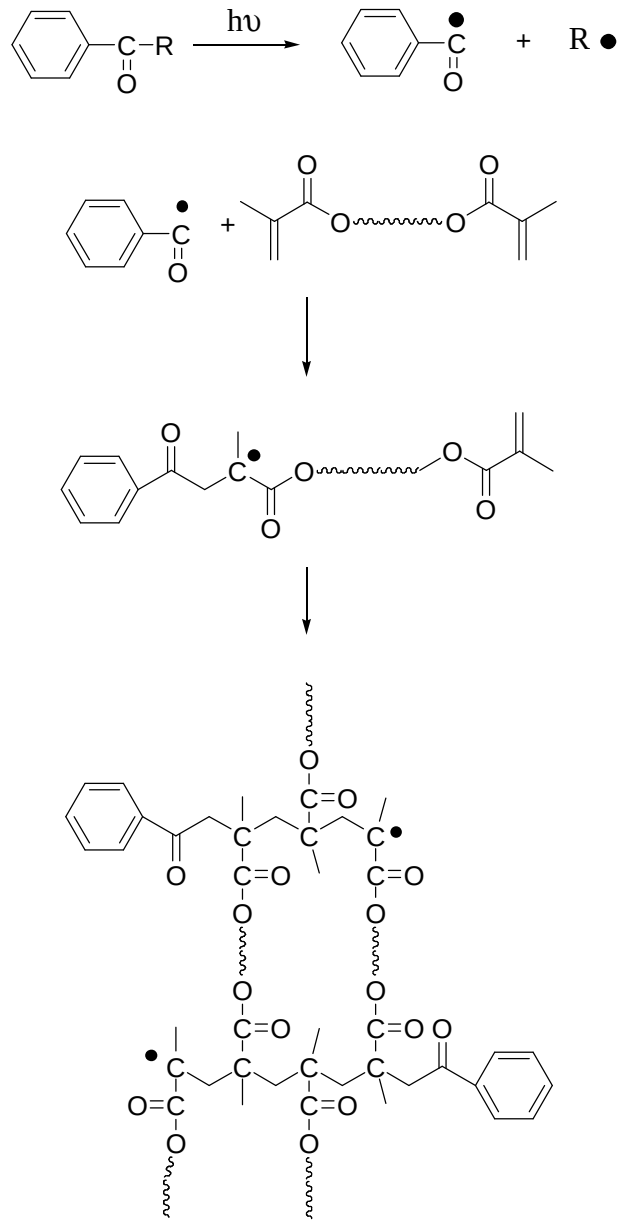

Figure 1.15. Mechanism of the photopolymerization of a dimethacrylate monomer

For instance, monomers capable of hydrogen bonds generally shows higher rate of polymerizations (R_p) compared to their non-hydrogen-bonding analogues. A plausible explanation for this enhanced polymerization rate is that hydrogen bonding results in preorganization in the monomers, by forcing the double bonds in close to each other. As a consequence, the propagation rate constant (k_p) will be enhanced [71]. Furthermore, hydrogen bonding will increase the overall viscosity of the bulk monomer solution, thus hindering radical termination and causing an increase in radical concentration. This will

increase polymerization rate [72]. However, there is a critical distance between the double bond and the hydrogen-bonding moiety (alkyl bridge length) beyond which there is no effect on R_p in the case of the preorganization theory. This is because conformational mobility of the skeletal bonds between the hydrogen-bonding moiety, and the double bond will reach a level whereby the double bond can be regarded as isolated from the hydrogen-bonding moiety [71,72].

1.3.3. Light Sources

The light source is another critical factor in the photo-curing process because the initiation rate can be varied by changing the light intensity. Simply, increase in light intensity will lead to increase in polymerization rate. In general, two major light sources are used:

a) Arc light
b) Laser light

The basic arc light has clear fused quartz tubing in which a gas is enclosed. When a direct current is applied through two electrodes to generate an arc, the gas is discharged and light is emitted. The output of the lamp depends on the pressure and the type of gas used. The most commonly used gases are mercury and xenon. The gas pressure can be low (10^{-3} torr), medium (1-2 atm), or high (>2 atm). The medium-pressure mercury lamp is the most important light source used in the photo- or UV-curing industry [69].

Lasers offer the prospect of an excitation source of exceedingly high intensity compared to classical light sources. Their outputs are available in both UV and visible wavelengths. Some lasers offer fixed wavelength, whereas some others offer tunable wavelengths [69].

In dentistry, 420-500 nm light in visible region is used [73].

Correct choice of the light system is the first step toward success of a radiation curing process. Emission spectra of the lamps must match the absorption spectra of the

chosen photoinitiators, sensitizers, or charge transfer complexes. Stable output over a period of time and the intensities of the various emission lines are also important.

1.3.4. Other Factors Affecting Photopolymerization Process

Besides photoinitiator and monomer efficiencies and light intensity of the light source, there are some other factors influencing polymerization rate and/or final degree of conversion of photopolymerization, such as:

a) Polymerization temperature
b) Glass transition temperature (T_g) of the forming network
c) Oxygen inhibition

Higher polymerization temperatures will lead to higher rate of polymerization; this is the so called Arrhenius behavior. However, for hydrogen bonding monomers one can expect lower rate of polymerization at higher temperatures where extent of hydrogen bonding is reduced [71,74]. Moreover, the glass transition temperature (T_g) of the fully cured polymer has a strong influence on the final conversion at room temperature. The T_g of UV-cured dimethacrylate polymers increase steadily with monomer conversion as well as with irradiation temperature [74]. Also, atmospheric oxygen diffuses into the polymerizing system and scavenges both the initiating and polymer radicals resulting an inhibitory effect on the photopolymerization [68].

1.3.5. Photopolymerization Kinetics of Monomers

Various analytical methods are used to study the kinetics of photopolymerization. These are differential scanning calorimetry, dilatometry, fluorescence spectroscopy, and RT-FTIR spectroscopy. By these techniques, heat evolved, volume shrinkage, increase in viscosity or disappearance of the reactive groups of the monomers are monitored.

By using differential scanning calorimetry technique, the rate of polymerization, propagation, and termination rate constants can be calculated from heat flow during polymerization according to the following equations (Figure 1.16):

$$R_p = \frac{(Q/s)\ M}{n\ \Delta H_p\ m} \qquad \frac{k_p}{k_t^{1/2}} = \frac{R_p}{[M]\ (\Theta I_0 \varepsilon [A])^{1/2}}$$

(Q/s) : heat flow per second during reaction
M : molar mass of the monomer
n : number of double bonds per monomer molecule
ΔH_p : heat released per mol of double bonds reacted
m : the mass of the monomer in the sample
Θ : the initiator efficiency
[M] : molar concentration of the double bonds
I_0 : incident light intensity
ε : extinction coefficient of the initiator
[*A*] : initiator concentration

Figure 1.16. Equation of the rate of polymerization

At the very beginning of the irradiation autoacceleration occurs because of the rapid increase in viscosity until the reaction reaches its maximum rate value. It is followed by a period where the polymerization develops at a sustained pace during about 0.3 s, the time after which autodeceleration starts taking place when propagation becomes diffusion controlled. Ultimately, vitrification leads to a complete stop of the curing process through the end of the polymerization. A certain amount of unreacted acrylic double bonds remains in the crosslinked polymer, which may ultimately affect the long term properties of the UV-cured material [69] (Figure 1.17).

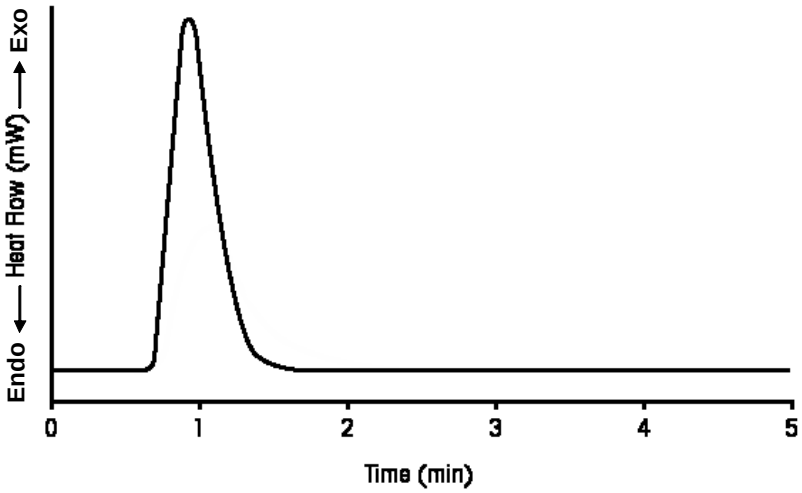

Figure 1.17. Representative heat flow versus time plot obtained from differential scanning calorimetry technique

1.3.6. Other Applications of Photopolymerizing Systems

Photocuring technology has found a variety of industrial applications due to the unique properties, such as high speed, solvent-free formulations, low energy consumption, ambient temperature operations, and tailor-made properties of the photocured polymers.

Besides its wide use in dental restorative filling systems, photopolymerization has also found applications in coating industry, for instance fast-drying varnishes, paints or printing inks, quick-setting adhesives, sealants; and also optical disks, microcircuits, and contact lenses are some of the other areas which photocuring technology is used [68,74,75].

2. OBJECTIVES

The objectives of this study were to develop new dental crosslinking monomers based on alkyl-α-hydroxymethyl acrylates with improved adhesion, volume shrinkage and stability properties, and investigate their photopolymerization behavior. The monomers were synthesized starting from Bisphenol A derivative of tert-butyl-α-bromomethyl acrylate. The carboxylic acid, ester, and amide monomers were prepared and the photopolymerization behaviors of the synthesized monomers with Bisphenol A glycolate dimethacrylate (Bis-GMA), triethyleneglycol dimethacrylate (TEGDMA) and 2-hydroxyethyl methacrylate (HEMA) were investigated using photodifferential scanning calorimeter (Photo-DSC).

3. EXPERIMENTAL

3.1. Materials and Apparatus

3.1.1. Materials

Chemicals used in this study were as follows:
tert-Butyl acrylate, paraformaldehyde, 1.4-diazobicyclo [2.2.2] octane (DABCO), $CaCl_2$, $CuCl_2$, PBr_3, NaCl, Bisphenol A, triethyl amine (TEA), NaOH, (3-aminopropyl)-triethoxy silane (APTES), benzyl amine, 3-acryloyloxy-2-hydroxypropyl methacrylate (AHM), Bisphenol A glycolate dimethacrylate (Bis-GMA), Triethyleneglycol dimethacrylate (TEGDMA), 2-hydroxyethyl methacrylate (HEMA), and 2,2-dimethoxy-2-phenyl acetophenone (Irgacure 651) were all purchased from Aldrich Chemical Co. and used as received. The solvents; ether, hexane, tetrahydrofuran (THF), methylene chloride, trifluoroacetic acid (TFA), methanol, dimethyl sulfoxide (DMSO), hydrochloric acid (HCl), N,N-dimethyl formamide (DMF), acetone, chloroform, ethyl acetate, and thionyl chloride were all purchased from Merck and used as received.

3.1.2. Apparatus

^{1}H-NMR and ^{13}C-NMR spectra were recorded using Varian Gemini 400 MHz spectrometer. IR analyses were performed by FT-IR Perkin Elmer using NaCl windows.

Photopolymerizations and kinetic investigations were carried out by TA Instruments Q 100 differential photocalorimeter containing a high-pressure mercury lamp.

3.2. Synthesis of tert-Butyl-α-Hydroxymethyl Acrylate (TBHMA)

tert-Butyl acrylate (64.05 g, 0.5 mol), paraformaldehyde (15 g, 0.5 mol), 1,4-Diazobicyclo [2.2.2] octane (DABCO) (7 g, 0.0625 mol), dimethyl sulfoxide (113.5 ml) and H_2O (42.5 ml) were added into a 500 ml round-bottom flask which was than fitted with a condenser and placed in a preheated oil bath at 70 ^{o}C. After the solution was heated

at 100 ^{o}C under nitrogen for 30 min, it was cooled and aqueous phase was separated. The organic phase was washed with 1wt% HCl (2x50 ml), dried with anhydrous $CaCl_2$ and filtered. After evaporation of excess tert-butyl acrylate, the solution was distilled under reduced pressure in the presence of a free radical inhibitor, $CuCl_2$, and pure TBHMA as a colorless liquid was collected at 60-65 ^{o}C head temperature in 30-40 per cent (17.2711 g) yield.

^{13}C-NMR ($CDCl_3$): δ= 28.1 (CH_3), 62.4 (CH_2-O), 81.2 [*C*-$(CH_3)_3$], 124.4 (*C*H_2=C), 140.6 (*C*=CH_2), 165.4 (*C*=O) ppm.

^{1}H-NMR ($CDCl_3$): δ= 1.49 (CH_3), 2.68 (O-H), 4.25 (CH_2-O), 5.72 (CH=C), 6.12 (CH=C) ppm.

FT-IR (NaCl): 3420 (OH), 2978-2934 (C-H), 1709 (C=O), 1639 (C=C), 1457-1369 [C-$(CH_3)_3$], 1159-1054 (C-O) cm^{-1}.

3.3. Synthesis of tert-Butyl-α-Bromomethyl Acrylate (TBBr)

TBHMA (27.29 g, 0.1725 mol), and ether (165 ml) were placed in 500 ml round-bottom flask. PBr_3 (8 ml) was added dropwise to the solution in an ice bath. Nitrogen gas was purged to remove HBr gas evolved. After complete addition, the solution was allowed to warm to room temperature and stirred for three hours under nitrogen. Then, 110 ml of water was added slowly to the flask and the aqueous phase was separated and extracted with hexane (3x35 ml). The organic phases were combined and washed with saturated NaCl solution (2x35 ml), dried with anhydrous $CaCl_2$ and filtered. After removal of ether by rotary evaporator, distillation under reduced pressure in the presence of $CuCl_2$ gave TBBr as a colorless liquid at 40-50 ^{o}C head temperature in 66.7 per cent (25.45 g) yield.

^{13}C-NMR ($CDCl_3$): δ= 27.9 (CH_3), 29.7 (CH_2-Br), 81.5 [*C*-$(CH_3)_3$], 127.8 (*C*H_2=C), 138.8 (*C*=CH_2), 164.1 (C=O) ppm.

^{1}H-NMR ($CDCl_3$): δ= 1.47 (CH_3), 4.09 (CH_2-Br), 5.79 (CH=C), 6.16 (CH=C) ppm.

FT-IR (NaCl): 2978-2934 (C-H), 1718 (C=O), 1621 (C=C), 1226-1158 (C-O), 720 (C-Br) cm^{-1}.

3.4. Synthesis and Photopolymerization of Novel Crosslinking Monomers

3.4.1. Synthesis of TBBr-Bisphenol A Diester Monomer

To a mixture of Bisphenol A (3.2 g, 0.01405 mol) and TEA (5.4 g, 0.05339 mol) in THF (15 ml) in an ice bath, TBBr (6.2 g, 0.028 mol) was added dropwise under nitrogen purge. After 24 hours of stirring at 60 ^oC, THF was evaporated. The residue was diluted with 25 ml of methylene chloride and 1-2 ml of 1% NaOH was added on ice. Then, the solution was washed with water (3x12 ml), dried with anhydrous $CaCl_2$ and filtered. After removal of CH_2Cl_2 by rotary evaporator, the pure product with the melting point of 66-67 ^oC, was obtained by precipitation into methanol in 64.3 per cent (4.5847 g) yield as a white solid.

^{13}C-NMR ($CDCl_3$): δ= 28.2 [$(CH_3)_3$-C], 31.1 (*C*H_3-C-Ar), 41.7 [*C*-$(CH_3)_2$], 66.3 (CH_2-O), 81.2 [*C*-$(CH_3)_3$], 124.9 (*C*H_2=C), 143.3 (*C*=CH_2), 164.6 (C=O) and C(Ar) (114.1, 127.6, 137.4, 156.1) ppm.

^{1}H-NMR ($CDCl_3$): δ= 1.42 [$(CH_3)_3$-C], 1.54 (CH_3-C-Ar), 4.59 (CH_2-O), 5.80 (CH=C), 6.17 (CH=C), C-H(Ar) (6.73, 7.01) ppm.

FT-IR (NaCl): 2972-2862 (C-H), 1712 (C=O), 1636 (C=C), 1150 (C-O) cm^{-1}.

3.4.2. Synthesis of TBBr-Bisphenol A Diacid Derivative

To a TBBr-Bisphenol A diester monomer (2.0 g, 0.004 mol), trifluoroacetic acid (TFA) (0.5 ml) was added dropwise in an ice bath under nitrogen purge. The solution was stirred at room temperature for 24 hours. The excess acid was removed under vacuum and the remaining solid was purified by recrystallization from methanol to give a white solid product with the melting point of 192 ^oC, in 56.7 per cent (2.26 g) yield.

^{13}C-NMR (CD_3OD): δ= 31.6 (*C*H_3-C-Ar), 42.8 [*C*-$(CH_3)_2$], 67.4 (*C*H_2-O), 126.6 (*C*H_2=C), 144.7 (*C*=CH_2), 168.5 (C=O) and C(Ar) (115.1, 128.7, 138.2, 157.5) ppm.

^{1}H-NMR (CD_3OD): δ= 1.62 (CH_3-C-Ar), 4.70 (CH_2-O), 5.95 (CH=C), 6.33 (CH=C), and C-H(Ar) 6.83, 7.13 ppm.

FT-IR (NaCl): 3050-2510 (OH), 1682 (C=O), 1633 (C=C), 1171 (C-O) cm^{-1}.

3.4.3. Synthesis of TBBr-Bisphenol A Diacid Chloride Intermediate

To a mixture of TBBr-Bisphenol A diester monomer (2.3 g, 0.0045 mol) and two drops of N,N-dimethyl formamide (DMF), thionyl chloride (6 ml) was added dropwise in an ice bath under nitrogen purge. After the complete addition, the solution was stirred at 40-45 ^oC for 48 hours under nitrogen. The excess $SOCl_2$ was removed by direct nitrogen bubbling into the solution.

3.4.4. Synthesis of TBBr-Bisphenol A – APTES Diamide Derivative

(3-aminopropyl)-triethoxy silane (APTES) (0.9846 g, 0.0044 mol) and triethyl amine (TEA) (0.4857 g, 0.0048 mol) are mixed in 12.5 ml of methylene chloride in 25 ml round-bottom flask. Then, TBBr-Bisphenol A diacid chloride intermediate (0.9171 g, 0.0021 mol) was added dropwise into the solution in an ice bath under nitrogen purge. After being stirred at room temperature for overnight under nitrogen, the solution was washed with cold water (2x8 ml) gently. The organic phase was dried with anhydrous $CaCl_2$ and filtered. After removal of CH_2Cl_2 by rotary evaporator, remaining crude product was precipitated into hexane to get the pure product with the melting point of 101 ^oC as white solid in 80.3 per cent (1.3655 g) yield.

^{13}C-NMR ($CDCl_3$): δ= 7.9 (CH_2-Si), 18.4 (*C*H_3-CH_2-O), 23.0 (*C*H_2-CH_2-Si), 31.1 (*C*H_3-C), 41.8 [*C*-$(CH_3)_2$], 41.9 (CH_2-NH), 58.5 (CH_2-O-Si), 67.9 (CH_2-O-Ar), 122.2 (*C*H_2=C), 143.7 (*C*=CH_2), 166.1 (C=O) and C(Ar) (114.2, 127.7, 139.5, 155.6) ppm.

^{1}H-NMR ($CDCl_3$): δ= 0.67 (CH_2-Si), 1.22 (*CH_3*-CH_2-O), 1.64 (CH_3-C), 1.68 (*CH_2*-CH_2-Si), 3.35 (*CH_2*-NH), 3.80 (CH_2-O-Si), 4.74 (CH_2-O), 5.67 (CH=C), 6.02 (CH=C), C-H(Ar) (6.82, 7.14), 7.25 (N-H) ppm.

FT-IR (NaCl): 3317 (NH), 2972-2886 (C-H), 1660 (C=O), 1613 (C=C), 1180 (C-O) cm^{-1}.

3.4.5. Synthesis of TBBr-Bisphenol A – Benzylamide Derivative

To a mixture of benzyl amine (0.689 g, 0.0064 mol) and 15 ml of triethyl amine (TEA) (0.651 g, 0.0064 mol) in 15 ml of methylene chloride, TBBr-Bisphenol A diacid chloride intermediate (1.2664 g, 0.0029 mol) was added dropwise in an ice bath under nitrogen purge. The solution was stirred at room temperature for overnight under nitrogen. Then, the solution was washed with 1N HCl (3x10 ml). The organic phase was dried with anhydrous $CaCl_2$ and filtered. After removal of CH_2Cl_2 by rotary evaporator, the pure product with the melting point of 105 ^{o}C, was obtained by recrystallization from methanol as white solid in 62.7 per cent (1.0541 g) yield.

^{13}C-NMR ($CDCl_3$): δ= 31.1 (*C*H_3-C), 41.9 [*C*-$(CH_3)_2$], 43.7 (CH_2-NH), 68.1 (CH_2-O), 123.1 (*C*H_2=C), 143.8 (*C*=CH_2), 166.0 (C=O) and C(Bis. ring) (114.3, 128.6, 137.8, 155.5), C(Benzyl. ring) (127.4, 127.5, 127.7, 139.1) ppm.

^{1}H-NMR ($CDCl_3$): δ= 1.54 (CH_3-C), 4.44 (*CH_2*-NH), 4.68 (CH_2-O), 5.61 (CH=C), 6.01 (CH=C), 6.58 (N-H), C-H(Bis. ring) (6.70, 7.00), C-H(Benzyl. ring) (7.16, 7.20, 7.22) ppm.

FT-IR (NaCl): 3308 (NH), 2966-2868 (C-H), 1660 (C=O), 1616 (C=C), 1180 (C-O) cm^{-1}.

3.4.6. Synthesis of AHM-APTES Monomer

3-acryloyloxy-2-hydroxypropyl methacrylate (AHM) (1.0742 g, 0.005 mol) and (3-aminopropyl)-triethoxy silane (APTES) (0.555 g, 0.0025 mol) were added into 10 ml round-bottom flask. The solution was stirred at room temperature for 24 hours under open atmosphere. Then, the product was obtained as a colorless liquid.

^{13}C-NMR ($CDCl_3$): δ= 7.9 (CH_2-Si), 18.3 (*C*H_3-CH_2-O, CH_3), 19.4 (*C*H_2-CH_2-Si), 32.7 (*C*H_2-CO), 49.2 (CH_2-N), 56.4 (CH_2-N), 58.3 (O-*C*H_2-CH_3), 65.2 (CH_2-O), 65.3 (CH-OH), 67.7 (CH_2-O), 126.0 (*C*H_2=C), 135.6 (*C*=CH_2), 166.9 (C=O), 172.2 (C=O) ppm.

^{1}H-NMR ($CDCl_3$): δ= 0.56 (CH_2-Si), 1.22 (*CH*$_3$-CH_2-O), 1.52 (*CH*$_2$-CH_2-Si), 1.95 (CH_3), 2.46 (CH_2-CO), 2.50 (CH_2-N), 2.78 (CH_2-N), 3.80 (O-*CH*$_2$-CH_3), 4.13 (O-H), 4.21 (CH_2-O), 4.22 (CH_2-O), 4.30 (*CH*-OH), 5.59 (CH=C), 6.13 (CH=C) ppm.

FT-IR (NaCl): 3450 (OH), 2974-2888 (C-H), 1732, 1719 (C=O), 1637 (C=C), 1170 (C-O) cm^{-1}.

3.5. Photopolymerizations

3.5.1. Sample Preparation

All the synthesized crosslinking monomers were mixed with two different commercially used dental systems (Bis-GMA/TEGDMA and Bis-GMA/HEMA) with the mol ratio of 50:45:5 (Bis-GMA:TEGDMA:Monomer or Bis-GMA:HEMA:Monomer). In this way two sets of polymerizing systems were obtained. Because of the miscibility problems of TBBr-Bisphenol A diacid and TBBr-Bisphenol A – benzylamide derivatives, samples of these two with the mole ratio of 50:49.5:0.5 were also prepared. Also, the homopolymerization of the AHM-APTES monomer, the only liquid monomer of all at RT was carried out.

Finally, 50:50 Bis-GMA:TEGDMA and Bis-GMA:HEMA mixtures were prepared to make a comparison between synthesized structures and the commercial systems.

3.5.2. Polymerization Procedure

All the photopolymerizations were carried out by TA Instruments Q 100 Photo-DSC using 2,2-dimethoxy-2-phenyl acetophenone (Irgacure 651) as the photoinitiator.

The initiator (5.5 mg for TEGDMA containing samples, 6.5 mg for HEMA containing ones) was first dissolved in methylene chloride (1 ml). Approximately 4.0 mg of sample (approximately 250 nm thickness) was carefully weighed in an aluminum DSC pan. Then, the initiator solution was added with a microsyringe to give a final concentration in the monomer of 2 mol% after evaporation of the solvent. After placing the sample and reference pans to sample compartment, the DSC chamber was purged with nitrogen for 10 min to remove air and allow for complete evaporation of solvent prior to the polymerization. The samples were irradiated for 10 min at either 40 ^{o}C or 60 ^{o}C under nitrogen purge.

Monochromatic 365 nm ultraviolet light with 15 mW/cm^2 light intensity was used for all photopolymerizations. The heat flux as a function of reaction time was monitored using DSC under isothermal conditions and both the rate of polymerizations and conversions were calculated as a function of time. The heat of reaction value, ΔH_p= 13.1 kcal/mol was used as the theoretical heat evolved for methacrylate double bonds [76]. Polymerization rates were calculated according to the following formula:

$$\mathbf{R_p = \frac{(Q/s)\,M}{n\,\Delta H_p\,m}}$$

Figure 3.1. Equation of the rate of polymerization

Where **Q/s** is heat flow per second, **M** is molar mass of the monomer, **n** is the number of double bonds per monomer molecule, and **m** is the mass of the monomer in the sample.

All the photopolymerizations in this study were carried out by the same procedure as mentioned above.

4. RESULTS AND DISCUSSION

4.1. Synthesis and Photopolymerization of Novel Crosslinking Monomers

New carboxylic acid, ester, and amide containing crosslinking monomers were synthesized starting from the Bisphenol A derivative of tert-butyl-α-hydroxymethyl acrylate (TBHMA) (Figure 4.1).

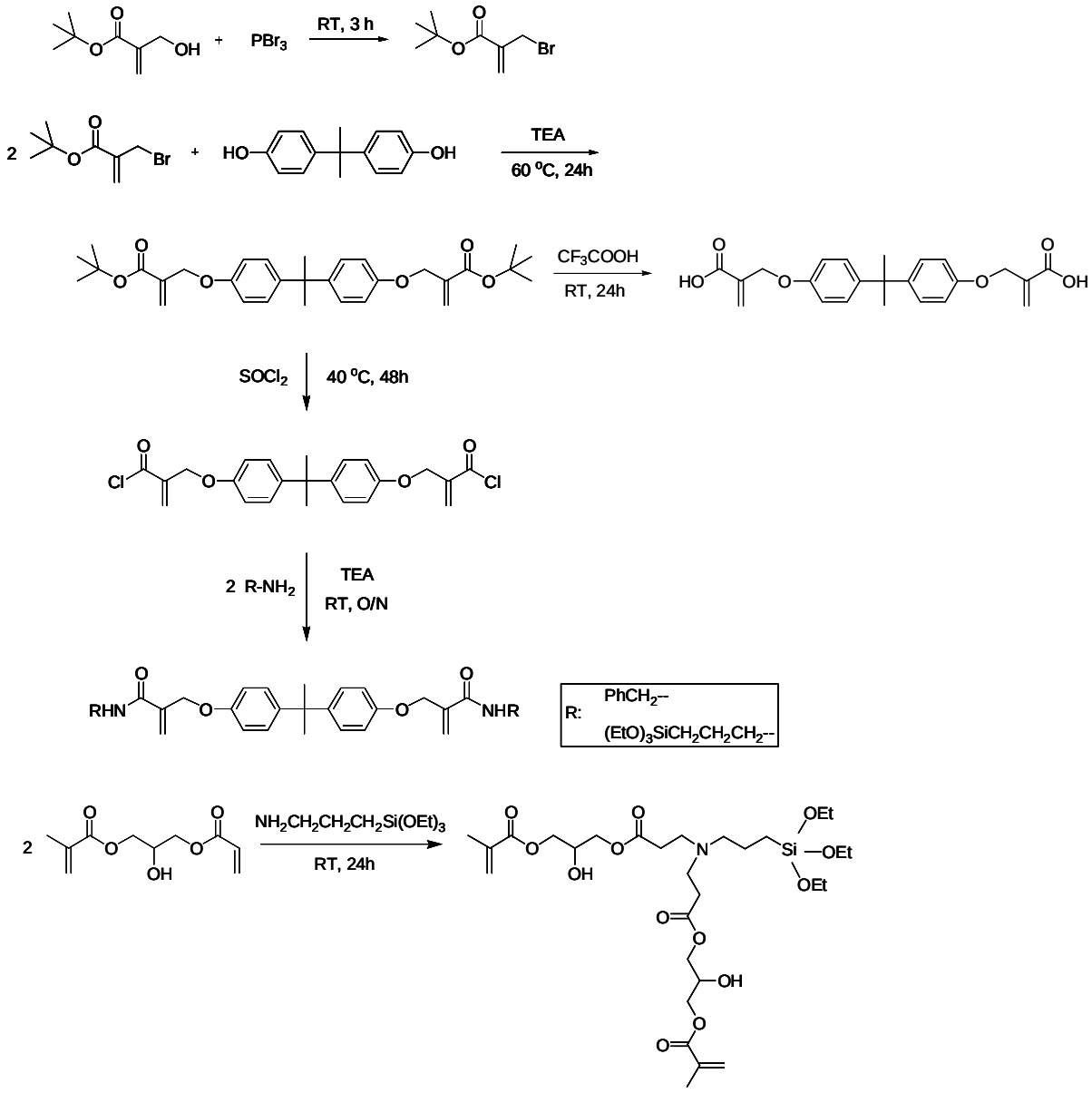

Figure 4.1. General synthetic scheme of new crosslinking monomers

The tert-butyl ester groups are well known for acid-catalyzed elimination yielding the carboxylic acid and isobutylene. We utilized this reaction to obtain the monomer with diacid functionality.

Two new amide derivatives were synthesized from the reactions of Bisphenol A derivative of TBHMA with either (3-aminopropyl)-triethoxy silane (APTES) or benzyl amine.

Another amide-linked monomer was obtained from the Michael addition of APTES to 3-acryloyloxy-2-hydroxypropyl methacrylate (AHM).

The reactivity of synthesized monomers was investigated using photodifferential scanning calorimeter (Photo-DSC). After mixing the commercial benchmarks such as Bis-GMA, TEGDMA, and HEMA, the polymerization rates and conversions were determined for each of the monomers. The effect of monomer structure on reactivity was examined.

The acid and silane containing monomers may have a potential for adhesion to dentin and enamel, whereas the amide-linked and bulky end groups containing ones are expected to improve hydrolytic and thermal stability, and other mechanical properties of the material.

4.1.1. Synthesis of tert-Butyl-α-Hydroxymethyl Acrylate (TBHMA)

TBHMA was synthesized from the Baylis-Hillman reaction between tert-butyl acrylate and paraformaldehyde in the presence of 1.4-diazobicyclo [2.2.2] octane (DABCO) as catalyst (Figure 4.2) using literature procedures [77,78]. Continued reaction

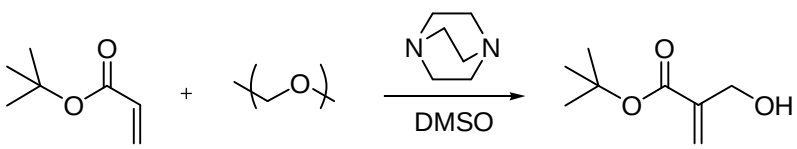

Figure 4.2. Synthesis of TBHMA

leads to the conversion to the ether dimer of this material (TBEED) (Figure 4.3). Conversion of TBHMA to the ether dimer is thermodynamically favorable and merely requires continued heating of the reaction mixture.

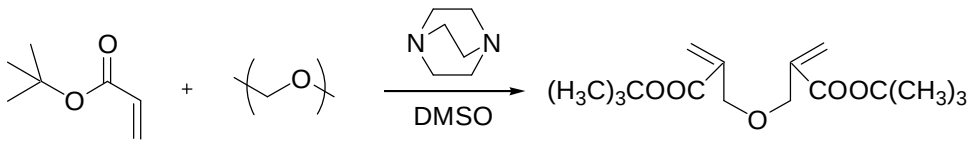

Figure 4.3. Synthesis of TBEED

The ^{13}C-NMR spectrum of TBHMA (Figure 4.4) was characterized by methylene carbon attached to hydroxyl at 62.4 ppm, tert-butyl carbons at 28.1 and 81.2 ppm, double bond carbons at 124.4 and 140.6 ppm, and carbonyl carbon peak at 165.4 ppm.

The ^{1}H-NMR spectrum of TBHMA (Figure 4.5) showed tert-butyl protons at 1.49 ppm, methylene protons at 4.25 ppm, hydroxyl proton at 2.68 ppm, and double bond protons at 5.72 and 6.12 ppm.

The FT-IR spectrum showed a characteristic hydroxyl absorption peak at 3420 cm^{-1}, C-H vibrations at 2978-2934 cm^{-1}, ester carbonyl absorption at 1709 cm^{-1}, and C=C absorption at 1639 cm^{-1}.

The advantages offered by this material are giving polymers with high glass transition temperatures (T_g) and capability of functionalization before or after polymer formation, through either the alcohol or ester group.

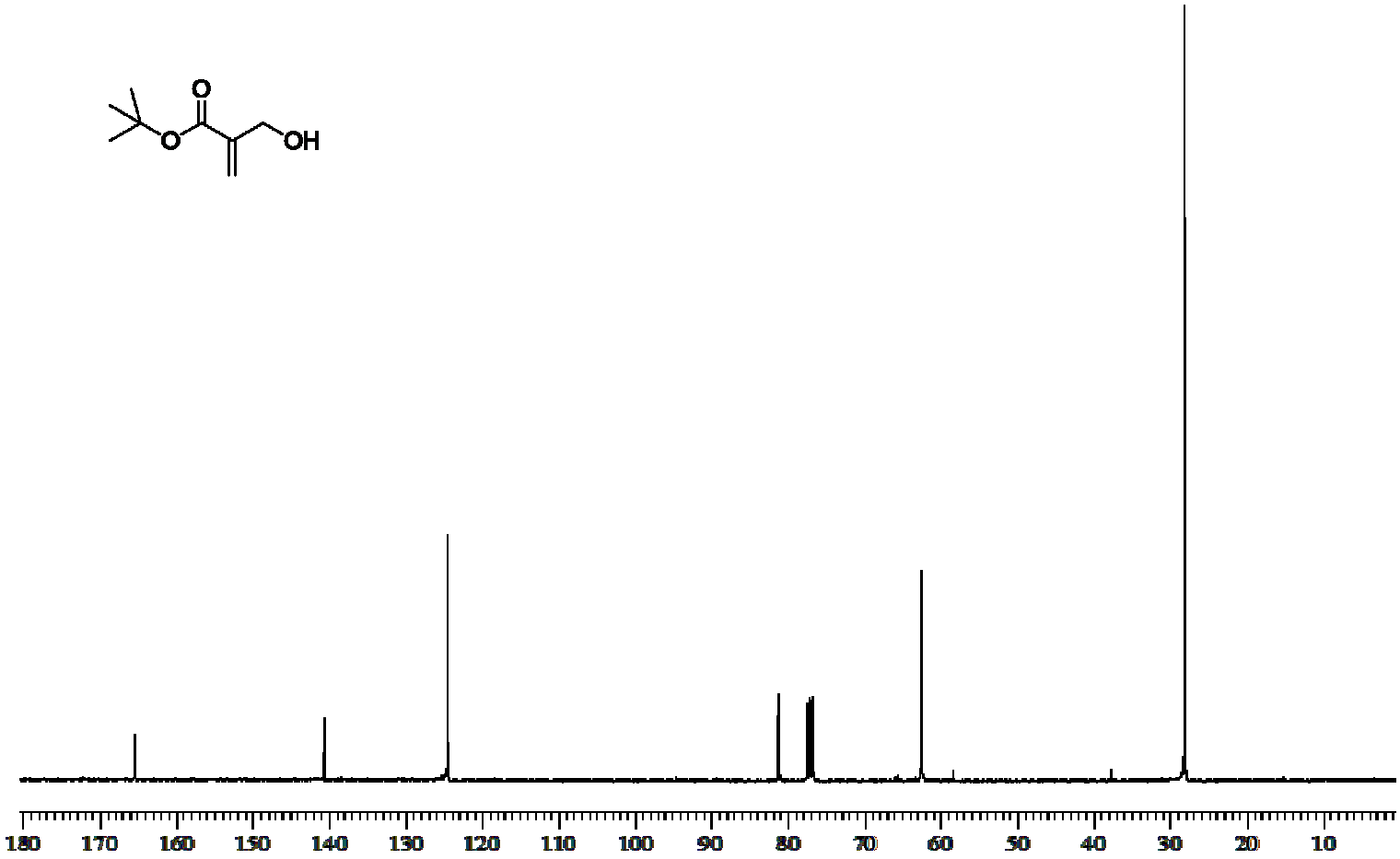

Figure 4.4. ^{13}C-NMR spectrum of TBHMA

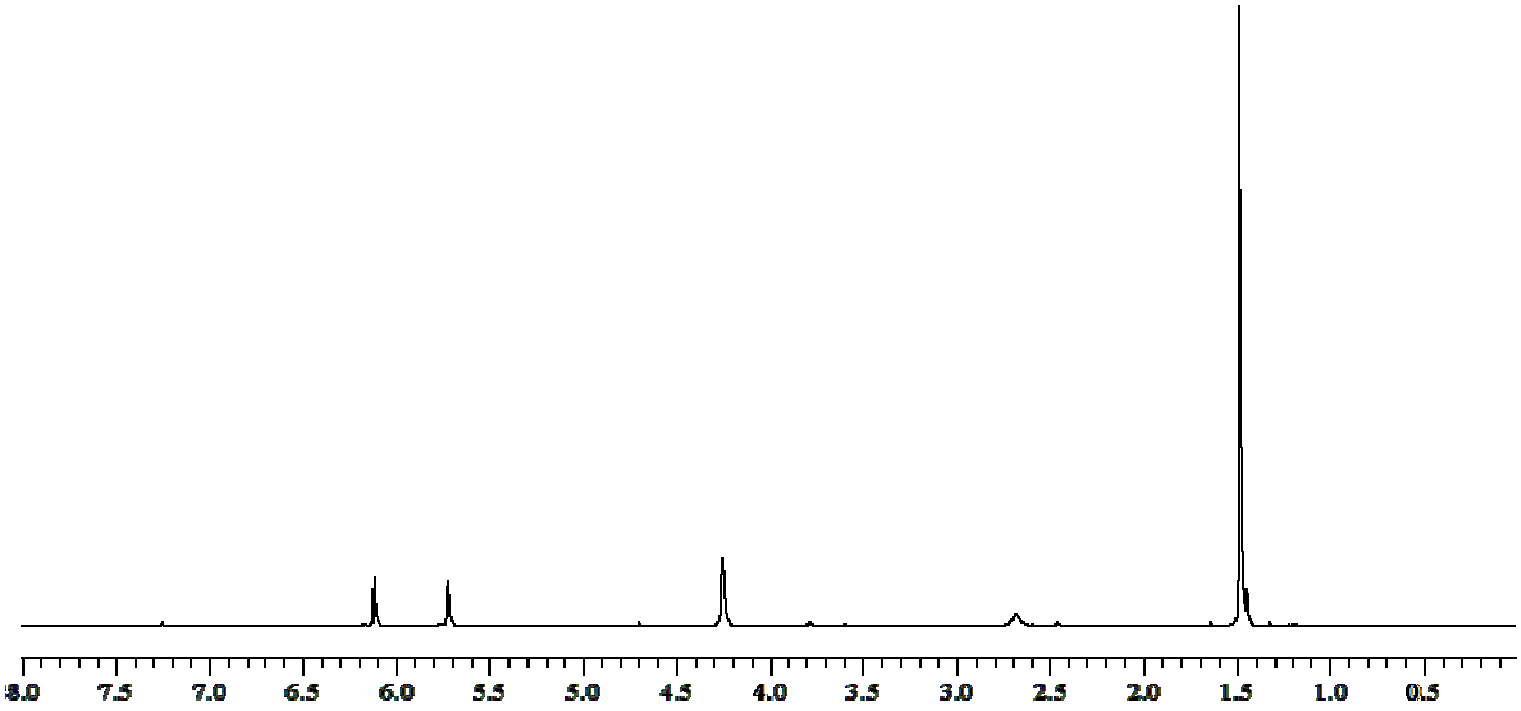

Figure 4.5. ^{1}H-NMR spectrum of TBHMA

4.1.2. Synthesis of tert-Butyl-α-Bromomethyl Acrylate (TBBr)

Reaction of TBHMA with excess PBr_3 in ether gave TBBr as a colorless liquid after 3 hours of mixing at room temperature (Figure 4.6). The reaction should be carried under nitrogen purge to remove HBr gas evolved during the reaction. Otherwise, HBr evolution may lead to the formation of side-products or may inhibit the expected product formation.

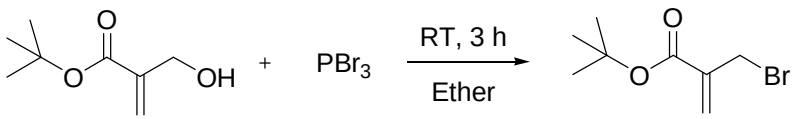

Figure 4.6. Synthesis of TBBr

The ^{13}C-NMR spectrum of TBBr (Figure 4.7) showed the disappearance of the peak of the methylene attached to hydroxyl at 62.4 ppm and appearance of new peak at 29.7 ppm corresponding methylene carbon attached to Br.

The ^{1}H-NMR spectrum (Figure 4.8) showed complete disappearance of hydroxyl proton peak at 2.68 ppm. Also, in the IR spectrum, hydroxyl absorption peak at 3420 cm^{-1} was not observed.

TBBr is the precursor for the synthesis of Bisphenol A derivative of TBHMA.

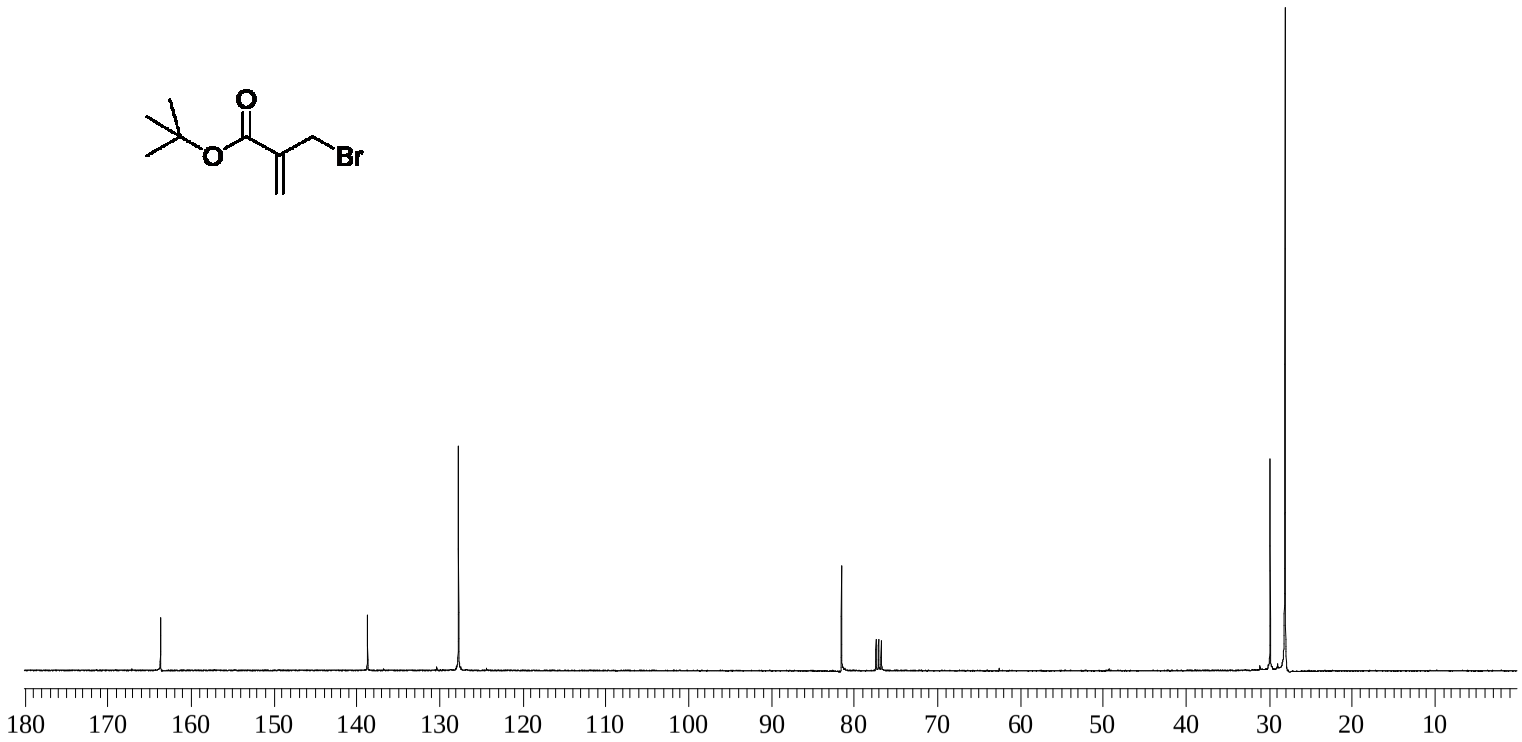

Figure 4.7. ^{13}C-NMR spectrum of TBBr

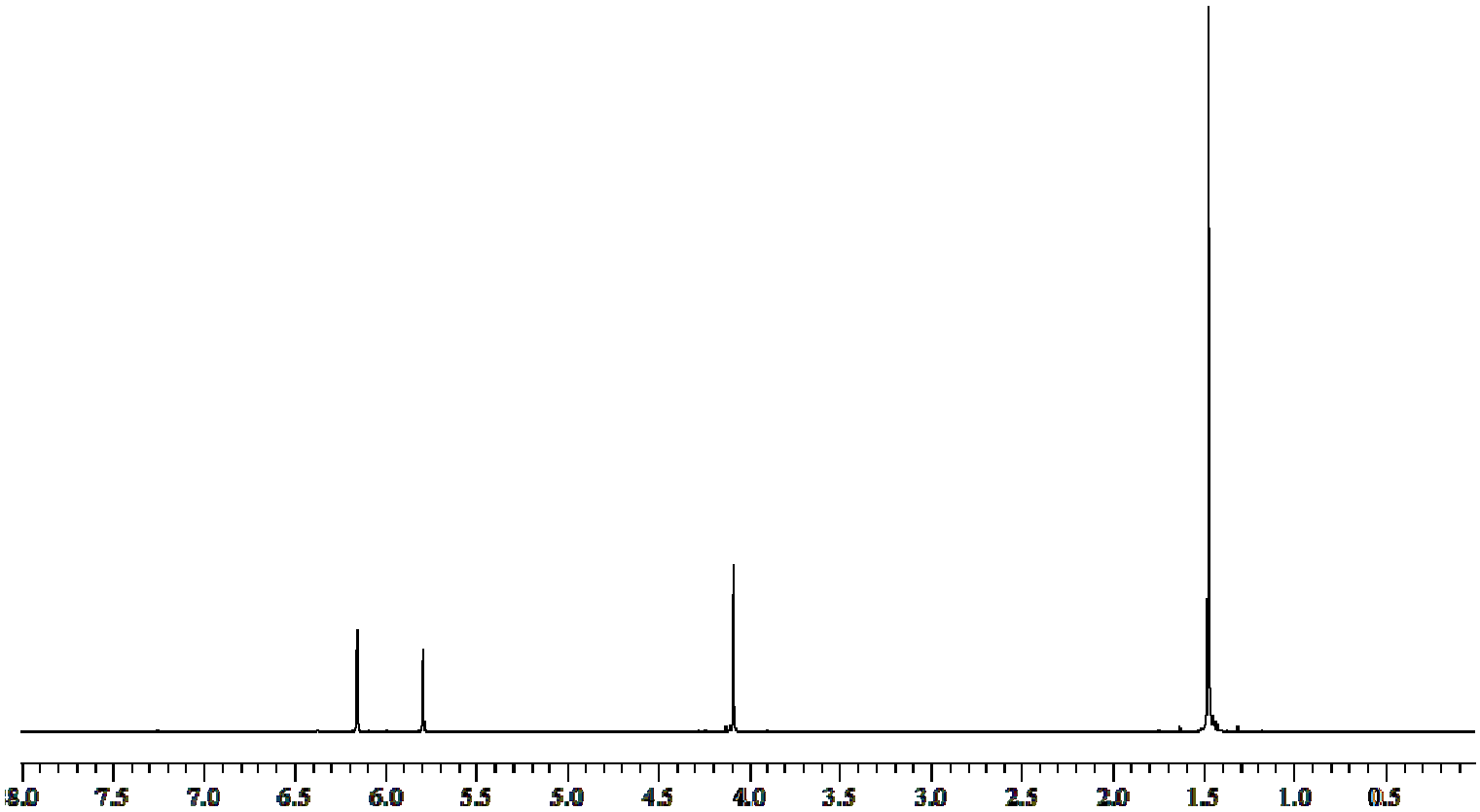

Figure 4.8. ^{1}H-NMR spectrum of TBBr

4.1.3. Synthesis of TBBr-Bisphenol A Diester Monomer

This first proposed monomer was synthesized from the reaction between TBBr and Bisphenol A in THF with TEA as catalyst (Figure 4.9). The second role of TEA is to trap HBr gas evolved during the reaction. The pure product was obtained in 64.3 per cent yield as a white solid with the melting point of 66-67 ^{o}C.

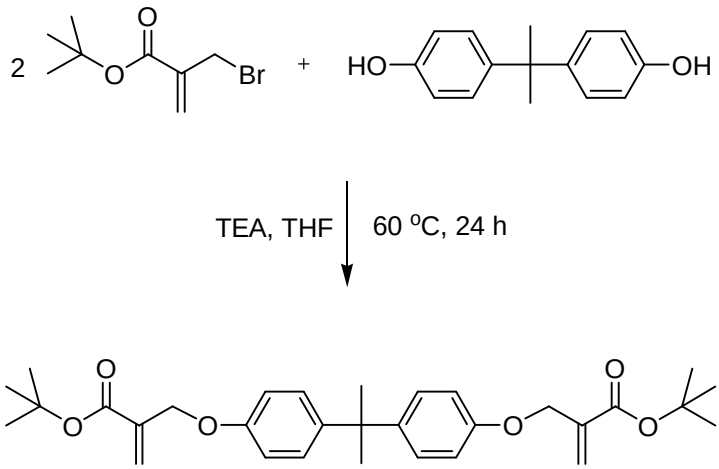

Figure 4.9. Synthesis of TBBr-Bisphenol A diester monomer

TBBr-Bisphenol A diester monomer was soluble in THF, ether, and acetone, whereas insoluble in water, hexane, and methanol.

In the ^{13}C-NMR spectrum (Figure 4.10), characteristic peaks corresponded to t-butoxy group at 28.2 (CH_3) and 81.2 (C-tert) ppm, carbons in the middle of bisphenol at 31.1 (CH_3) and 41.7 (C-tert) ppm, methylene carbon attached to oxygen at 66.3 ppm, double bond carbons at 124.9 and 143.3 ppm, carbonyl peak at 164.6 ppm, and the carbons in bisphenol rings at 114.1, 127.6, 137.4, 156.1 ppm.

The ^{1}H-NMR spectrum (Figure 4.11) showed methyl protons of t-butoxy at 1.42 and of bisphenol at 1.54 ppm, methylene protons at 4.59 ppm, double bond protons at 5.80 and 6.17 ppm, and ring protons at 6.73, 7.01 ppm.

The FT-IR spectrum of the product (Figure 4.12) showed C-H vibrations between 2972-2862 cm^{-1}, ester carbonyl at 1712 cm^{-1}, C=C stretching peak at 1636 cm^{-1}, and C-O vibrations at 1150 cm^{-1}.

The advantageous property of this monomer is capability of improving thermal and mechanical properties of the ultimate material, due to the bulky tert-butyl end groups contained and the rigidity of the monomer itself.

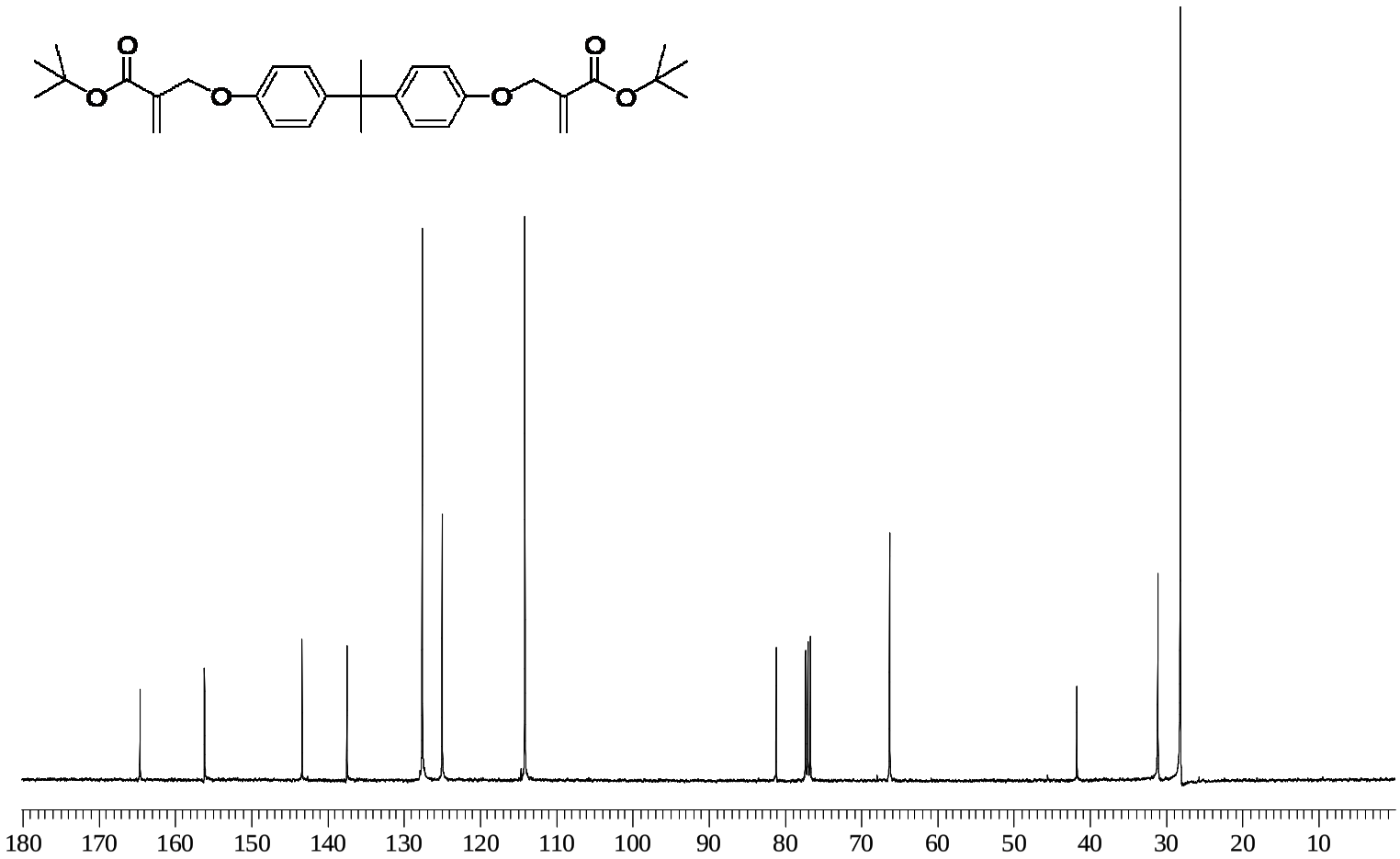

Figure 4.10. ^{13}C-NMR spectrum of TBBr-Bisphenol A diester monomer

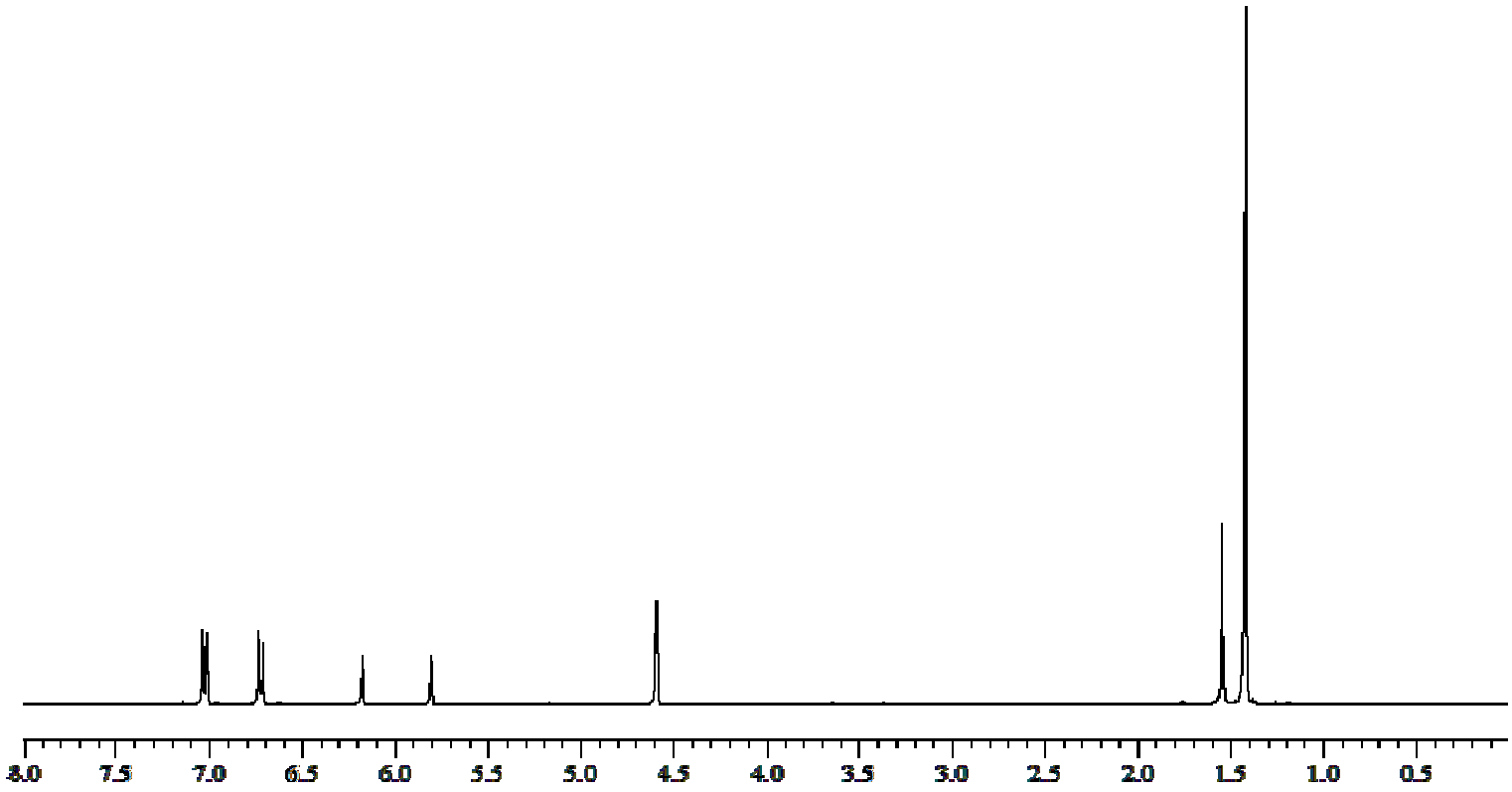

Figure 4.11. ^{1}H-NMR spectrum of TBBr-Bisphenol A diester monomer

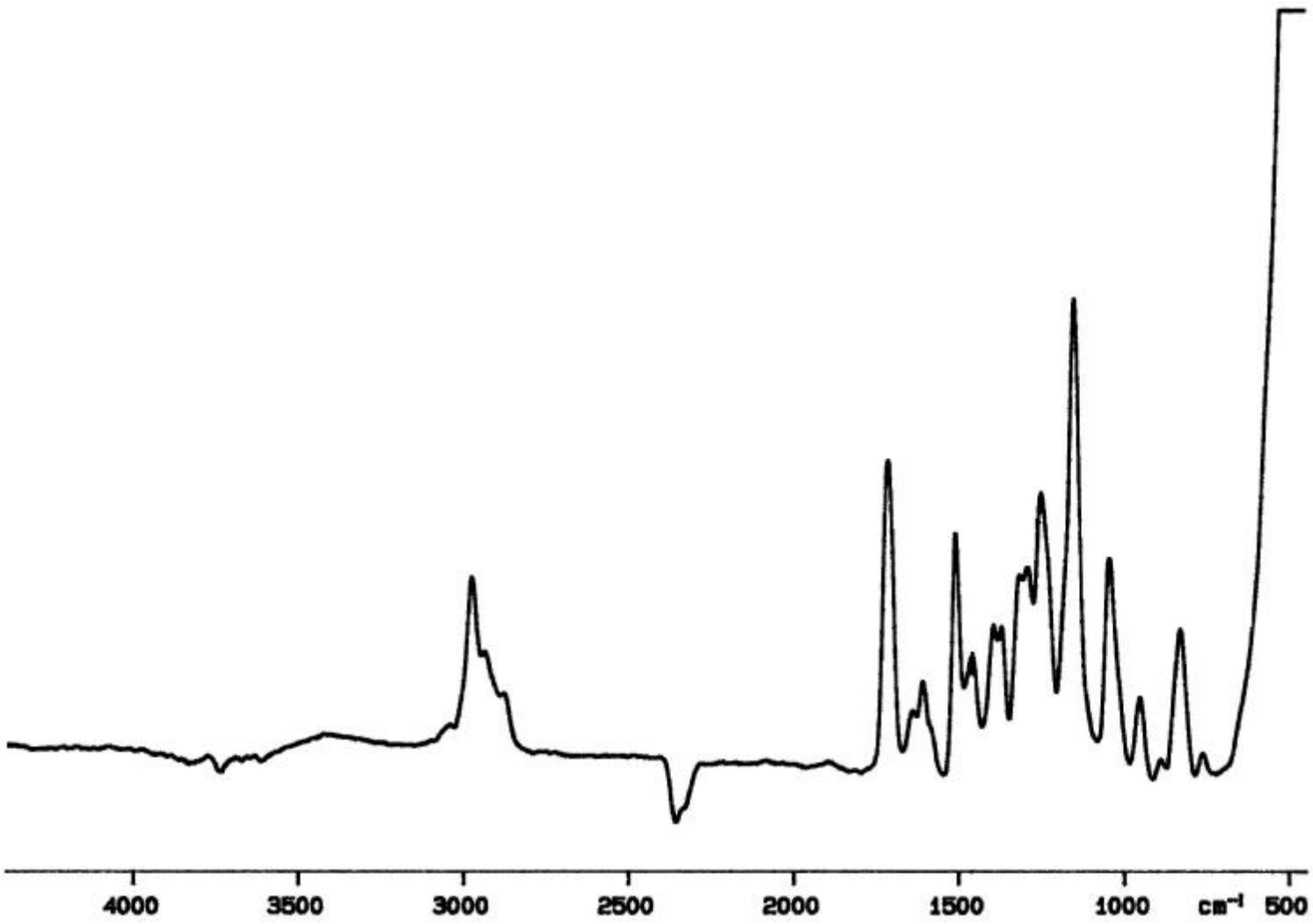

Figure 4.12. FT-IR spectrum of TBBr-Bisphenol A diester monomer

4.1.4. Synthesis of TBBr-Bisphenol A Diacid Derivative

Synthesized TBBr-Bisphenol A diester monomer was hydrolyzed with CF_3COOH (Figure 4.13). After recrystallization from methanol, the diacid monomer was obtained in 56.7 per cent yield as a white solid with the melting point of 192 ^oC.

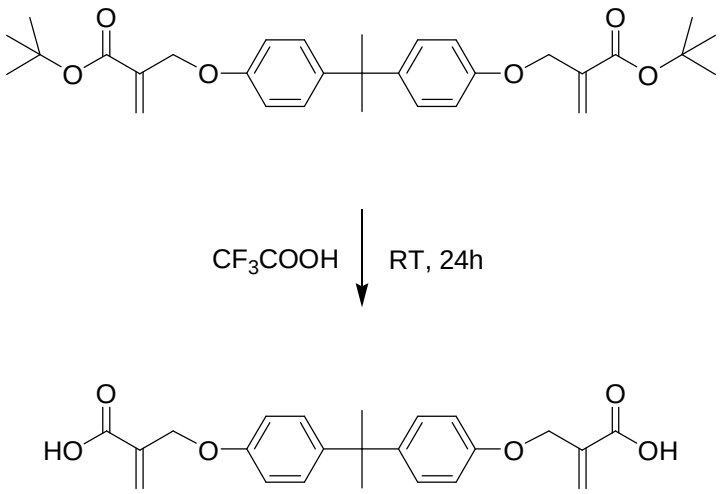

Figure 4.13. Synthesis of TBBr-Bisphenol A diacid derivative

TBBr-Bisphenol A diacid derivative was soluble in methanol and DMSO, but insoluble in water, chloroform, methylene chloride, and hexane. It was also partially soluble in ether.

In the ^{13}C-NMR spectrum (Figure 4.14), the peaks corresponding to t-butyl groups disappeared at 28.2 and 81.2 ppm. Two methyls of bisphenol group shifted to 42.8 ppm. The carbons of ether groups appeared at 67.4 and ring carbons at 115.1, 128.7, 138.2, and 157.5 ppm. Carbonyl and double bond carbons shifted to 168.5, 126.6, and 144.7 ppm.

The ^1H-NMR spectrum (Figure 4.15) showed two methyl protons at 1.62 ppm, ether methylenes at 4.70 ppm, double bond protons at 5.95 and 6.33 ppm and aromatic protons at 6.83 and 7.13 ppm.

The FT-IR spectrum of the product (Figure 4.16) showed the ester carbonyl peak at 1682 cm^{-1}, C=C stretching at 1633 cm^{-1}, and C-O vibrations at 1171 cm^{-1}. The broad absorption

peak between 3050 and 2510 cm^{-1} was due to the OH stretching which confirmed the formation of the product.

This monomer is able to react with other methacrylate monomers by radical polymerization and also by glass-ionomer reaction with the ions leached from the glass used in dental materials. It may also provide bonding to tooth tissue by complexation of Ca^{2+} ions on the tooth surface.

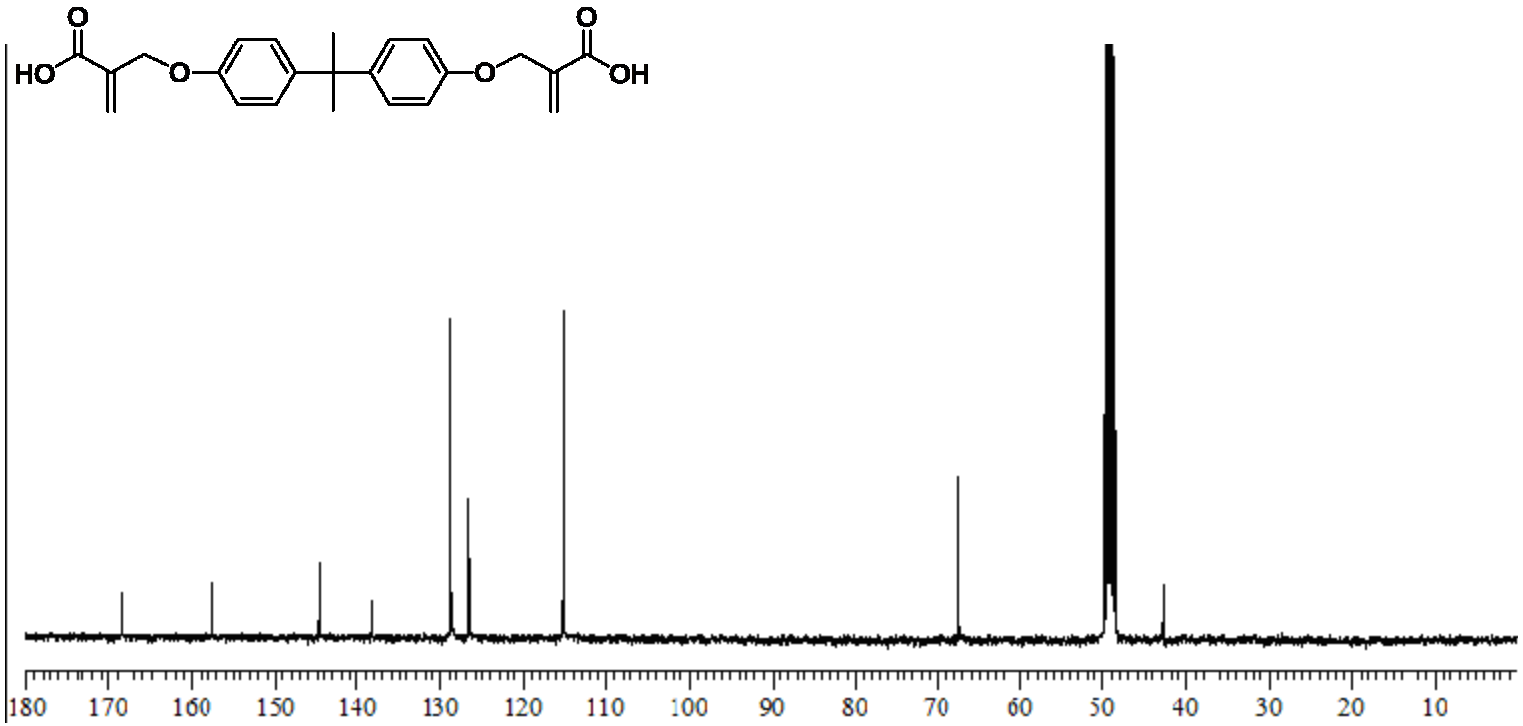

Figure 4.14. ^{13}C-NMR spectrum of TBBr-Bisphenol A diacid derivative

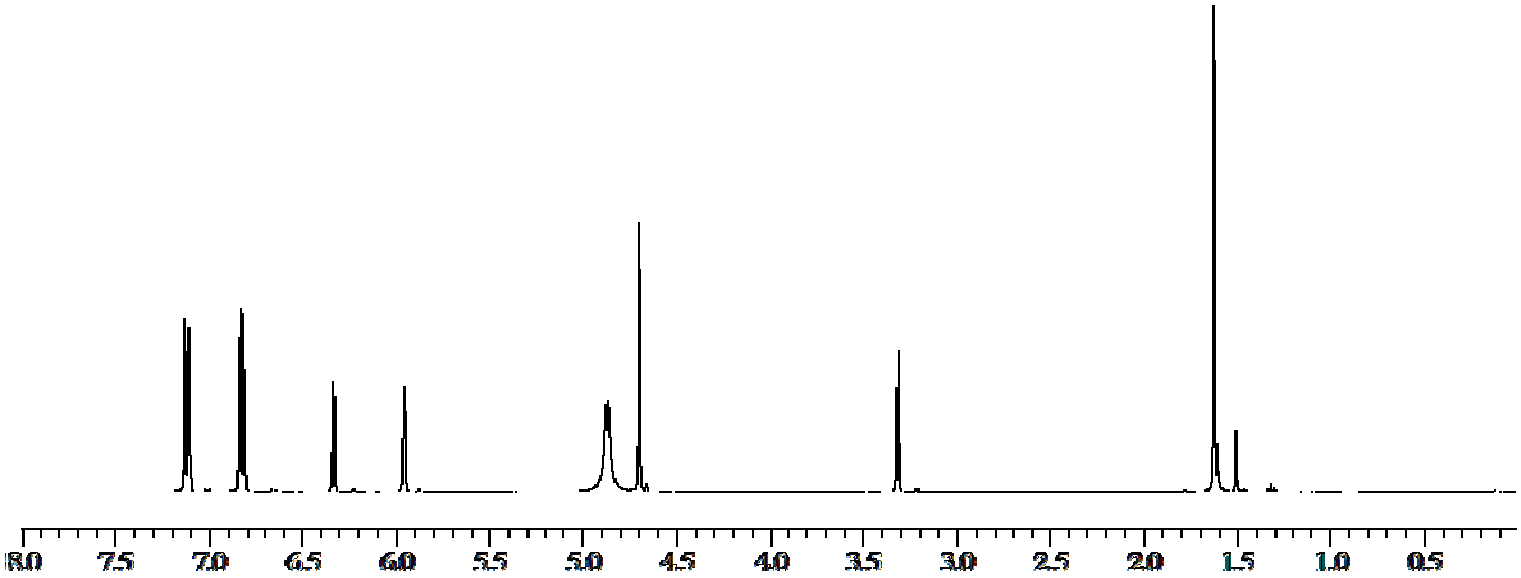

Figure 4.15. ^{1}H-NMR spectrum of TBBr-Bisphenol A diacid derivative

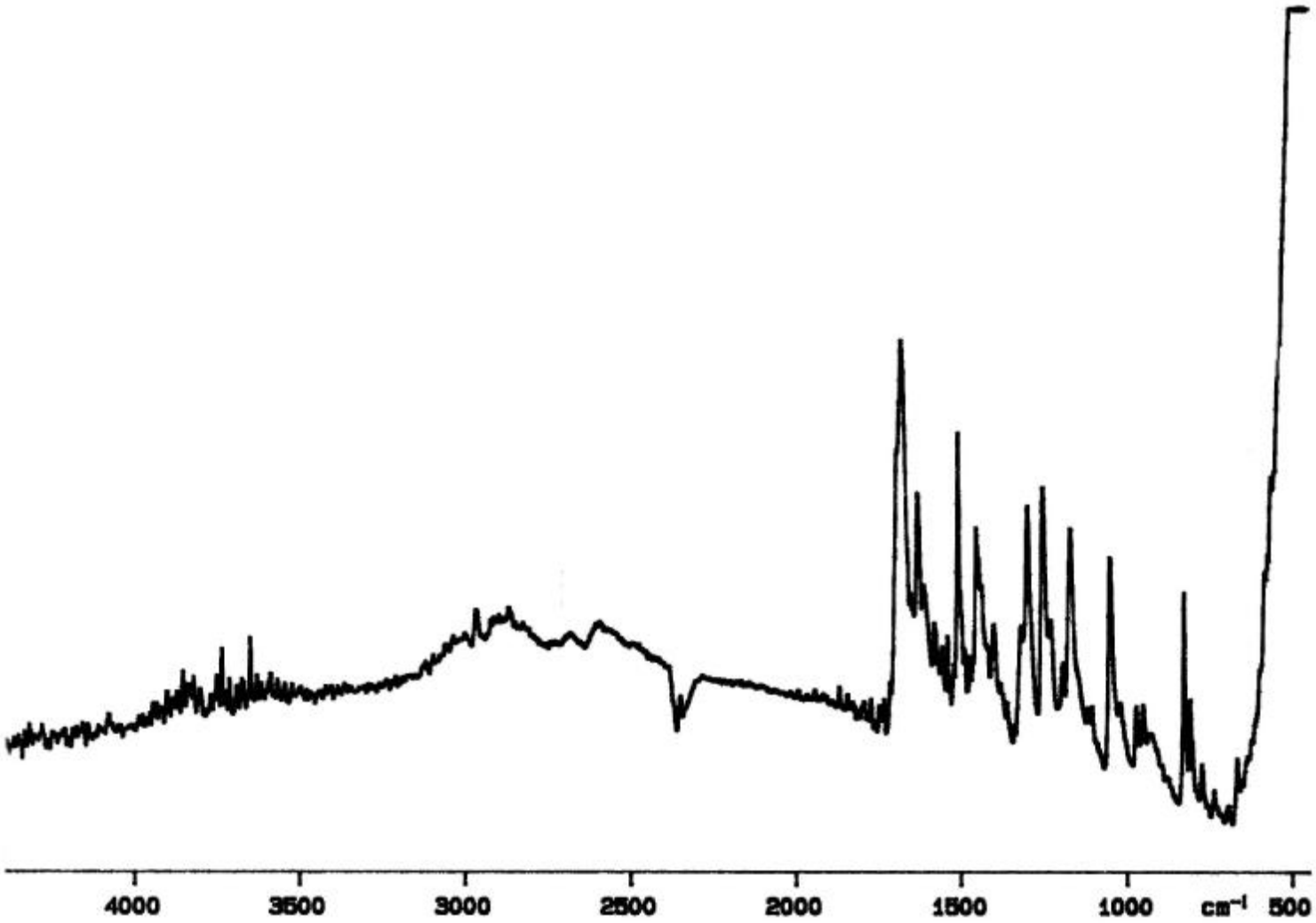

Figure 4.16. FT-IR spectrum of TBBr-Bisphenol A diacid derivative

4.1.5. Synthesis of TBBr-Bisphenol A Diacid Chloride Intermediate

Addition of excess thionyl chloride into the TBBr-Bisphenol A monomer with the catalysis of DMF, gave TBBr-Bisphenol A diacid chloride intermediate after mixing for 48 hours at 40-45 ^{o}C (Figure 4.17). The excess $SOCl_2$ was removed by direct nitrogen bubbling into the solution.

Continued reaction may lead to formation of side-products due to the HCl attacks resulting from the HCl gas evolved during the reaction.

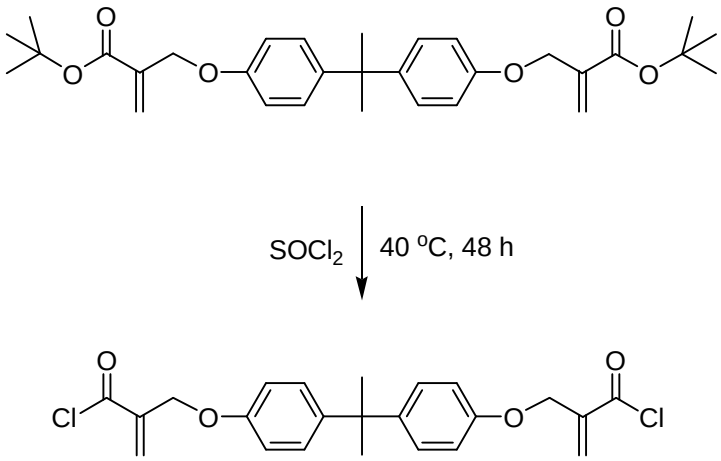

Figure 4.17. Synthesis of TBBr-Bisphenol A diacid chloride intermediate

The reaction was monitored using ^{13}C-NMR by observing disappearance of t-butyl carbon peaks at 28.2 and 81.2 ppm.

TBBr-Bisphenol A diacid chloride intermediate is the precursor for the syntheses of the further proposed crosslinking monomers.

4.1.6. Synthesis of TBBr-Bisphenol A – APTES Diamide Derivative

This amide-containing crosslinking monomer was obtained from the reaction between TBBr-Bisphenol A diacid chloride intermediate and (3-aminopropyl)-triethoxy

silane (APTES) in methylene chloride with TEA as catalyst (Figure 4.18). It is very important to be careful while washing the crude reaction mixture with water, due to the possible polymerization through the ethoxy silane end groups. It is suggested to use cold water and be very gentle for washing procedure. After precipitation into hexane, the pure white solid with the melting point of 101 ^{o}C was obtained in 80.3 per cent yield.

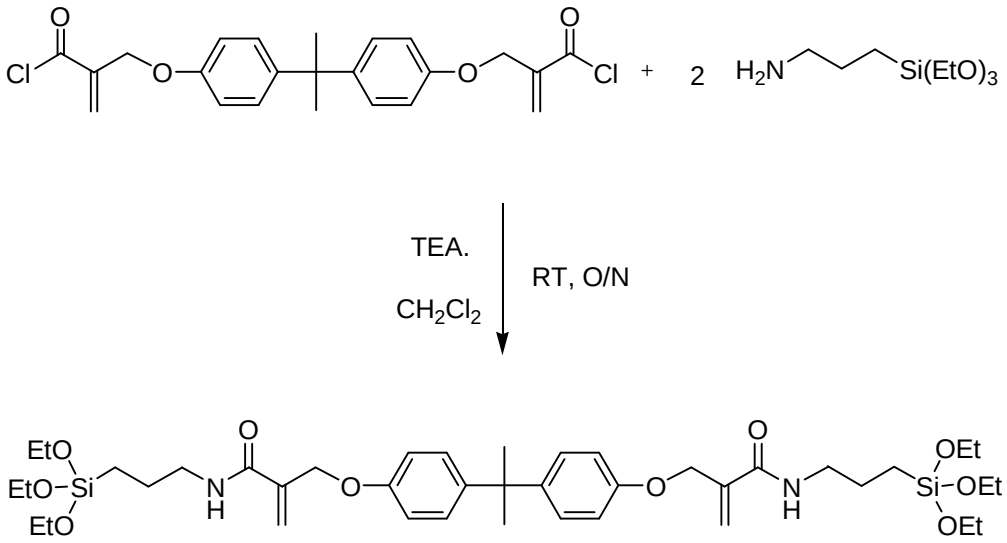

Figure 4.18. Synthesis of TBBr-Bisphenol A – APTES diamide derivative

TBBr-Bisphenol A – APTES diamide monomer was soluble in ether, acetone, ethyl acetate, and methanol. On the other hand it was insoluble in water and hexane.

In the ^{13}C-NMR spectrum (Figure 4.19), methyl and methylene carbons of ethoxysilane at 18.4 and 58.5 ppm, methylenes attached to silicon at 7.9 and 23.0 ppm, methyl carbons at 31.1 ppm, tertiary carbon peak at 41.8 ppm, methylenes attached to nitrogen at 41.9 ppm, methylene attached to oxygen at 67.9 ppm, double bond and carbonyl carbons at 122.2, 143.7, and 166.1 ppm, and carbons of bisphenol rings at 114.2, 127.7, 139.5, and 155.6 ppm were characterized.

The ^{1}H-NMR spectrum (Figure 4.20) showed protons of APTES at 0.67, 1.22, 1.68, 3.35, and 3.80 ppm, methyl protons at 1.64, methylene protons attached to oxygen at 4.74, double bonds at 5.67 and 6.02 ppm, ring protons at 6.82 and 7.14, and the proton attached to nitrogen at 7.25 ppm.

The FT-IR spectrum of the product (Figure 4.21) showed C-H vibrations between 2972-2886 cm^{-1}, amide carbonyl at 1660 cm^{-1}, C=C stretching peak at 1613 cm^{-1}, and C-O vibrations at 1180 cm^{-1}. The broad peak at 3317 cm^{-1} was due to NH stretching which confirmed the formation of the product.

This new organic-inorganic hybrid material structurally looks like ormocers. It has both polymerizable double bonds and the adhesive alkoxy silane end groups in the same molecule. This compound can be polymerized not only by free radical polymerization, but also condensation through the alkoxy silane groups.

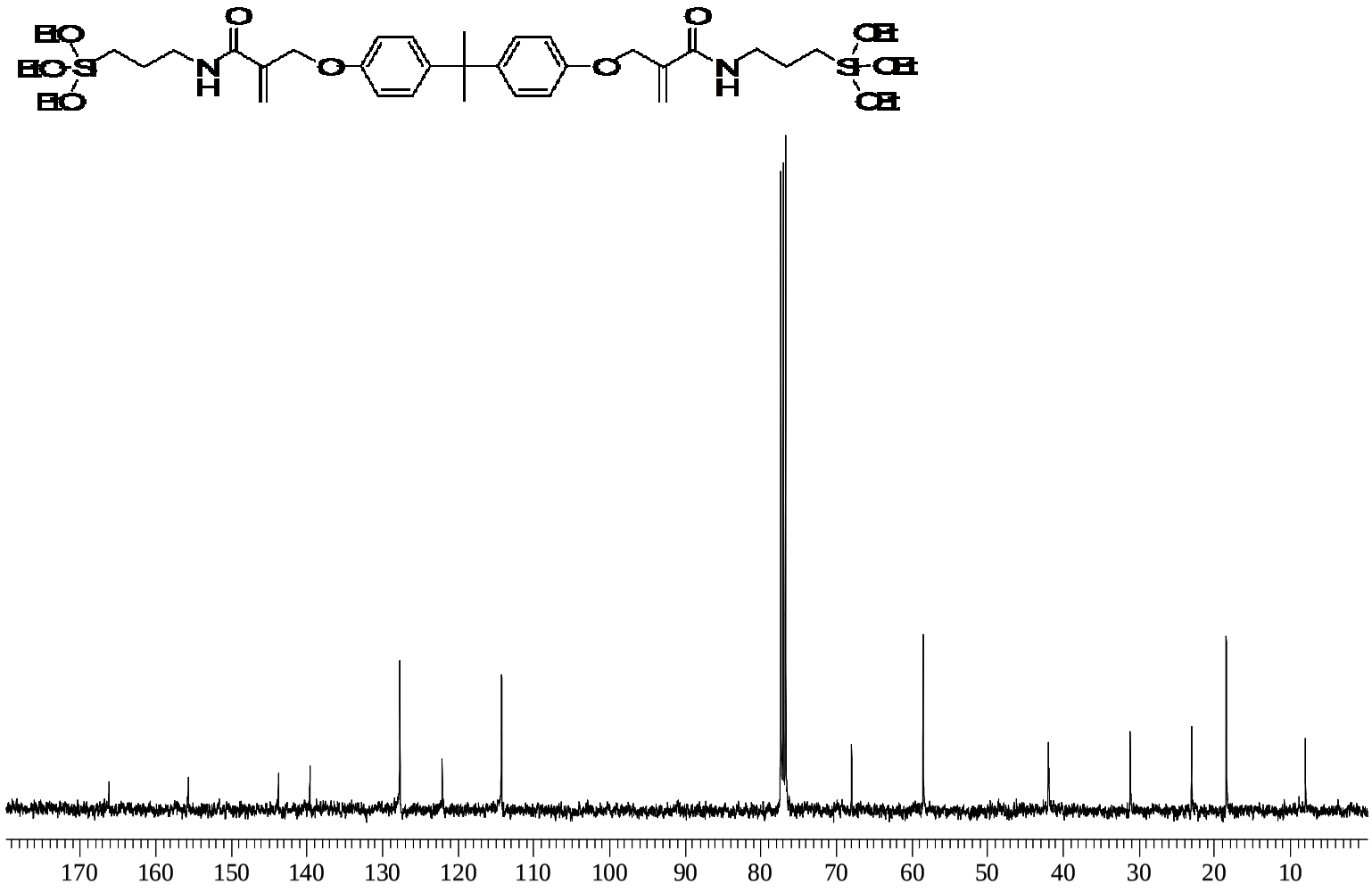

Figure 4.19. ^{13}C-NMR spectrum of TBBr-Bisphenol A – APTES diamide derivative

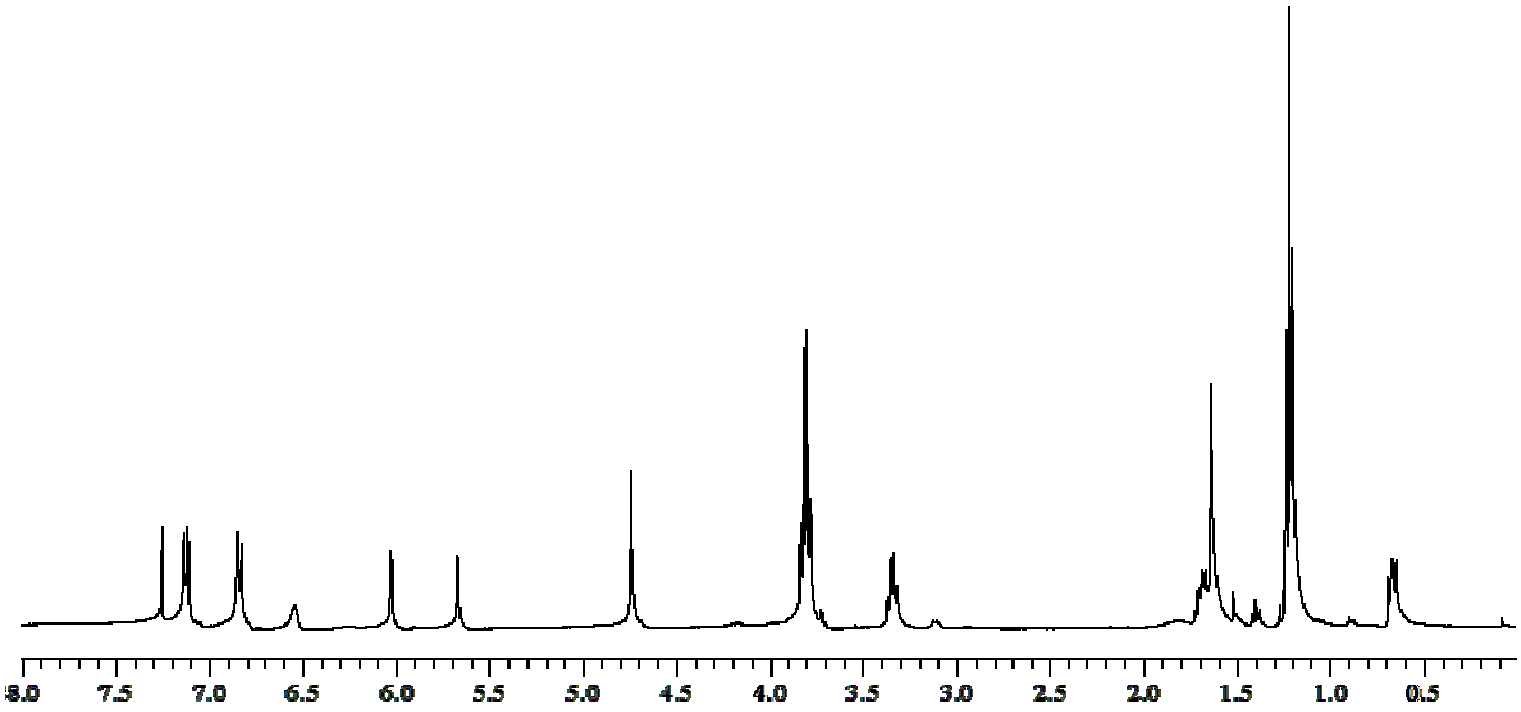

Figure 4.20. ^{1}H-NMR spectrum of TBBr-Bisphenol A – APTES diamide derivative

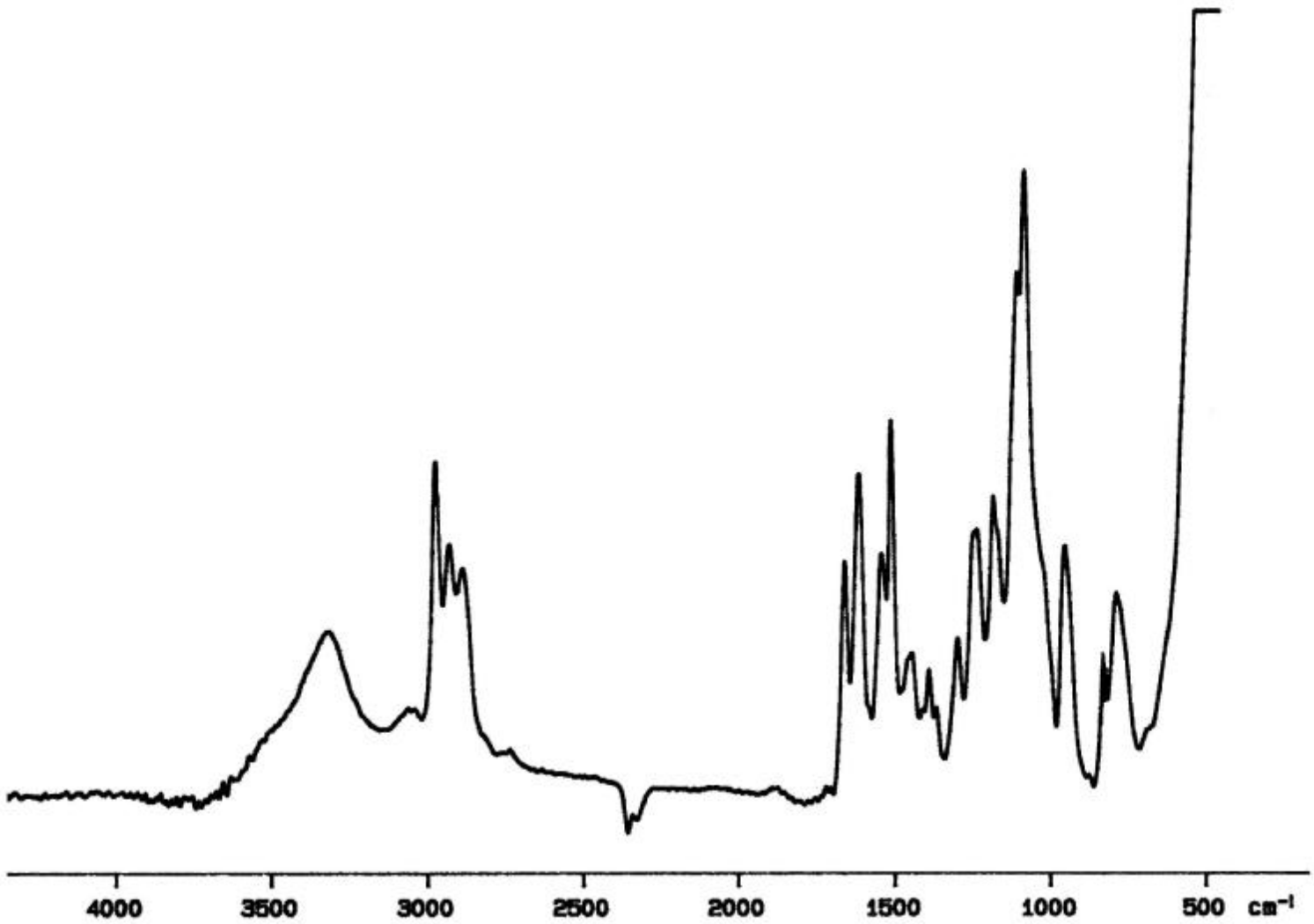

Figure 4.21. FT-IR spectrum of TBBr-Bisphenol A – APTES diamide derivative

4.1.7. Synthesis of TBBr-Bisphenol A – Benzylamide Derivative

Another amide-linked monomer was synthesized from the reaction of TBBr-Bisphenol A diacid chloride intermediate with benzyl amine in the presence of TEA (Figure 4.22). The pure product with the melting point of 105 ^{o}C, was obtained by recrystallization from methanol as white solid in 62.7 per cent yield.

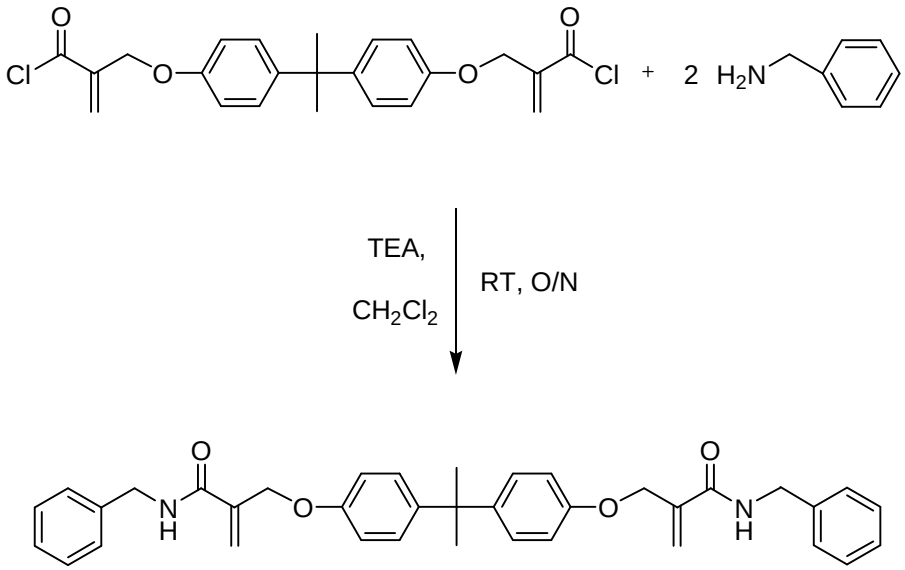

Figure 4.22. Synthesis of TBBr-Bisphenol A – benzylamide derivative

TBBr-Bisphenol A – benzylamide monomer was soluble in THF and acetone, whereas insoluble in water, hexane, and ether. It was also partially soluble in methanol.

The ^{13}C-NMR spectrum of the product (Figure 4.23) showed methyl and tertiary carbon peaks of bisphenol group at 31.1 and 41.9 ppm, methylene of benzyl amine at 43.7 ppm, carbon peak attached to oxygen at 68.1 ppm, double bond and carbonyl peaks at 123.1, 143.8, and 166.0 ppm, carbons of bisphenol rings at 114.3, 128.6, 137.8, and 155.5 ppm, and finally the carbons of benzyl ring at 127.4, 127.5, 127.7, and 139.1 ppm.

In the ^{1}H-NMR spectrum (Figure 4.24), methyl protons of bisphenol at 1.54 ppm, protons of methylene attached to amide group at 4.44 ppm, methylene protons of ether group at 4.68 ppm, double bond protons at 5.61 and 6.01 ppm, amide proton at 6.58 ppm,

protons of bisphenol rings at 6.70 and 7.00 ppm, and protons of benzyl ring at 7.16, 7.20, and 7.22 ppm were observed.

The FT-IR spectrum (Figure 4.25) showed C-H vibrations between 2966-2868 cm^{-1}, amide carbonyl at 1660 cm^{-1}, C=C stretching peak at 1616 cm^{-1}, and C-O vibrations at 1180 cm^{-1}. The broad peak at 3308 cm^{-1} was due to NH stretching which confirmed the formation of the product.

TBBr-Bisphenol A – benzylamide derivative has a very stiff structure. Especially, the rigid benzyl end groups and amide linkages are expected to improve thermal and hydrolytic properties of the ultimate material. Also, hydrogen bonding ability makes this material attractive for binding to dentine and enamel structures.

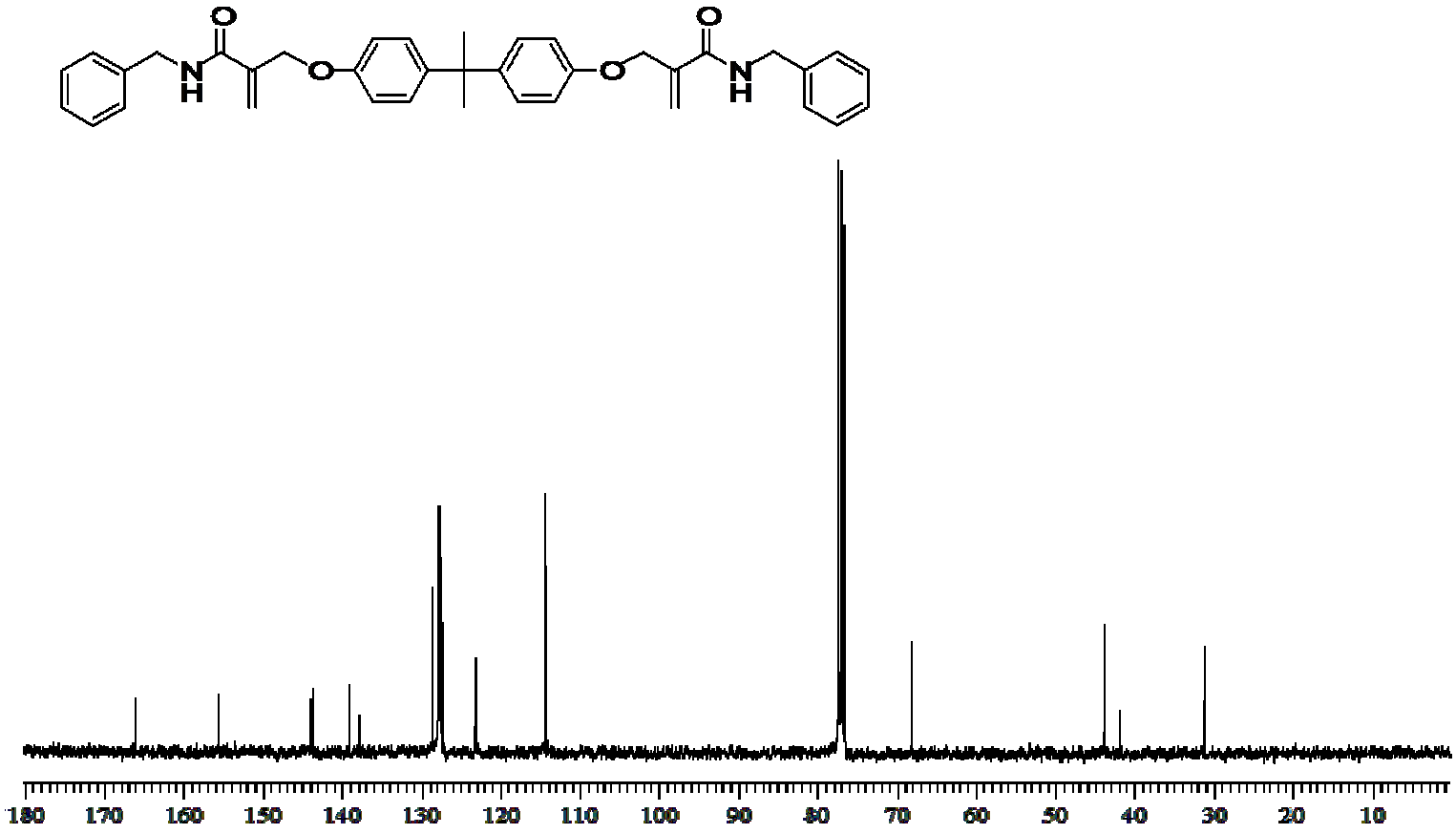

Figure 4.23. ^{13}C-NMR spectrum of TBBr-Bisphenol A – benzylamide derivative

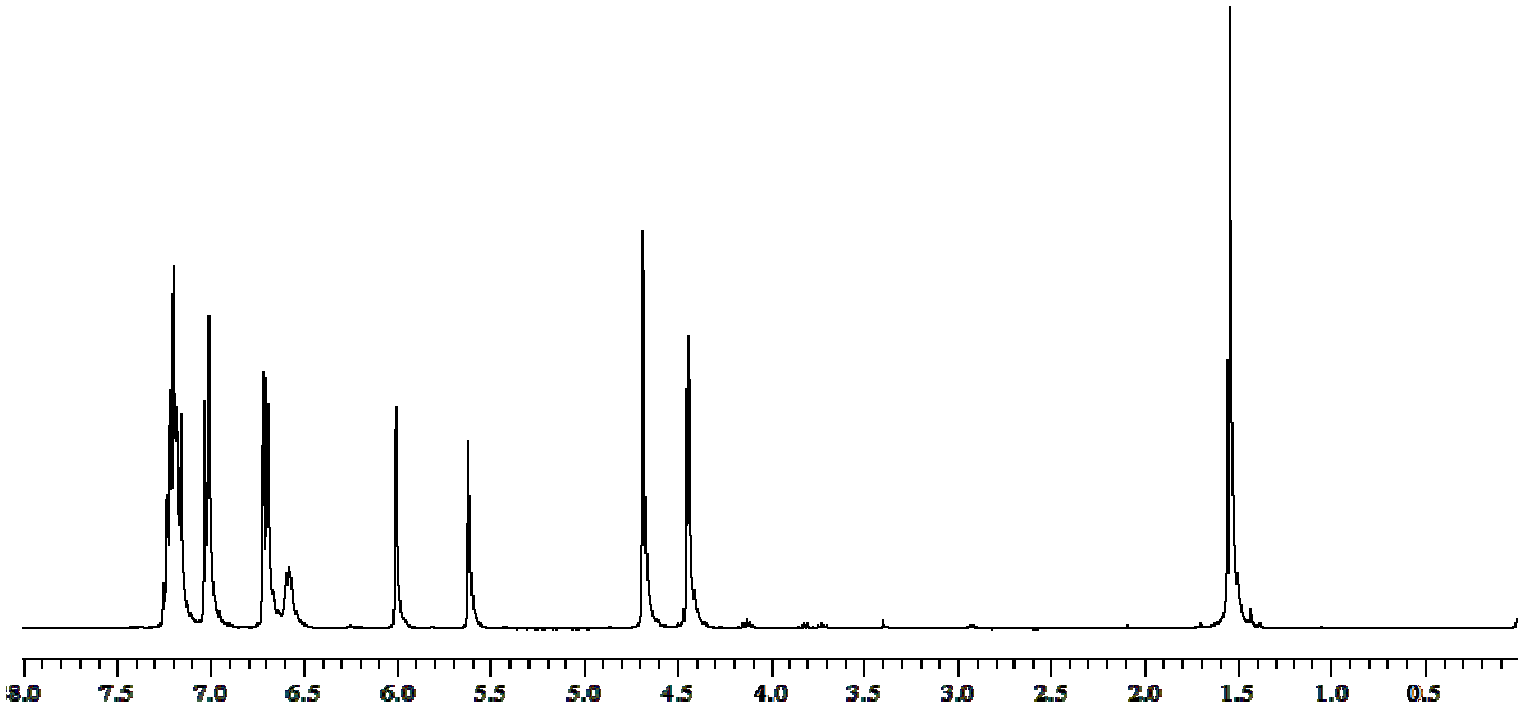

Figure 4.24. ^{1}H-NMR spectrum of TBBr-Bisphenol A – benzylamide derivative

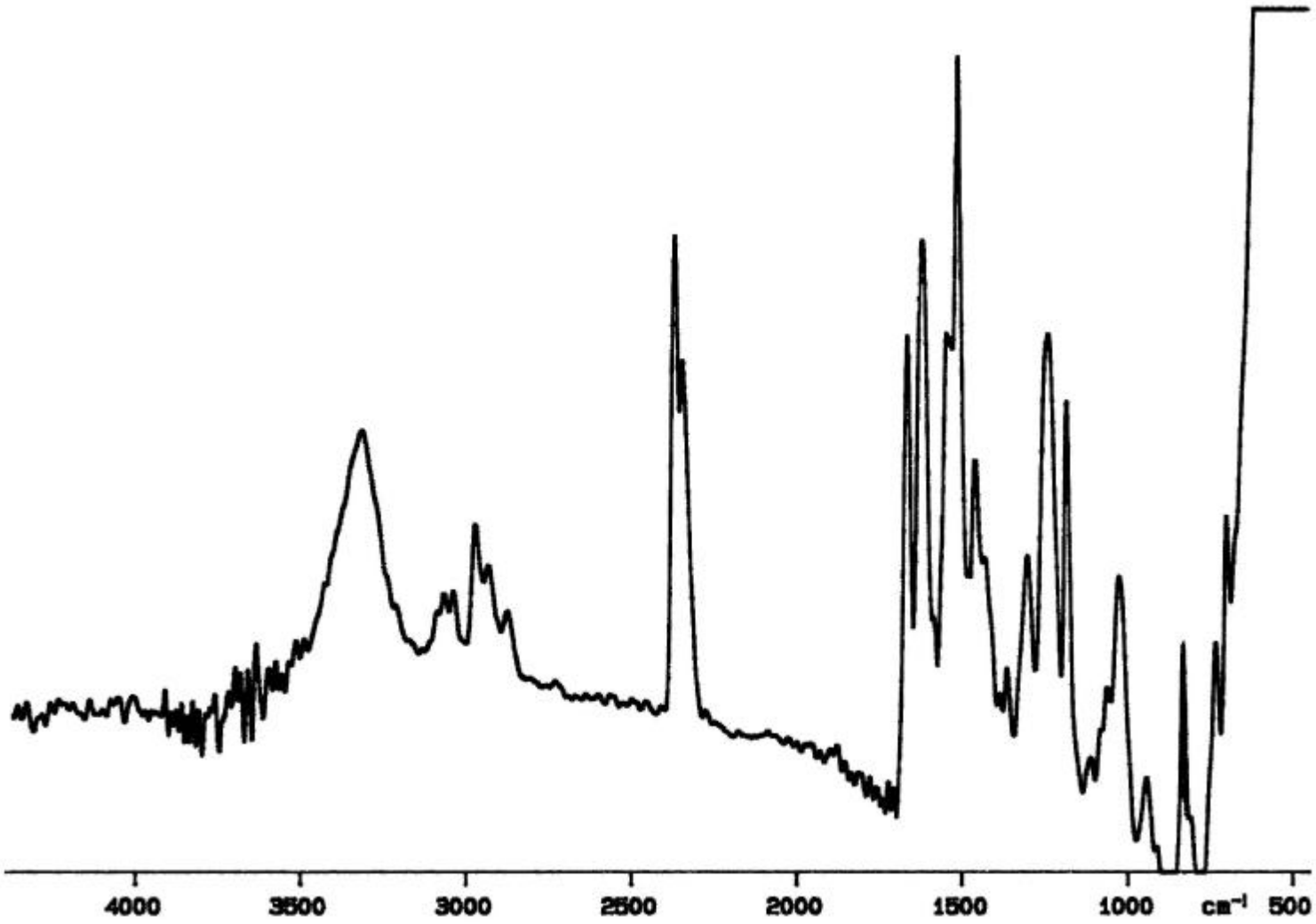

Figure 4.25. FT-IR spectrum of TBBr-Bisphenol A – benzylamide derivative

4.1.8. Synthesis of AHM-APTES Monomer

The Michael addition of 2 equiv. mol of 3-acryloyloxy-2-hydroxypropyl methacrylate (AHM) to 1 equiv. mol of APTES (Figure 4.26) gave the AHM-APTES monomer as a colorless liquid.

AHM is a mixture of two isomers in different ratios. These isomers are formed from 1,3 or 1,2 substitution reactions of glycerol giving one isomer with primary hydroxyl group (unsymmetrical isomer) and the other with secondary hydroxyl group (symmetrical isomer).

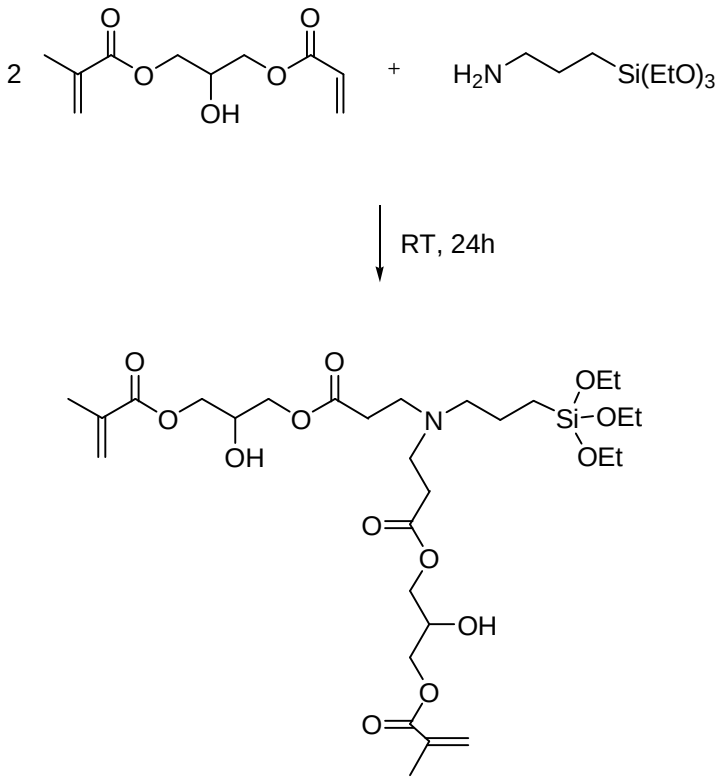

Figure 4.26. Synthesis of AHM-APTES monomer

The AHM-APTES monomer was soluble in methanol, methylene chloride, and acetone. On the other hand it was insoluble in ether and hexane.

The ^{13}C-NMR spectrum of the AHM-APTES monomer (Figure 4.27) showed the peaks at the aminopropyl site of APTES at 7.9, 19.4, and 56.4 ppm, and those at the

triethoxy site at 18.3 and 58.3 ppm. Methylene carbon attached to carbonyl at 32.7 ppm, and the others attached to nitrogen and oxygen at 49.2, 65.2, and 67.7 ppm, CH-OH peak at 65.3 ppm, double bonds and carbonyls at 126.0, 135.6, 166.9, and 172.2 ppm were detected. The small peaks at 61.1, 62.5, and 72.4 ppm indicated the presence of a small amount of product obtained from the 1,2-glycerol diester isomer of AHM.

In the ^{1}H-NMR spectrum (Figure 4.28), proton peaks of APTES appeared at 0.56, 1.22, 1.52, 2.50, 3.80 ppm, methyl protons at 1.95 ppm, methylene protons attached to carbonyl at 2.46 ppm, and the ones attached to nitrogen at 2.78 ppm, methylene protons attached to oxygens at 4.21 and 4.22 ppm, the hydroxyl, and the protons of carbon attached to hydroxyl at 4.13 and 4.30 ppm, respectively. The double bond protons appeared at 5.59, 6.13 ppm.

The FT-IR spectrum (Figure 4.29) showed C-H vibrations between 2974-2888 cm^{-1}, ester carbonyl at 1719 cm^{-1}, C=C stretching peak at 1637 cm^{-1}, and C-O vibrations at 1100 cm^{-1}. The broad peak at 3450 cm^{-1} was due to OH.

This unique monomer has an ormocer-like structure. Like TBBr-Bisphenol A – APTES diamide derivative, this compound can be polymerized both by free radical polymerization and condensation through the alkoxy silane group, too. A distinguishing property of this material is being contained two different types of possible binding groups (alcohol and silane) in three different sites of the molecule instead of two those in the previous structures.

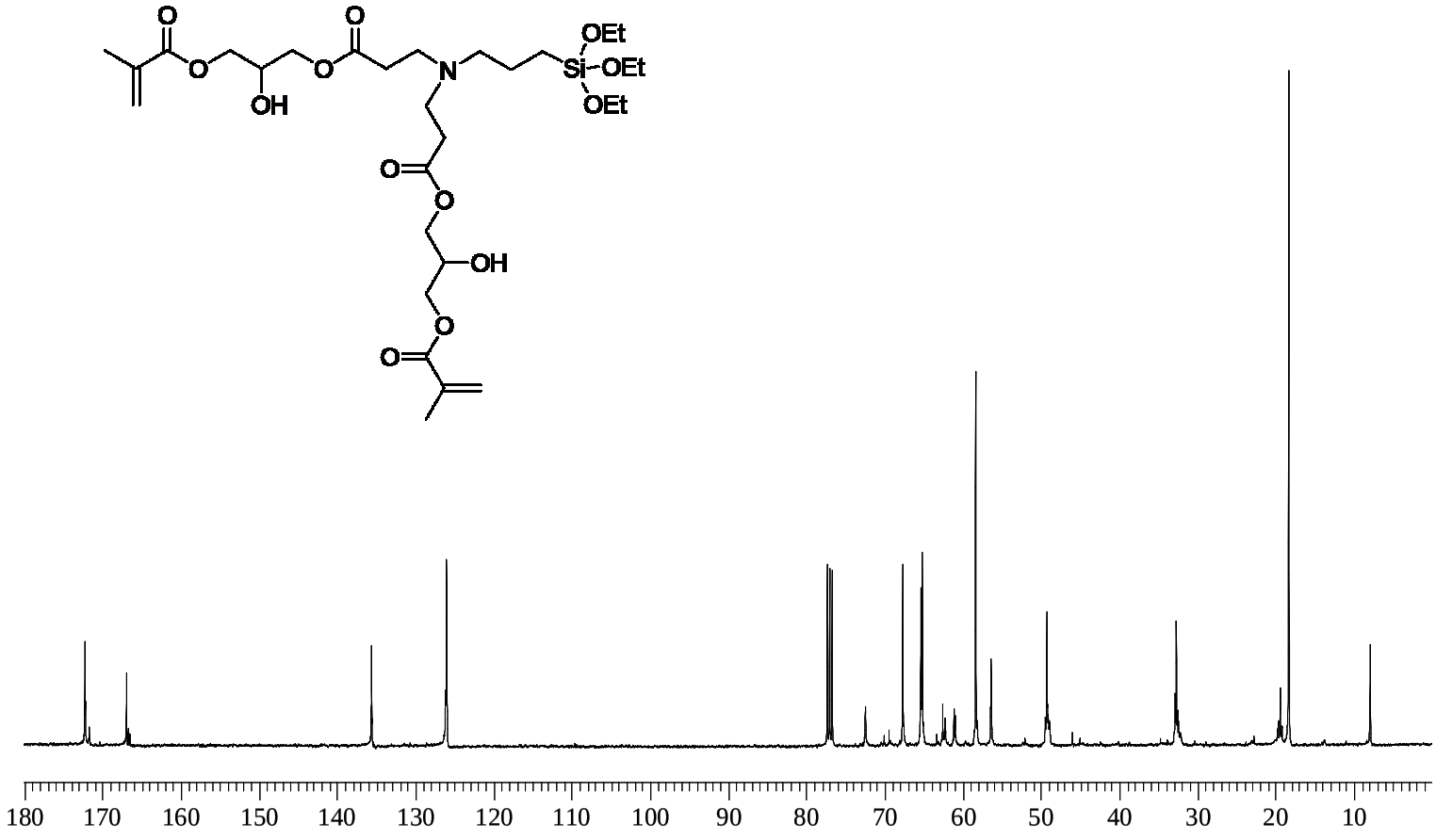

Figure 4.27. ^{13}C-NMR spectrum of AHM-APTES monomer

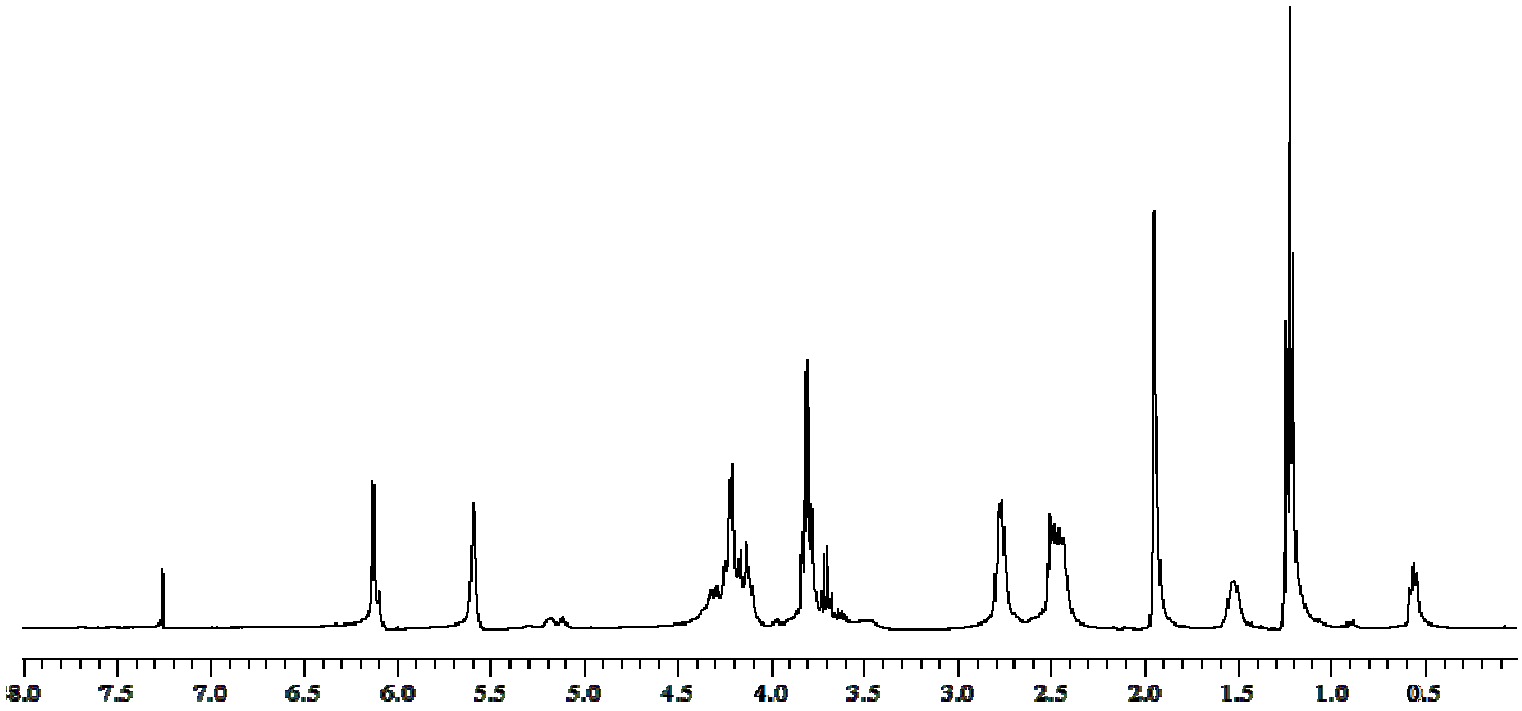

Figure 4.28. ^{1}H-NMR spectrum of AHM-APTES monomer

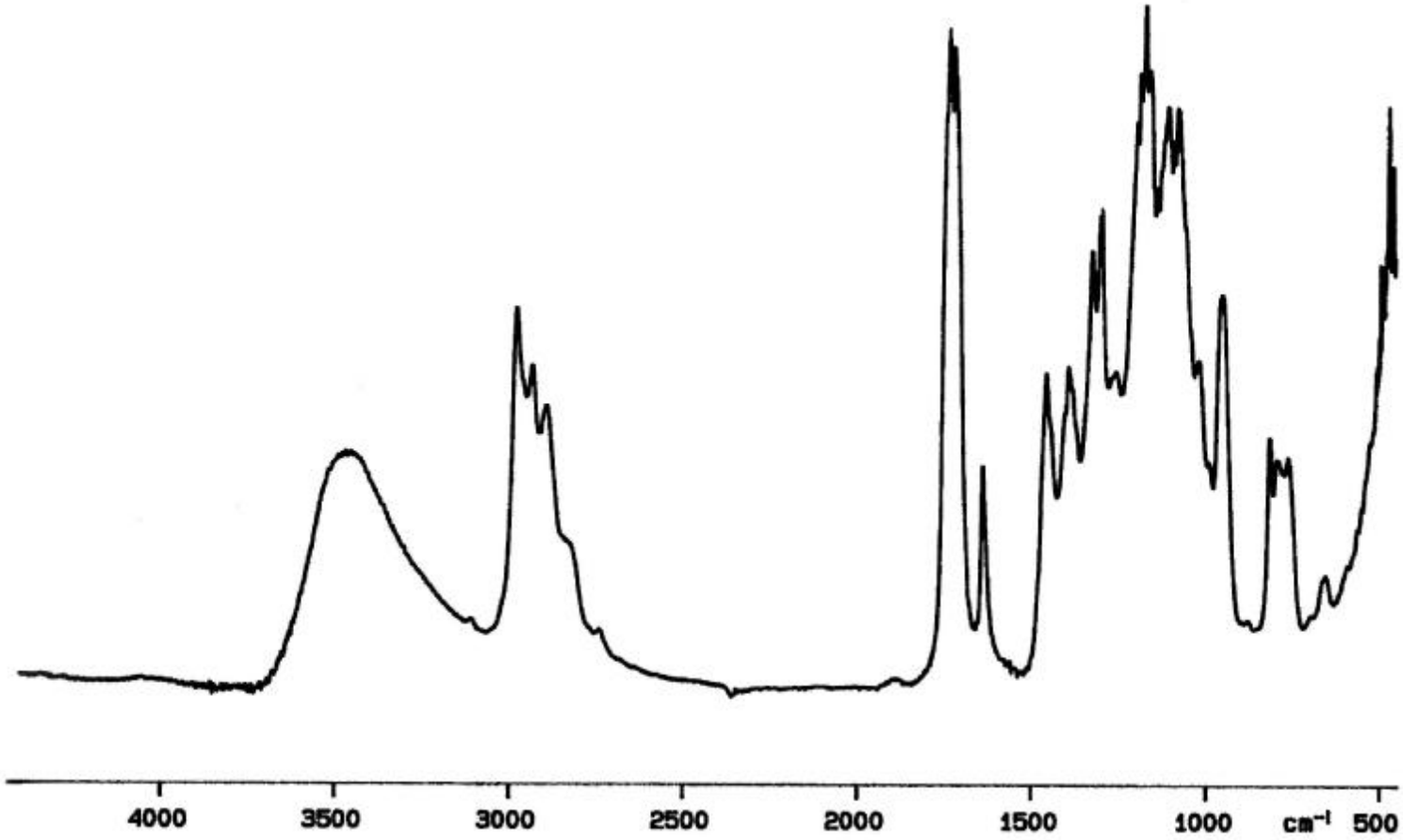

Figure 4.29. FT-IR spectrum of AHM-APTES monomer

4.1.9. Photopolymerizations

The photopolymerization behavior of all prepared polymerizing systems was investigated using photodifferential scanning calorimeter (Photo-DSC). All the polymerizations were performed under identical conditions of initiator concentration (2.0 mol%) and UV light intensity (15 mW/cm^2), but at two different temperatures (at 40 ^{o}C and 60 ^{o}C). All the rate of polymerization and conversion data obtained from the photopolymerization experiments throughout this study are given in Appendix A.

In the first set of polymerizing systems, very rigid and H-bonding capable Bis-GMA monomer was diluted with flexible and non H-bonding TEGDMA reactive diluent monomer in the mol ratio of 50:45, and then, 5 mol% of synthesized novel crosslinking monomers were added. Synthesized TBBr-Bisphenol A diacid and TBBr-Bisphenol A benzylamide monomers were not miscible with Bis-GMA:TEGDMA mixture in this ratio. Rate of polymerization and conversions of both miscible and immiscible mixtures (after mixing in an ultrasonic bath) were determined. Figure 4.30 shows the rate versus time plots for Bis-GMA:TEGDMA (50:50) and Bis-GMA:TEGDMA:Monomer (50:45:5) polymerizing systems at 40 ^{o}C.

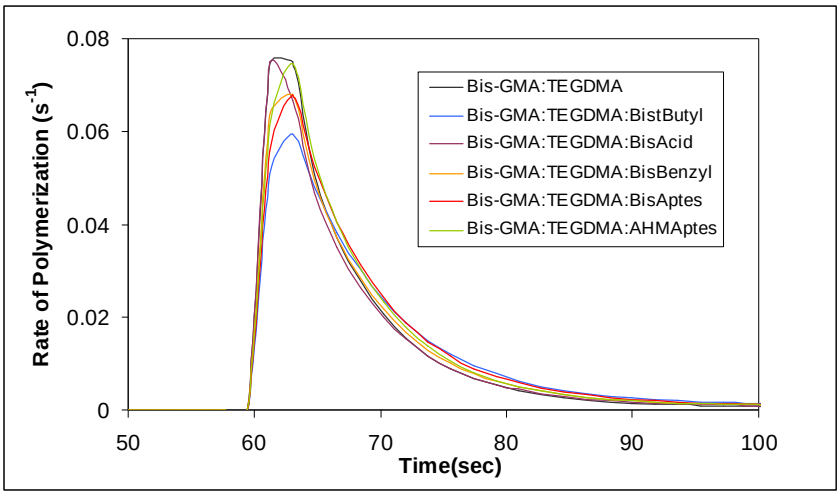

Figure 4.30. Rate versus time plot of Bis-GMA:TEGDMA system with synthesized novel crosslinking monomers at 40 ^{o}C

Addition of H-bonding, flexible AHM-APTES monomer and H-bonding, rigid TBBr-Bisphenol A diacid derivative did not result in a significant change in the maximum rate of polymerization. A slight decrease in the rate was observed in the systems containing TBBr-Bisphenol A – APTES diamide and TBBr-Bisphenol A – benzylamide derivatives. Highly sterically hindered, non H-bonding crosslinking monomer, TBBr-Bisphenol A diester monomer showed about 20 per cent decrease in the rate of polymerization.

The overall conversions of the Bis-GMA:TEGDMA:Monomer (50:45:5) systems at 40 ^{o}C (65.7-78.1) were very similar or higher than that of commercial Bis-GMA:TEGDMA (50:50) resin (67.4-67.6) (Figure 4.31). This result reveals that addition of 5 per cent synthesized monomers do not increase the amount of unreacted monomer in the polymerizing system. Unreacted monomers in the dental materials may act as plasticizers and affect the mechanical properties of the material, and also they may irritate the soft tooth tissue.

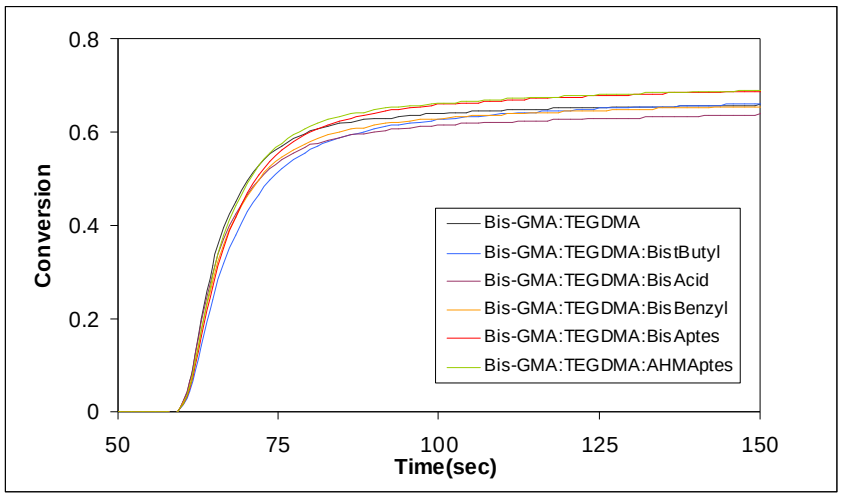

Figure 4.31. Conversion versus time plot of Bis-GMA:TEGDMA system with synthesized novel crosslinking monomers at 40 ^{o}C

In the second set of polymerizing systems, non H-bonding diluent TEGDMA monomer was replaced by H-bonding monomethacrylate diluent monomer HEMA. In this way highly hydrogen bonding mixtures was obtained. Synthesized TBBr-Bisphenol A diacid and TBBr-Bisphenol A benzylamide monomers were not miscible with Bis-

GMA:HEMA mixture in this ratio. Rate of polymerizations and conversions of both miscible and immiscible mixtures (after mixing in an ultrasonic bath) were determined.

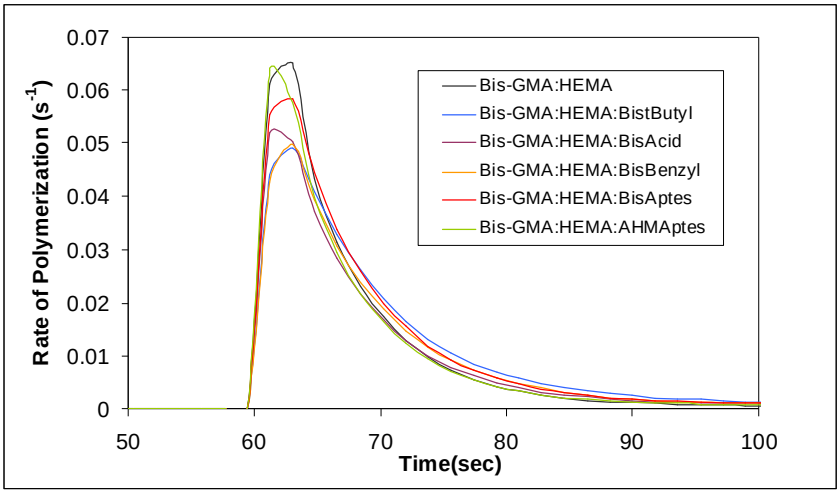

Figure 4.32. Rate versus time plot of Bis-GMA:HEMA system with synthesized novel crosslinking monomers at 40 ^{o}C

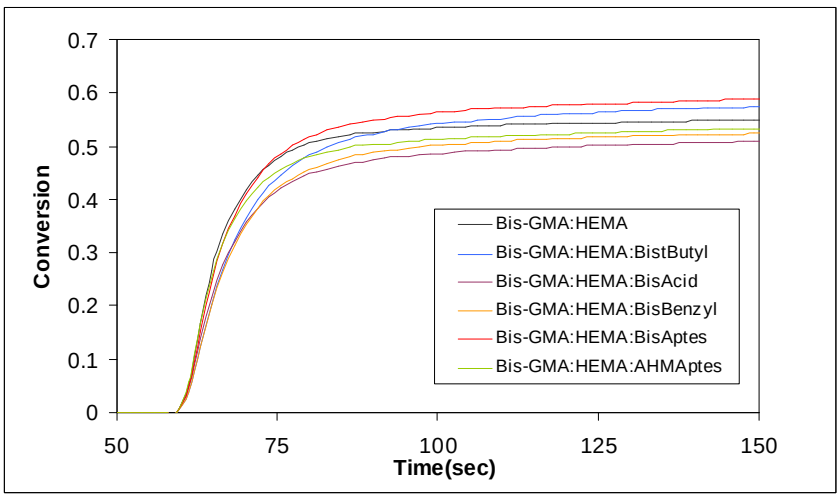

Figure 4.33. Conversion versus time of Bis-GMA:HEMA system with synthesized novel crosslinking monomers at 40 ^{o}C

Figures 4.32 and 4.33 show the rate versus time and conversion versus time plots for Bis-GMA:HEMA (50:50) and Bis-GMA:HEMA:Monomer (50:45:5) polymerizing systems at 40 ^{o}C. Similar trend to Bis-GMA:TEGDMA:Monomer systems was seen in the

Bis-GMA:HEMA:Monomer systems regarding the addition of proposed crosslinking monomers. However, a significant polymerization rate and conversion decrease was observed in the HEMA containing systems when compared to TEGDMA containing ones. The dilution of H-bonding capacity might be responsible for this type of behavior. In the Bis-GMA:TEGDMA:Monomer systems, non H-bonding TEGDMA monomer dilutes the overall H-bonding and provides more flexible systems. On the other hand, by addition of H-bonding HEMA monomer, dilution of H-bonding groups is suppressed and about 100 per cent H-bonding capable systems are obtained. This will reduce the molecular mobility of the system. Then, the restricted mobility of the network might suppress the propagation reaction, by hindering the diffusion of the free monomer [8].

In order to investigate the effect of diluent monomer on the rate of polymerization of viscous Bis-GMA, homopolymerizations of Bis-GMA, TEGDMA and HEMA were also carried out at 40 ^{o}C. The polymerization of Bis-GMA showed an immediate autoacceleration region caused by the rigid environment and the maximum rate was reached at very low conversion (Figure 4.34 and Figure 4.35). This monomer has the highest reactivity for quick network formation compared to HEMA and TEGDMA.

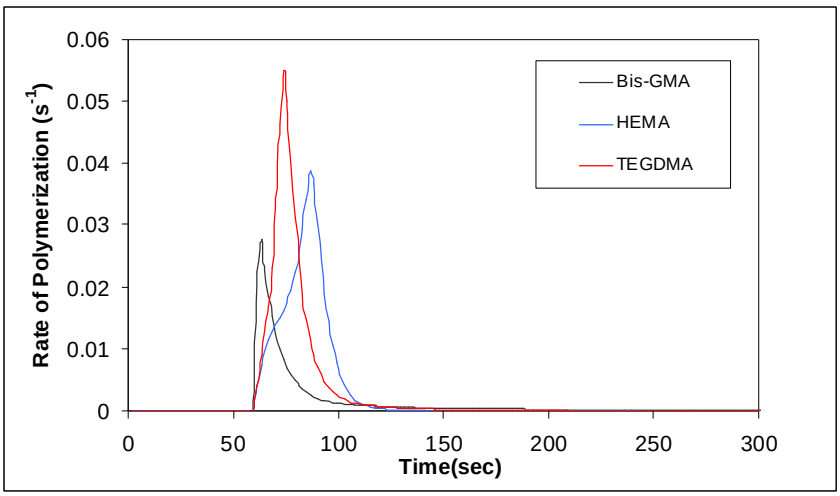

Figure 4.34. Rate versus time plot of Bis-GMA, TEGDMA and HEMA homopolymerizations at 40 ^{o}C

Interestingly, Figures 4.30, 4.32 and 4.34 show that Bis-GMA:TEGDMA and Bis-GMA:HEMA mixtures showed higher polymerization rates than that of neat Bis-GMA,

TEGDMA, and HEMA. When Bis-GMA was polymerized, the maximum rate was low (0.026-0.027 s^{-1}) and the final conversion reached was 42-45 per cent. The polymerization of TEGDMA gave the maximum rate and conversion of 0.05-0.055 s^{-1} and 80-83 per cent. Combining equal moles of the two monomers resulted in a rate of 0.075 s^{-1}. Conversions were not as high as that of TEGDMA but higher than Bis-GMA.

Furthermore, Figures 4.31 and 4.35 show that addition of the reactive diluent TEGDMA to Bis-GMA results in an important increase in the monomer conversion of Bis-GMA monomer. The conversions reached for Bis-GMA and Bis-GMA:TEGDMA (50:50 mol %) were about 42-45 and 67 per cent. Similarly, the addition of HEMA as a diluent monomer increased the conversions to 56-57 per cent. These results reveal a synergistic effect of components of these mixtures on the polymerization rate, which may be most probably due to the good plasticizing effect of TEGDMA and HEMA.

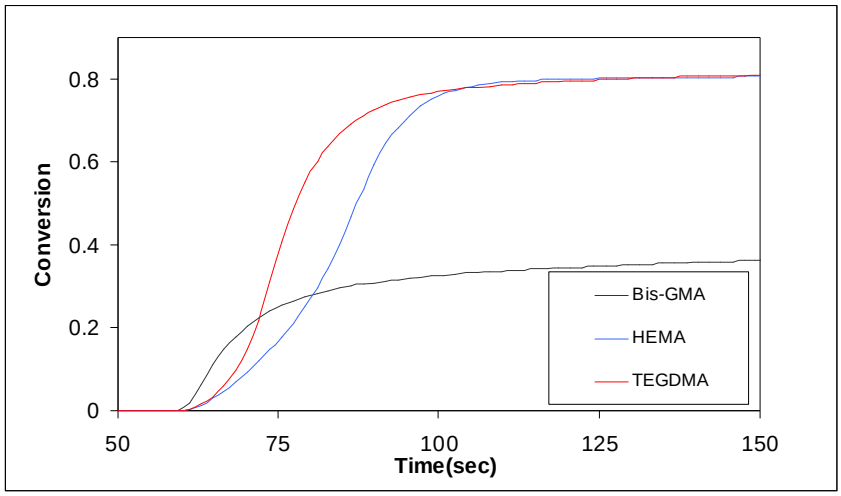

Figure 4.35. Conversion versus time plot of Bis-GMA, TEGDMA and HEMA homopolymerizations at 40 ^{o}C

Synthesized TBBr-Bisphenol A diacid and TBBr-Bisphenol A – benzylamide monomers were not miscible in both Bis-GMA:TEGDMA and Bis-GMA:HEMA mixtures in the 50:45:5 mol ratio. So, to make a more accurate interpretation, a ratio which they make homogenous mixtures had to be found. These monomers gave completely miscible, homogenous mixtures in the ratio of 50:49.5:0.5. Figures 4.36 and 4.37 show the rate versus time and conversion versus time plots for these systems at 40 ^{o}C.

These mixtures were faster than their 5 per cent monomer containing immiscible counterparts, and they were also faster or similar in rate even to neat Bis-GMA:TEGDMA and Bis-GMA:HEMA mixtures, whereas the overall conversions did not change.

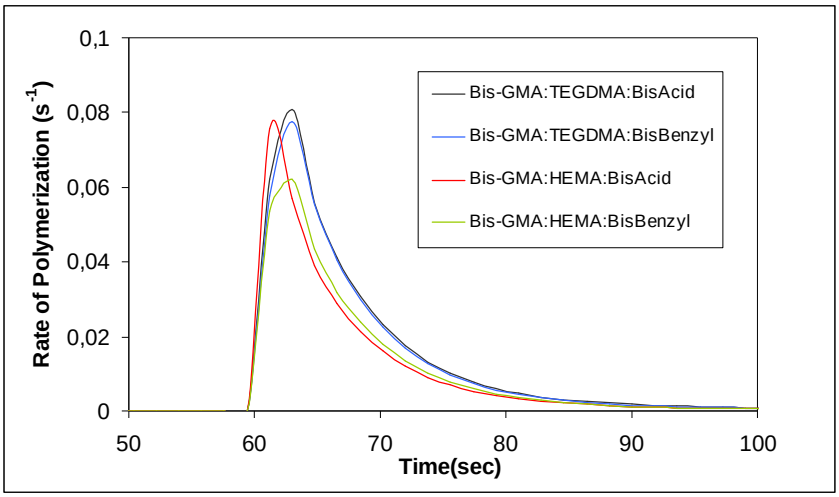

Figure 4.36. Rate versus time plot of Bis-GMA:TEGDMA and Bis-GMA:HEMA systems with synthesized TBBr-Bisacid and TBBr-Bisphenol A – benzylamide monomers (50:49.5:0.5) at 40 ^{o}C

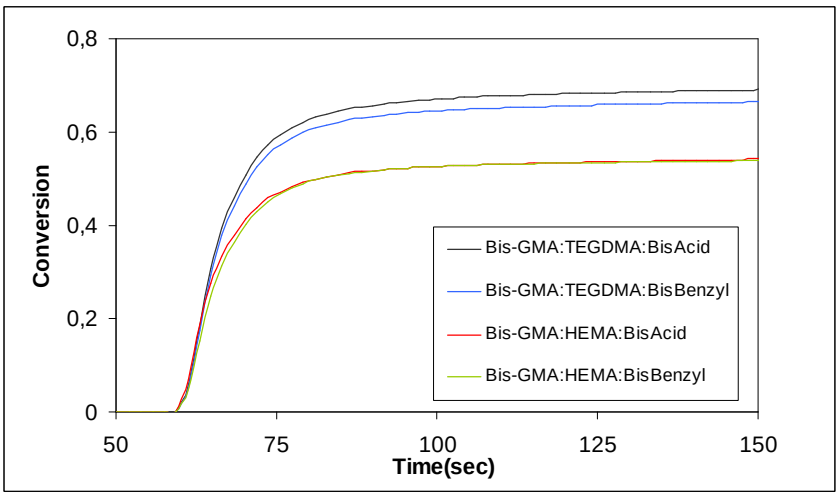

Figure 4.37. Conversion versus time plot of Bis-GMA:TEGDMA and Bis-GMA:HEMA systems with synthesized TBBr-Bisphenol A diacid and TBBr-Bisphenol A – benzylamide monomers (50:49.5:0.5) at 40 ^{o}C

In order to see the temperature effect on polymerization rate, conversion, and H-bonding efficiency, 50:50 mol per cent Bis-GMA:TEGDMA and Bis-GMA:HEMA mixtures and their 50:45:5 per cent TBBr-Bisphenol A diester, TBBr-Bisphenol A – APTES diamide and AHM-APTES analogues were also polymerized at 60 ^{o}C under identical initiator concentration and UV light intensity.

In the Bis-GMA:TEGDMA and Bis-GMA:TEGDMA:AHM-APTES systems the Arrhenius behavior was observed. The rate of polymerization increased from 4 to 8 per cent for them when compared to that in the polymerizations at 40 ^{o}C. On the other hand, a significant change in the polymerization rate was not observed in the Bis-GMA:TEGDMA:BisAptes system, whereas Bis-GMA:TEGDMA:Bistbutyl mixture showed about 11 per cent decrease (Figure 4.38).

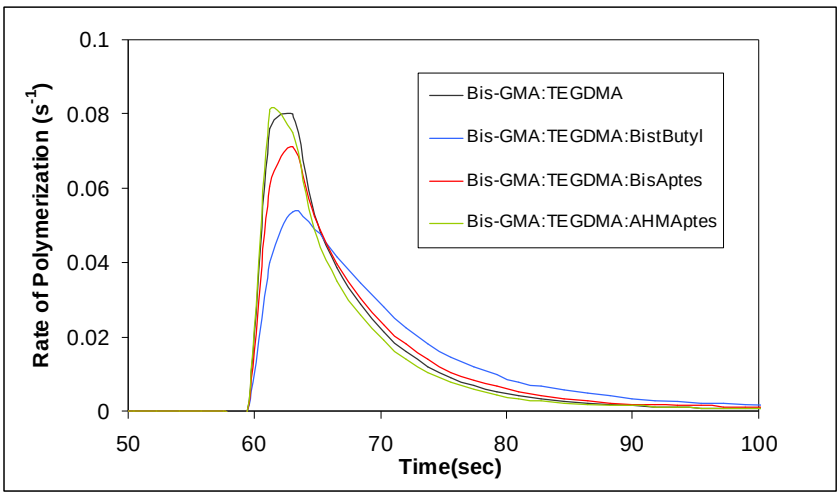

Figure 4.38. Rate versus time plot of Bis-GMA:TEGDMA system with synthesized novel crosslinking monomers at 60 ^{o}C

The similar trend in the rate of polymerization was seen in the HEMA containing polymerizing systems. 22 to 25 per cent rate increase was observed in Bis-GMA:HEMA and Bis-GMA:HEMA:AHM-APTES mixtures, whereas Bis-GMA:TEGDMA:Bistbutyl system showed decrease in 18 to 24 per cent. The rate of Bis-GMA:TEGDMA:BisAptes system remained almost constant (Figure 4.39).

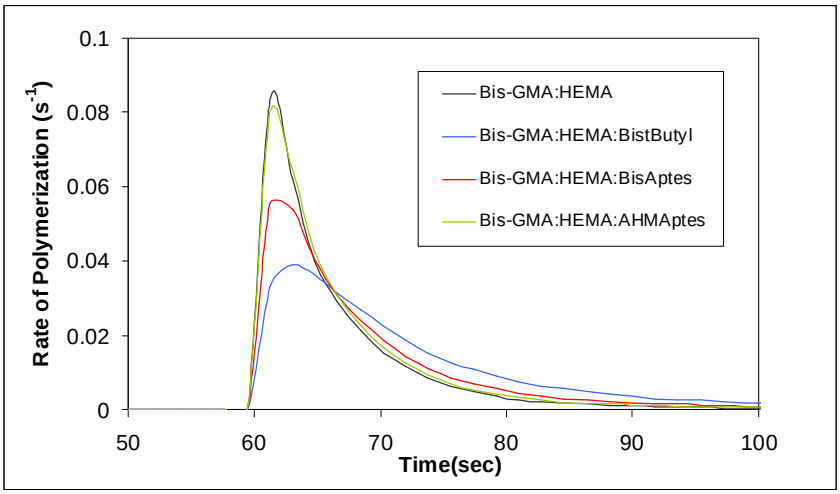

Figure 4.39. Rate versus time plot of Bis-GMA:HEMA system with synthesized novel crosslinking monomers at 60 ^{o}C

The overall conversions of the polymerizing systems at 60 ^{o}C were similar to those at 40 ^{o}C. Figures 4.40 and 4.41 show the conversions of Bis-GMA:TEGDMA and Bis-GMA:HEMA systems with synthesized monomers at 60 ^{o}C.

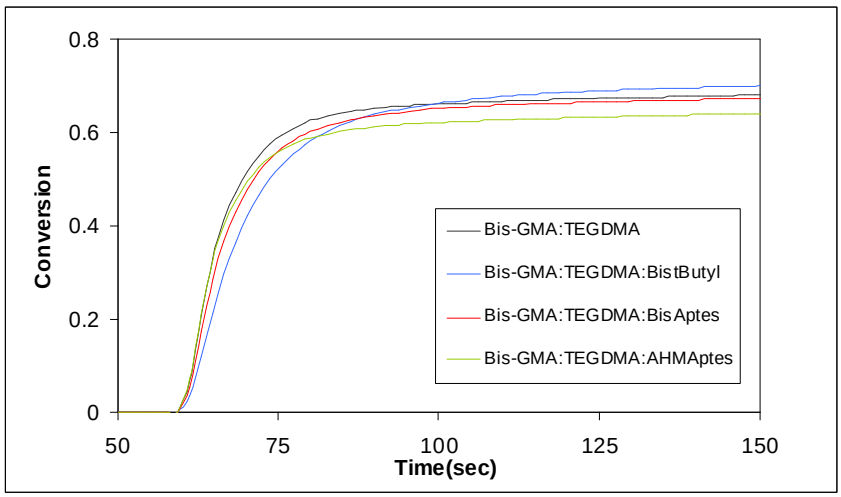

Figure 4.40. Conversion versus time plot of Bis-GMA:TEGDMA system with synthesized novel crosslinking monomers at 60 ^{o}C

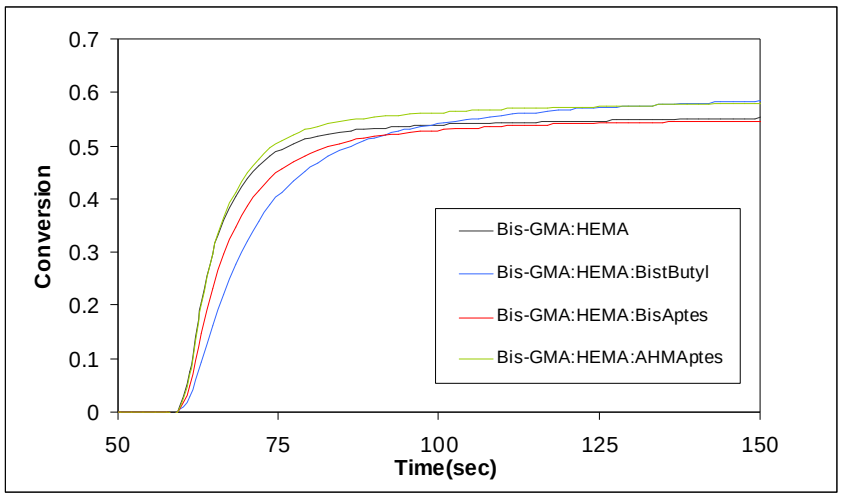

Figure 4.41. Conversion versus time plot of Bis-GMA:HEMA system with synthesized novel crosslinking monomers at 60 ^{o}C

Finally, the homopolymerization of the only liquid monomer of all the synthesized ones, AHM-APTES was carried out at 40 ^{o}C. As seen in Figures 4.42 and 4.43 this flexible, H-bonding material showed higher polymerization rate and conversion than Bis-GMA:TEGDMA and Bis-GMA:HEMA (50:50) systems and also their 5 per cent AHM-APTES containing counterparts.

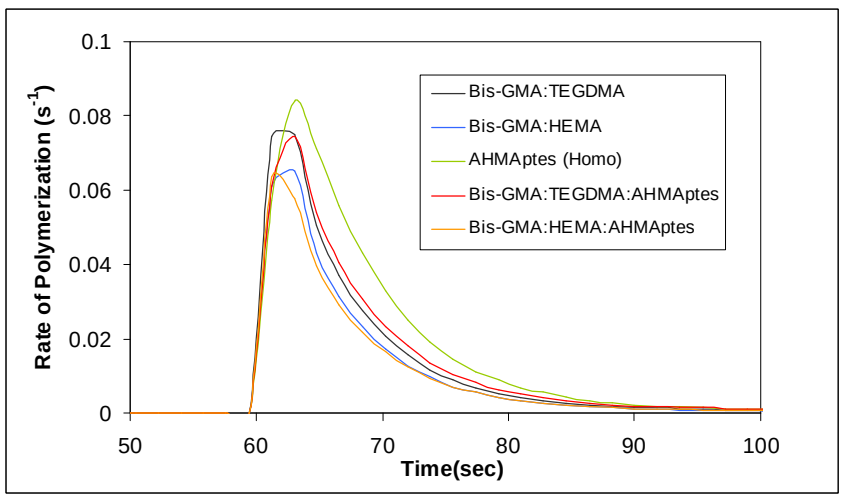

Figure 4.42. Rate versus time plot of AHM-APTES crosslinking monomer with several other polymerizing systems at 40 ^{o}C

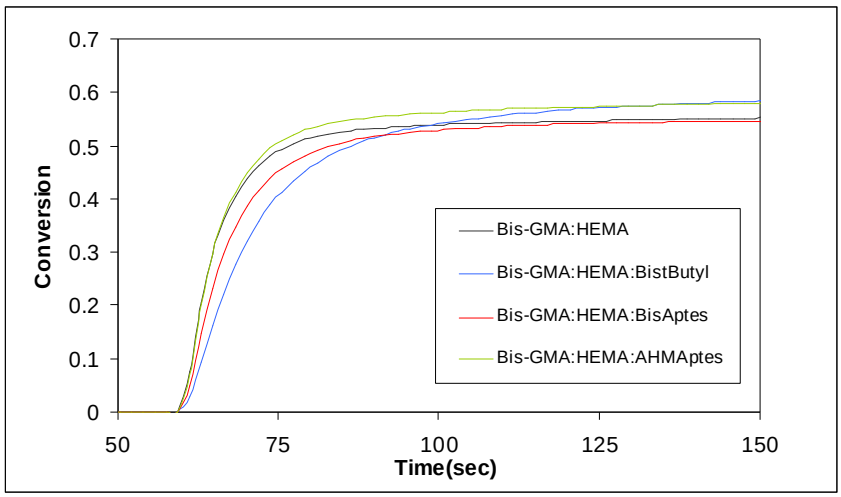

Figure 4.43. Conversion versus time plot of AHM-APTES crosslinking monomer with several other polymerizing systems at 40 ^{o}C

5. CONCLUSIONS

In this study, five new dental crosslinking monomers with adhesive groups to tooth tissue were developed using simple synthetic methods. Three of the monomers contained hydrolytically stable amide, carboxylic acid and ether linkages which is important for dental composites.

Synthesized monomers were added to Bis-GMA:TEGDMA and Bis-GMA:HEMA systems in different ratios (0.5 and 5 mol %), then their photopolymerization behaviors were investigated by photodifferential scanning calorimeter.

The mobility of the systems was found to have a significant effect on the photopolymerization behavior. For example, addition of diluent TEGDMA to reactive Bis-GMA increased both rate and conversion due to increased mobility of the system. However addition of HEMA as a reactive diluent to Bis-GMA did not increase the conversion due to formation of a rigid system caused by H-bonding. Also, increasing the amount of TEGDMA in Bis-GMA:TEGDMA:Monomer mixtures resulted in an increase in rate of these systems, whereas a significant change was not observed in overall conversions.

The polymerization behavior of the mixtures of the synthesized monomers with Bis-GMA:TEGDMA and Bis-GMA:HEMA systems showed similar rate and conversions. Only, BisGMA:TEGDMA:TBBr-Bisphenol A diester system showed significantly lower rate of polymerization and conversion probably due to steric effect.

The effect of cure temperature on the polymerization kinetic was investigated. By elevating the temperature, viscosity of the systems decreased and mobility increased which allowed increased rate of polymerization except BisGMA:TEGDMA:TBBr-Bisphenol A diester and BisGMA:HEMA:TBBr-Bisphenol A diester systems.

APPENDIX A: TABLES OF THE OBTAINED POLYMERIZATION RATE AND CONVERSION DATA IN THE STUDY

Table A.1. Rate and conversion data of Bis-GMA, HEMA, TEGDMA, and AHM-APTES homopolymerizations at 40 ^{o}C

Composition	Rate (s^{-1})	Conversion (%)
Bis-GMA	0.0261	44.6
	0.0277	41.6
HEMA	0.0370	83.0
	0.0388	80.8
TEGDMA	0.0508	79.6
	0.0550	82.6
AHM-APTES	0.0812	89.2
	0.0838	77.7
	0.0943	92.5

Table A.2. Rate and conversion data of Bis-GMA:TEGDMA system with synthesized novel crosslinking monomers (50:45:5) at 40 ^{o}C

Composition	Rate (s^{-1})	Conversion (%)
Bis-GMA:TEGDMA (50:50)	0.0748	67.6
	0.0769	67.4
Bis-GMA:TEGDMA:BistButyl	0.0591	67.8
	0.0594	69.6
Bis-GMA:TEGDMA:BisAcid	0.0704	68.6
	0.0743	65.7
Bis-GMA:TEGDMA:BisBenzyl	0.0679	69.0
	0.0680	69.2
Bis-GMA:TEGDMA:BisAptes	0.0620	66.0
	0.0678	71.9
	0.0772	78.1
Bis-GMA:TEGDMA:AHMAptes	0.0746	73.4
	0.0799	77.0

Table A.3. Rate and conversion data of Bis-GMA:HEMA system with synthesized novel crosslinking monomers (50:45:5) at 40 ^{o}C

Composition	Rate (s^{-1})	Conversion (%)
Bis-GMA:HEMA (50:50)	0.0651	57.1
	0.0664	56.2
Bis-GMA:HEMA:BistButyl	0.0478	58.9
	0.0490	60.5
Bis-GMA:HEMA:BisAcid	0.0520	53.4
Bis-GMA:HEMA:BisBenzyl	0.0473	56.8
	0.0497	54.7
Bis-GMA:HEMA:BisAptes	0.0555	61.2
	0.0584	61.4
Bis-GMA:HEMA:AHMAptes	0.0628	60.5
	0.0637	57.4

Table A.4. Rate and conversion data of Bis-GMA:TEGDMA and Bis-GMA:HEMA systems with synthesized -Bisphenol A diacid and TBBr-Bisphenol A – benzylamide monomers (50:49.5:0.5) at 40 ^{o}C

Composition	Rate (s^{-1})	Conversion (%)
Bis-GMA:TEGDMA:BisAcid	0.0728	67.9
	0.0810	70.5
Bis-GMA:TEGDMA:BisBenzyl	0.0776	68.5
	0.0839	72.3
Bis-GMA:HEMA:BisAcid	0.0756	55.9
	0.0769	55.5
Bis-GMA:HEMA:BisBenzyl	0.0621	54.9
	0.0654	60.8

Table A.5. Rate and conversion data of Bis-GMA:TEGDMA system with synthesized novel crosslinking monomers (50:45:5) at 60 ^{o}C

Composition	Rate (s^{-1})	Conversion (%)
Bis-GMA:TEGDMA (50:50)	0.0798	70.9
	0.0807	72.6
Bis-GMA:TEGDMA:BistButyl	0.0514	72.6
	0.0537	73.6
Bis-GMA:TEGDMA:BisAptes	0.0698	68.4
	0.0711	68.4
Bis-GMA:TEGDMA:AHMAptes	0.0806	66.3
	0.0861	72.0

Table A.6. Rate and conversion data of Bis-GMA:HEMA system with synthesized novel crosslinking monomers (50:45:5) at 60 ^{o}C

Composition	Rate (s^{-1})	Conversion (%)
Bis-GMA:HEMA (50:50)	0.0832	57.8
	0.0867	58.0
Bis-GMA:HEMA:BistButyl	0.0374	58.2
	0.0391	62.4
Bis-GMA:HEMA:BisAptes	0.0538	56.7
	0.0554	55.4
Bis-GMA:HEMA:AHMAptes	0.0797	60.2
	0.0868	60.2

REFERENCES

1. *Tooth Anatomy*, http://www.tooth.net/info/Anotomyoftooth.htm, 2005.

2. *Dental Glossary*, http://www.dentalreview.com/Glossary.htm, 2005.

3. Tao, S. X., M. Takahashi, Y. Miyagawa, and S. Nakahara, "Comparison of the Histological Structure and Elemental Composition Between Primordial and Degenerative Third Molar Enamels", *Anthropology Journal*, Vol. 12, pp. 2-3, 2005.

4. Verde, A. V., M. Ramosa, M. Stoneham, and R. M. Ribeiro, "Mesoscopic Modelling of the Interaction of Infrared Lasers with Composite Materials: An Application to Human Dental Enamel", *Applied Surface Science*, Vol. 238, pp. 410-414, 2004.

5. Nicholson, J. and M. Anstice, "The Development of Modified Glass-Ionomer Cements for Dentistry", ***TRIP.***, Vol. 2, No. 8, pp. 272-276, 1994.

6. Culbertson, B. M., "Glass-Ionomer Dental Restoratives", ***Prog. Polym. Sci.***, Vol. 26, pp. 577-604, 2001.

7. Espevik, S., "Dental Amalgam", ***Ann. Rev. Mater. Sci.***, Vol. 7, pp. 55-72, 1977.

8. Sideridou, I., V. Tserki, and G. Papanastasiou, "Effect of Chemical Structure on Degree of Conversion in Light-Cured Dimethacrylate-Based Dental Resins", ***Biomaterials***, Vol. 23, pp. 1819-1829, 2002.

9. Bogdal, D., J. Pielichowski, and A. Boron, "Application of Diol Dimethacrylates in Dental Composites and Their Influence on Polymerization Shrinkage", ***J. Appl. Polym. Sci.***, Vol. 66, pp. 2333-2337, 1997.

10. Holland, R. I., "Release of Mercury Vapor from Corroding Amalgam in Vitro", ***Dent. Mater.***, Vol. 9, pp. 99-103, 1993.

11. Chew, C. L., G. Soh, A. S. Lee, and T. S. Yeoh, "Comparison of Release of Mercury from Three Dental Amalgams", *Dent. Mater.*, Vol. 5, pp. 244-246, 1989.

12. Moszner, N., "New Monomers for Dental Application", *Macromol. Symp.*, Vol. 217, pp. 63-75, 2004.

13. Lu, H., J. W. Stansbury, J. Nie, K. A. Berchtold, and C. N. Bowman, "Development of Highly Reactive Mono-(meth)acrylates as Reactive Diluents for Dimethacrylate-Based Dental Resin Systems", *Biomaterials*, Vol. 26, pp. 1329-1336, 2005.

14. Ahn, K. D., D. K. Han, S. H. Lee, and C. W. Lee, "New Aromatic tert-Amines for Application as Photoinitiator Components in Photocurable Dental Materials", *Macromol. Chem. Phys.*, Vol. 204, pp. 1628-1635, 2003.

15. Ullrich, G., D. Herzog, R. Liska, P. Burtscher, and N. Moszner, "Photoinitiators with Functional Groups VII, Covalently Bonded Camphorquinone-Amines", *J. Polym. Sci., Part A: Polym. Chem.*, Vol. 42, pp. 4948–4963, 2004.

16. Lu, H., J. W. Stansbury, and C. N. Bowman, "Towards the Elucidation of Shrinkage Stress Development and Relaxation in Dental Composites", *Dent. Mater.*, Vol. 20, pp. 979-986, 2004.

17. Davy, K. W. M., S. Kalachandra, M. S. Pandain, and M. Braden, "Relationship Between Composite Matrix Molecular Structure and Properties", *Biomaterials*, Vol. 19, pp. 2007-2014, 1998.

18. Chung, C. M., J. G. Kim, M. S. Kim, K. M. Kim, and K. N. Kim, "Development of a New Photocurable Composite Resin with Reduced Curing Shrinkage", *Dent. Mater.*, Vol. 18, pp. 174-178, 2002.

19. Meyer, J., M. A. Cattani-Lorente, and V. Dupuis, "Compomers: Between Glass-Ionomer Cements and Composites", *Biomaterias*, Vol. 19, pp. 529-539, 1998.

20. Nie, J., L. G. Lovell, and C. N. Bowman, “Synthesis and Characterization of *N*-isopropyl, *N*-methacryloxyethyl methacrylamide as a Possible Dental Resin”, *Biomaterials*, Vol. 22, pp. 535-540, 2001.

21. Weir, M. D., C. A. Khatri, and J. M. Antonucci, “Facile Synthesis of Hydroxylated Dimethacrylates for Use in Biomedical Applications”, *ACS Polym. Prepr.*, Vol. 42, No. 2, pp. 131-132, 2001.

22. Klee, J. E., U. Walz, D. Holter, H. Frey, and R. Mulhaupt, “Branched Macromonomers and Their Application in Dental Composites”, *Die Angew. Makromol. Chem.*, Vol. 260, pp. 71-75, 1998.

23. Chappelow, C. C., M. D. Power, C. Q. Bowles, R. G. Miller, C. S. Pinzino, and J.D. Eick, “Novel Priming and Crosslinking Systems for Use with Isocyanatomethacrylate Dental Adhesives”, *Dent. Mater.*, Vol. 16, pp. 396-405, 2000.

24. Stansbury, J. W. and J. M. Antonucci, “Dimethacrylate Monomers with Varied Fluorine Contents and Distributions”, *Dent. Mater.*, Vol. 15, pp. 166-173, 1999.

25. Sibold, N., P. J. Madec, S. Masson, and T.N. Pham, “Synthesis and Characterization of (co)Polymers Containing a Phosphonate Function for Use in Dental Composites”, *Polymer*, Vol. 43, pp. 7257-7267, 2002.

26. Moszner, N., F. Zeuner, and V. Rheinberger, “Polymerization of Cyclic Monomers 1, Radical Polymerization of Unsaturated Spiro Orthocarbonates”, *Macromol. Rapid Commun.*, Vol. 16, pp. 667- 672, 1995.

27. Moszner, N., F. Zeuner, U. K. Fischer, V. Rheinberger, A. De Meijere, and V. Bagutski, “Polymerization of Cyclic Monomers 10, Synthesis and Radical Polymerization of Methyl-2-(Bicyclo[3.1.0]hex-1-yl)acrylate”, *Macromol. Rapid Commun.*, Vol. 24, pp. 269-273, 2003.

28. De Meijere, A., V. Bagutski, F. Zeuner, U. K. Fischer, V. Rheinberger, and N. Moszner, "Synthesis and Radical Polymerization of Various 2-Cyclopropylacrylates", *Eur. J. Org. Chem.*, pp. 3669-3678, 2004.

29. Moszner, N., T. Volkel, and V. Rheinberger, "Synthesis, Characterization and Polymerization of Dendrimers with Methacrylic End Groups", *Macromol. Chem. Phys.*, Vol. 197, pp. 621- 631, 1996.

30. Moszner, N. and U. Salz, "New Developments of Polymeric Dental Composites", *Prog. Polym. Sci.*, Vol. 26 pp. 535-576, 2001.

31. Moszner, N., F. Zeuner, U. K. Fischer, and V. Rheinberger, "Monomers for Adhesive Polymers 2, Synthesis and Radical Polymerisation of Hydrolytically Stable Acrylic Phosphonic Acids", Macromol. Chem. Phys., Vo. 200, pp. 1062-1067, 1999.

32. Avci, D. and A. Z. Albayrak, "Synthesis and Copolymerization of New Phosphorus-Containing Acrylates", *J. Polym. Sci. Polym. Chem. Ed.*, Vol. 41, pp. 2207-2217, 2003.

33. Albayrak, A. Z. and D. Avci, "Novel Phosphorus-Containing Cyclopolymers from Ether Dimer of tert-Butyl-α-Hydroxymethyl Acrylate", *Designed Monomers and Polymers*, Vol. 7, No. 3, pp. 291-300, 2004.

34. Kalachandra, S., D. F. Taylor, J. E. McGrath, M. Sankarapandian, and H. K. Shobha, "Structure-Property Relationships in Dental Composites Based on Polydimethacrylates", *Polym. Prepr.*, Vol. 38, pp. 94-95, 1997.

35. McLean, J. W., J. W. Nicholson, and A. D. Wilson, "Proposed Nomenclature for Glass-Ionomer Dental Cements and Related Materials", *Quint. Int.*, Vol. 25, No. 9, pp. 587- 589, 1994.

36. Nicholson, J. W., "Chemistry of Glass-ionomer Cements: A Review", *Biomaterials*, Vol. 19, pp. 485-494, 1998.

37. Kent, B. E. and A. D. Wilson, "The Properties of a Glass-Ionomer Cement", *Br. Dent. J.*, Vol. 135, pp. 322-326, 1973.

38. Mount, G. J., *A Colour Atlas of Glass-Ionomer Cements*, 2nd edn., Martin Dunits, London, 1994.

39. Brook, J. M. and P. V. Hatton, "Glass-Ionomers: Bioactive Implant Materials", *Biomaterials*, Vol. 19, pp. 565-571, 1998.

40. Wasson, E. A. and J. W. Nicholson, "New Aspects of the Setting of Glass-Ionomer Cements", *J. Dent. Res.*, Vol. 72, pp. 481-483, 1993.

41. Philips, R. W., "Glass Ionomer Cements", *Alpha Omegan*, Vol. 81, No. 4, pp. 25-27, 1988.

42. Momoi, Y. and J. F. McCabe, "Fluoride Release from Light-Activated Glass Ionomer Restorative Cements", *Dent. Mater.*, Vol. 9, pp. 151-154, 1993.

43. Tobias, R. S., R. M. Browne, and C. D. Wilson, "Antibacterial Activity of Dental Restorative Materials", *Int. Endodont. J.*, Vol. 18, pp. 161-71, 1985.

44. McComb, D. and D. Ericson, "Antimicrobial Action of New, Proprietary Lining Cements", *J. Dent. Res.*, Vol. 66, pp. 1025-1028, 1987.

45. Scherer, W., N. Lippman, and J. Kaim, "Antimicrobial Properties of Glass-Ionomer Cements and Other Restorative Materials" *Oper. Dent.*, Vol. 14, pp. 77-81, 1989.

46. Berg, J. H., J. E. Farrell, and L. R. Brown, "Class II Glass Ionomer/Silver Cermet Restorations and Their Effect on Interproximal Growth of Mutans Streptococci", *Pediart. Dent.*, Vol. 12, No. 1, pp. 20-23, 1990.

47. Svanberg, M., J. A. Mjor, and D. J. Orstavik, “Mutans Streptococci in Plaque from Margins of Amalgam, Composite, and Glass-Ionomer Restorations”, *Dent. Res.*, Vol. 69, No. 3, pp. 861-864, 1990.

48. Koch, G. and S. Hatibovic-Kofman, “Glass Ionomer Cements as a Fluoride Release System in vivo” *Swed. Dent. J.*, Vol. 14, No. 6, pp. 267-273, 1990.

49. Svanberg, M., B. Krasse, and H. O. Ornerfeld, “Mutans Streptococci in Interproximal Plaque from Amalgam and Glass Ionomer Restorations”, *Caries Res.*, Vol. 24, No. 2, pp. 133-136, 1990.

50. Forss, H., J. Jokinen, S. Spets-Happonen, L. Seppa, and H. Luoma, “Fluoride and Mutans Streptococci in Plaque Grown on Glass Ionomer and Composite”, *Caries Res.*, Vol. 25, No. 6, pp. 454-458, 1991.

51. Weerheijm, K. L., J. J. de Soet, W. E. van Amerongen, and J. de Graaff, “The Effect of Glass-Ionomer Cement on Carious Dentine: An in vivo Study”, *Caries Res.*, Vol. 27, No. 5, pp. 417-423, 1993.

52. Garcia-Godoy, F. and W. F. Malone, “Effect of Various Etching Times on Two Glass Ionomer Lining Cements”, *Texas Dent. J.*, Vol. 104, No. 4, pp. 12-15, 1987.

53. Hotz, P. R., *Helv. Odont. Acta*, Vol. 23, pp. 89, 1979.

54. Garcia-Godoy, F. and M. E. Jensen, “Artificial Recurrent Caries in Glass Ionomer-Lined Amalgam Restorations”, *Am. J. Dent.*, Vol. 3, No. 3, pp. 89-93, 1990.

55. Jensen, M. E., F. Garcia-Godoy, and J. S. Wefel, “Artificial Root Caries in Amalgam Restorations: Effect of Light-Cured Fluoride Releasing Liners”, *Am. J. Dent.*, Vol. 3, No. 6, pp. 295-298, 1990.

56. Arcoria, C. J., M. A. Fischer, and M. J. Wagner, "Microleakage in Alloy-Glass Ionomer Lined Amalgam Restorations After Thermocycling", *J. Oral Rehabil.*, Vol. 18, No. 1, pp. 9-14, 1991.

57. Souto, M. and K. J. Donly, "Caries Inhibition of Glass Ionomers", *Am. J. Dent.*, Vol. 7, No. 2, pp. 122-124, 1994.

58. Griffin, F., K. J. Donly, and R. Erickson, *Am. J. Dent.*, Vol. 4, 293, 1992.

59. Tyas, M. J., "Cariostatic Effect of Glass Ionomer Cement: A Five-Year Clinical Study", *Aus. Dent. J.*, Vol. 36, No. 3, No. 9, pp. 236-239, 1991.

60. Feilzer, A. J., A. J. De Gee, and C. L. Davidson, "Curing Contraction of Composites and Glass-Ionomer Cements", *J. Prosthet. Dent.*, Vol. 59, No. 3, pp. 297-300, 1988.

61. Powis, D. R., T. Folleras, S. A. Merson, and A. D. Wilson, *J. Dent. Res.*, 59, 297, 1982.

62. Cook, P. A., J. Clin. Orthod., Vol. 24, pp. 509, 1990.

63. Guggenberger, R., R. May, and K. P. Stefan, "New Trends in Glass-Ionomer Chemistry", *Biomaterials*, Vol. 19, pp. 479-483, 1998.

64. Mathis, R. and I. L. Ferracane, "Properties of a New Glass-Ionomer/Composite Resin Hybrid Restorative", *J. Dent. Res.*, Vol. 66, pp. 113, 1987.

65. Wilson, A. D., "Resin-Modified Glass-Ionomer Cements", *Int. J. Prosthodontics*, Vol. 3, No. 5, pp. 425-429, 1990.

66. Croll, T. P., "Light-Hardened Class I Glass-Ionomer-Resin Cement Restoration of a Permanent Molar", *Quintessence Int.*, Vol. 24, No. 2, pp. 109-113, 1993.

67. Moszner, N., T. Volkel, S. C. von Clausbruch, E. Geiter, N. Batliner, and V. Rheinberger, "Sol-Gel Materials 1, Synthesis and Hydrolytic Condensation of New Cross-Linking Alkoxysilane Methacrylates and Light-Curing Composites Based upon the Condensates", *Macromol. Mater. Eng.*, Vol. 287, pp. 339-347, 2002.

68. Decker, C., "Kinetic Study and New Applications of UV Radiation Curing", *Macromol. Rapid Commun.*, Vol. 23, pp. 1067-1093, 2002.

69. Chandra, R. and R. K. Soni, "Recent Developments in Thermally Curable and Photocurable Systems", *Prog. Polym. Sci.*, Vol. 19, pp. 137-169, 1994.

70. Sunam Ayfer, B., *Synthesis and Photopolymerizations of New Methacrylate Crosslinkers and Antibacterial Quaternary Ammonium Monomers*, M.S. Thesis, Boğaziçi University, 2004.

71. Jansen, J., A. A. Dias, M. Dorschu, and B. Coussens, "Fast Monomers: Factors Affecting the Inherent Reactivity of Acrylate Monomers in Photoinitiated Acrylate Polymerization", *Macromolecules*, Vol. 36, pp. 3861-3873, 2003.

72. Beckel, E. R., J. Nie, J. W. Stansbury, and C. N. Bowman, "Effect of Aryl Substituents on the Reactivity of Phenyl Carbamate Acrylate Monomers", *Macromolecules*, Vol. 37, pp. 4062-4069, 2004.

73. *Dental composite depth of cure with halogen and blue LED technology*, http://www.spectravuitc.com/Downloads/Dental%20composite%20depth-of-cure%20Halogen%20vs%20LED.pdf, 2005.

74. Smith, T. J., B. J. Shemper, J. S. Nobles, A. M. Casanova, C. Ott, and L. J. Mathias, "Crosslinking Kinetics of Methyl and Ethyl (α-hydroxymethyl)acrylates: Effect of Crosslinker Type and Functionality", *Polymer*, Vol. 44, pp. 6211-6216, 2003.

75. Young, J. S., A. R. Kannurpatti, and C. N. Bowman, "Effect of Comonomer Concentration and Functionality on Photopolymerization Rates, Mechanical

Properties and Heterogeneity of the Polymer", *Macromol. Chem. Phys.*, Vol. 199, pp. 1043-1049, 1998.

76. Anseth, K. S., C. M. Wang, and C. N. Bowman, "Kinetic Evidence of Reaction Diffusion During the Polymerization of Multi(meth)acrylate Monomers", *Macromolecules*, Vol. 27, pp. 650-655, 1994.

77. Yu, C. and L. Hu, "Successful Baylis-Hillman Reaction of Acrylamide with Aromatic Aldehydes", *J. Org. Chem.*, Vol. 67, pp. 219-223, 2002.

78. Yu, C., B. Liu, and L. Hu, "Efficient Baylis-Hillman Reaction Using Stoichiometric Base Catalyst and an Aqueous Medium", *J. Org. Chem.*, Vol. 66, pp. 5413-5418, 2001.